

Modeling of Cell Adhesion and Deformation Mediated by Receptor-Ligand
Interaction

by

Amirreza F. Golestaneh
B.Sc., Shahrekord University, 2005
M.Sc., UPM, 2009

A Dissertation Submitted in Partial Fulfillment of the
Requirements for the Degree of

DOCTOR OF PHILOSOPHY

in the Department of Mechanical Engineering

© Amirreza Fahim Golestaneh, 2015
University of Victoria

All rights reserved. This dissertation may not be reproduced in whole or in part, by
photocopying or other means, without the permission of the author.

Modeling of Cell Adhesion and Deformation Mediated by Receptor-Ligand
Interaction

by

Amirreza F. Golestaneh
B.Sc., Shahrekord University, 2005
M.Sc., UPM, 2009

Supervisory Committee

Dr. Ben Nadler, Supervisor
(Department of Mechanical Engineering)

Dr. Stephanie Willerth, Departmental Member
(Department of Mechanical Engineering)

Prof. Reuven Gordon, Outside Member
(Department of Electrical and Computer Engineering)

Supervisory Committee

Dr. Ben Nadler, Supervisor
(Department of Mechanical Engineering)

Dr. Stephanie Willerth, Departmental Member
(Department of Mechanical Engineering)

Prof. Reuven Gordon, Outside Member
(Department of Electrical and Computer Engineering)

ABSTRACT

Cell adhesion to a substrate or another cell plays an important role in the activities of the cell, such as cell growth, cell migration and cell signaling and communication with extracellular environment or other cells. The adhesion of the cell to the extracellular matrix also plays a vital role in life, as it involves in healing process of a wound and formation of the blood clot inside a vessel. The spread of cancer metastasis tumors inside the body is mostly dependent on the mechanisms of the cell adhesion. The current work is devoted to studying deformation and adhesion of the cell membrane mediated by receptors and ligands in order to enhance the existing models. In fact phospholipid molecules as the constructive units of the cell membrane grant sufficient in-plane continuity and fluidity to the cell membrane that it can be acceptably modeled as a continuum fluid medium. Therefore a two dimensional isotropic continuum fluid model is proposed in here for cell under implementation of membrane theory. In accordance to lack of sufficient study on direct effect of presence of receptors on membrane dilation, the developed model engages the intensity of presence of receptors with membrane deformation and adhesion. This influence is considered through introduction of spontaneous areal dilation. Another innovation is introduced regarding conception of receptor-ligand bonds formation such that a nonlinear constitutive relation is developed for binding force based on charge-induced dipole interaction,

which is physically admissible. This relation becomes also enriched by considering one-to-one shielding phenomenon. Diffusion of the receptors is formulated along the membrane under the influence of receptor-receptor and receptor-ligand interactions. Then the presented models in this work are implemented to an axisymmetric configuration of a cell to study the deformation and adhesion of its membrane. Another target of this work is to clarify the impacts of variety of material, binding and diffusion constitutive factors on membrane deformation and adhesion and to declare a rational comparison among them.

Contents

Supervisory Committee	ii
Abstract	iii
Table of Contents	v
List of Tables	vii
List of Figures	viii
Acknowledgements	xii
Dedication	xiii
1 Introduction	1
1.1 Membrane deformation	3
1.2 Membrane Adhesion	4
2 Formulation and Application of the Model	9
2.1 Mathematical modeling of the cell	9
2.1.1 Constitutive equation of the cell membrane	10
2.1.2 Stress in the cell membrane	17
2.1.3 Spontaneous areal dilation	21
2.1.4 Binding force	23
2.1.5 Diffusion of the receptors	26
2.2 Implementation of the models	29
2.2.1 Geometry and deformation of the cell	30
2.2.2 Equilibrium condition of the cell	41
2.2.3 Initial fluid pressure	49
2.2.4 Initial contact pressure	50

2.2.5	Receptor diffusion on the cell	51
2.2.6	Nondimensionalized formulation	53
2.2.7	Numerical Solution	57
3	Results and Discussion	62
4	Conclusions	86
5	Future Work	88
A	Additional Results	89
	Bibliography	101

List of Tables

Table 2.1	Summary of the developed models, which govern the deformation of the cell and diffusion of the receptors on the membrane. . . .	29
Table 2.2	Summary of the five nonlinear first order ODEs and the boundary conditions, which govern the deformation of the cell and diffusion of the receptors on the membrane.	61

List of Figures

Figure 2.1	Referential (undeformed), natural (stress-free) and spatial (deformed) configurations and related deformation gradients. . . .	13
Figure 2.2	Referential (undeformed), natural (stress-free) and spatial (deformed) area elements and related area dilations [26].	22
Figure 2.3	Reference (undeformed) configuration mapped by injective immersion $\hat{\mathbf{X}}$ and associated covariant and contravariant bases. . .	31
Figure 2.4	Spatial (deformed) configuration mapped by injective immersion $\hat{\mathbf{x}}$ and associated covariant and contravariant bases.	35
Figure 2.5	Reference (undeformed) and spatial (deformed) configurations mapped by injective immersions and the deformation gradient \mathbf{F} between them.	38
Figure 2.6	The relation between bases in different coordinate systems. . . .	40
Figure 3.1	Cell configurations for different nondimensionalized ligand densities $\bar{\rho}_l = \{0.0, 0.1, 0.5, 1.0\}$ and $\{\bar{r}_0 = 3, \bar{\gamma} = 10^{-4}, \gamma_3 = 10^{-5}, \bar{K} = 0.025, \bar{\zeta} = 0.5, \bar{h}_0 = 0.35\}$ [26].	63
Figure 3.2	Nondimensionalized receptor density $\bar{\rho}_r$ versus dimensionless vertical distance \bar{h} for different nondimensionalized ligand densities $\bar{\rho}_l = \{0.0, 0.1, 0.5, 1.0\}$ and $\{\bar{r}_0 = 3, \bar{\gamma} = 10^{-4}, \gamma_3 = 10^{-5}, \bar{K} = 0.025, \bar{\zeta} = 0.5, \bar{h}_0 = 0.35\}$ [26].	64
Figure 3.3	Distribution of the nondimensionalized binding force \bar{f}_b on the membrane versus dimensionless vertical distance \bar{h} for different nondimensionalized ligand densities $\bar{\rho}_l = \{0.0, 0.1, 0.5, 1.0\}$ and $\{\bar{r}_0 = 3, \bar{\gamma} = 10^{-4}, \gamma_3 = 10^{-5}, \bar{K} = 0.025, \bar{\zeta} = 0.5, \bar{h}_0 = 0.35\}$ [26].	65
Figure 3.4	The nondimensionalized pressure of the enclosed fluid, \bar{p}_f , versus dimensionless ligand density, $\bar{\rho}_l$, and $\{\bar{r}_0 = 3, \bar{\gamma} = 10^{-4}, \gamma_3 = 10^{-5}, \bar{K} = 0.025, \bar{\zeta} = 0.5, \bar{h}_0 = 0.35\}$ [26].	66

- Figure 3.5 The membrane area dilation, J , versus the dimensionless vertical distance, \bar{h} , for different nondimensionalized ligand densities $\bar{\rho}_l = \{0.0, 0.1, 0.5, 1.0\}$ and $\{\bar{r}_0 = 3, \bar{\gamma} = 10^{-4}, \gamma_3 = 10^{-5}, \bar{K} = 0.025, \bar{\zeta} = 0.5, \bar{h}_0 = 0.35\}$ [26]. 67
- Figure 3.6 The spontaneous area dilation, J_{sp} , on the membrane versus the dimensionless vertical distance, \bar{h} , for different nondimensionalized ligand densities $\bar{\rho}_l = \{0.0, 0.1, 0.5, 1.0\}$ and $\{\bar{r}_0 = 3, \bar{\gamma} = 10^{-4}, \gamma_3 = 10^{-5}, \bar{K} = 0.025, \bar{\zeta} = 0.5, \bar{h}_0 = 0.35\}$ [26]. 68
- Figure 3.7 The nondimensionalized resultant adhesion force of the cell, \bar{F}_{ad} , versus the dimensionless ligand density $\bar{\rho}_l$ and $\{\bar{r}_0 = 3, \bar{\gamma} = 10^{-4}, \gamma_3 = 10^{-5}, \bar{K} = 0.025, \bar{\zeta} = 0.5, \bar{h}_0 = 0.35\}$ [26]. 70
- Figure 3.8 The nondimensionalized pressure, \bar{p}_m , in the membrane versus the dimensionless ligand density, $\bar{\rho}_l$, and $\{\bar{r}_0 = 3, \bar{\gamma} = 10^{-4}, \gamma_3 = 10^{-5}, \bar{K} = 0.025, \bar{\zeta} = 0.5, \bar{h}_0 = 0.35\}$ [26]. 71
- Figure 3.9 Deformed configurations of the cell for different values of the dimensionless coefficient of spontaneous area dilation $\bar{\zeta} = \{0.0, 0.1, 0.25, 0.5\}$ and $\{\bar{r}_0 = 3, \bar{\gamma} = 10^{-4}, \gamma_3 = 10^{-5}, \bar{K} = 0.025, \bar{h}_0 = 0.35, \bar{\rho}_l = 1.0\}$ [26]. 74
- Figure 3.10 The nondimensionalized adhesion force of the cell \bar{F}_{ad} versus dimensionless coefficient of spontaneous area dilation $\bar{\zeta}$ and $\{\bar{r}_0 = 3, \bar{\gamma} = 10^{-4}, \gamma_3 = 10^{-5}, \bar{K} = 0.025, \bar{h}_0 = 0.35, \bar{\rho}_l = 1.0\}$ [26]. 75
- Figure 3.11 Deformed configurations of the cell for different values of Debye length inverse $\bar{K} = \{0.025, 0.25, 2.5, 25\}$ and $\{\bar{r}_0 = 3, \bar{\gamma} = 10^{-4}, \gamma_3 = 10^{-5}, \bar{\zeta} = 0.5, \bar{h}_0 = 0.35, \bar{\rho}_l = 1.0\}$ [26]. 76
- Figure 3.12 The nondimensionalized adhesion force of the cell \bar{F}_{ad} versus the inverse of the Debye length \bar{K} and $\{\bar{r}_0 = 3, \bar{\gamma} = 10^{-4}, \gamma_3 = 10^{-5}, \bar{\zeta} = 0.5, \bar{h}_0 = 0.35, \bar{\rho}_l = 1.0\}$ [26]. 78
- Figure 3.13 Deformed configurations of the cell for different dimensionless binding-membrane parameters $\bar{\gamma} = \{10^{-7}, 10^{-6}, 10^{-5}, 10^{-4}\}$ and $\{\bar{r}_0 = 3, \gamma_3 = \{10^{-8}, 10^{-7}, 10^{-6}, 10^{-5}\}, \bar{K} = 0.025, \bar{\zeta} = 0.5, \bar{h}_0 = 0.35, \bar{\rho}_l = 1.0\}$ [26]. 80
- Figure 3.14 The nondimensionalized adhesion force of the cell \bar{F}_{ad} versus dimensionless binding-membrane parameter $\bar{\gamma}$ and $\{\bar{r}_0 = 3, \gamma_3 = \{10^{-8}, 10^{-7}, 10^{-6}, 10^{-5}\}, \bar{K} = 0.025, \bar{\zeta} = 0.5, \bar{h}_0 = 0.35, \bar{\rho}_l = 1.0\}$ [26]. 81

Figure 3.15 The distributions of the areal dilation J versus dimensionless vertical distance \bar{h} for various dimensionless diffusion parameter $\gamma_3 = \{10^{-8}, 10^{-7}, 10^{-6}, 10^{-5}\}$ and $\{\bar{r}_0 = 3, \bar{\gamma} = 10^{-4}, \bar{K} = 0.025, \bar{\zeta} = 0.5, \bar{h}_0 = 0.35\}$ 82

Figure 3.16 The nondimensionalized adhesion force of the cell \bar{F}_{ad} versus dimensionless diffusion parameter γ_3 and $\{\bar{r}_0 = 3, \bar{\gamma} = 10^{-4}, \bar{K} = 0.025, \bar{\zeta} = 0.5, \bar{h}_0 = 0.35, \bar{\rho}_l = 1.0\}$ 83

Figure 3.17 The distributions of the spontaneous areal dilation J_{sp} versus dimensionless vertical distance \bar{h} for various dimensionless diffusion parameter $\gamma_3 = \{10^{-8}, 10^{-7}, 10^{-6}, 10^{-5}\}$ and $\{\bar{r}_0 = 3, \bar{\gamma} = 10^{-4}, \bar{K} = 0.025, \bar{\zeta} = 0.5, \bar{h}_0 = 0.35\}$ 84

Figure 3.18 The distributions of the nondimensionalized receptor density $\bar{\rho}_r$ versus dimensionless vertical distance \bar{h} for various dimensionless diffusion parameter $\gamma_3 = \{10^{-8}, 10^{-7}, 10^{-6}, 10^{-5}\}$ and $\{\bar{r}_0 = 3, \bar{\gamma} = 10^{-4}, \bar{K} = 0.025, \bar{\zeta} = 0.5, \bar{h}_0 = 0.35\}$ 85

Figure A.1 Variation of the membrane area dilation, J , for various values of the dimensionless coefficient of spontaneous area dilation $\bar{\zeta} = \{0.0, 0.1, 0.25, 0.5\}$ and $\{\bar{r}_0 = 3, \bar{\gamma} = 10^{-4}, \gamma_3 = 10^{-5}, \bar{K} = 0.025, \bar{h}_0 = 0.35, \bar{\rho}_l = 1.0\}$ 90

Figure A.2 The nondimensionalized pressure of the enclosed fluid, \bar{p}_f versus nondimensionalized coefficient of spontaneous area dilation $\bar{\zeta}$ and $\{\bar{r}_0 = 3, \bar{\gamma} = 10^{-4}, \gamma_3 = 10^{-5}, \bar{K} = 0.025, \bar{h}_0 = 0.35, \bar{\rho}_l = 1.0\}$ 91

Figure A.3 The distribution of the dimensionless receptor density $\bar{\rho}_r$ versus dimensionless \bar{h} for various values of Debye length inverse $\bar{K} = \{0.025, 0.25, 2.5, 25\}$ and $\{\bar{r}_0 = 3, \bar{\gamma} = 10^{-4}, \gamma_3 = 10^{-5}, \bar{\zeta} = 0.5, \bar{h}_0 = 0.35, \bar{\rho}_l = 1.0\}$ 92

Figure A.4 Variation of the dimensionless binding force \bar{f}_b on the membrane versus dimensionless vertical distance \bar{h} for various values of Debye length inverse $\bar{K} = \{0.025, 0.25, 2.5, 25\}$ and $\{\bar{r}_0 = 3, \bar{\gamma} = 10^{-4}, \gamma_3 = 10^{-5}, \bar{\zeta} = 0.5, \bar{h}_0 = 0.35, \bar{\rho}_l = 1.0\}$ 93

Figure A.5 Variation of the membrane area dilation J on the membrane versus dimensionless vertical distance \bar{h} for various values of Debye length inverse $\bar{K} = \{0.025, 0.25, 2.5, 25\}$ and $\{\bar{r}_0 = 3, \bar{\gamma} = 10^{-4}, \gamma_3 = 10^{-5}, \bar{\zeta} = 0.5, \bar{h}_0 = 0.35, \bar{\rho}_l = 1.0\}$ 94

- Figure A.6 Variation of the spontaneous area dilation J_{sp} on the membrane versus dimensionless vertical distance \bar{h} for various values of Debye length inverse $\bar{K} = \{0.025, 0.25, 2.5, 25\}$ and $\{\bar{r}_0 = 3, \bar{\gamma} = 10^{-4}, \gamma_3 = 10^{-5}, \bar{\zeta} = 0.5, \bar{h}_0 = 0.35, \bar{\rho}_l = 1.0\}$ 95
- Figure A.7 The dimensionless pressure of the enclosed fluid, \bar{p}_f , versus Debye length inverse $\bar{K} = \{0.025, 0.25, 2.5, 25\}$ and $\{\bar{r}_0 = 3, \bar{\gamma} = 10^{-4}, \gamma_3 = 10^{-5}, \bar{\zeta} = 0.5, \bar{h}_0 = 0.35, \bar{\rho}_l = 1.0\}$ 96
- Figure A.8 Variation of the membrane area dilation J versus the dimensionless vertical distance \bar{h} for various dimensionless binding-membrane parameters $\bar{\gamma} = \{10^{-7}, 10^{-6}, 10^{-5}, 10^{-4}\}$ and $\{\bar{r}_0 = 3, \gamma_3 = \{10^{-8}, 10^{-7}, 10^{-6}, 10^{-5}\}, \bar{K} = 0.025, \bar{\zeta} = 0.5, \bar{h}_0 = 0.35, \bar{\rho}_l = 1.0\}$ 97
- Figure A.9 Variation of the spontaneous area dilation J_{sp} versus the dimensionless vertical distance \bar{h} for various dimensionless binding-membrane parameters $\bar{\gamma} = \{10^{-7}, 10^{-6}, 10^{-5}, 10^{-4}\}$ and $\{\bar{r}_0 = 3, \gamma_3 = \{10^{-8}, 10^{-7}, 10^{-6}, 10^{-5}\}, \bar{K} = 0.025, \bar{\zeta} = 0.5, \bar{h}_0 = 0.35, \bar{\rho}_l = 1.0\}$ 98
- Figure A.10 The dimensionless pressure of the enclosed fluid, \bar{p}_f , versus dimensionless binding-membrane parameters $\bar{\gamma} = \{10^{-7}, 10^{-6}, 10^{-5}, 10^{-4}\}$ and $\{\bar{r}_0 = 3, \gamma_3 = \{10^{-8}, 10^{-7}, 10^{-6}, 10^{-5}\}, \bar{K} = 0.025, \bar{\zeta} = 0.5, \bar{h}_0 = 0.35, \bar{\rho}_l = 1.0\}$ 99
- Figure A.11 The nondimensionalized pressure of the enclosed fluid \bar{p}_f versus dimensionless diffusion parameter γ_3 and $\{\bar{r}_0 = 3, \bar{\gamma} = 10^{-4}, \bar{K} = 0.025, \bar{\zeta} = 0.5, \bar{h}_0 = 0.35, \bar{\rho}_l = 1.0\}$ 100

ACKNOWLEDGEMENTS

I would like to deeply thank:

Dr. Ben Nadler for supporting me during my study. He provided me with very bit of guidance and assistance, such that he step by step helped me to learn the fundamentals of continuum mechanics and differential geometry, I required for my research.

DEDICATION

Dedicated to my beloved mom and dad and my supervisor Dr. Ben Nadler.

Chapter 1

Introduction

Cell adhesion strongly influences various activities of the cell including cell growth, cell differentiation, cell neutralization and even communication of the cell with extracellular environment and other cells. Most of the functions of a cell at both sides of the membrane is implemented by the transmembrane proteins called integrins which play a significant role in adhesion. Additionally, cell adhesion to the extracellular matrix (ECM) plays a vital role in human life, saving life or sometime imposing danger on life, where phenomena such as movement and adhesion of the fibroblast cells during wound healing, spreading of the cancer cells from one organ to another in far distance and formation of the blood clot inside the vessel which might prevent and obstruct the flow of the blood to parts of the body are only a few examples. Therefore, cell adhesion and deformation have attracted many attentions from scientists of different fields including engineering.

Vesicle is a bubble of liquid enclosed by a phospholipid bilayer membrane, which stores and transfers the substances within a cell or to the environment (see figure 10-6 in [2]). Vesicles are divided into two groups based on the structure of their membrane; 1) unilamellar vesicles in which the enclosing membrane consists of one bilayer and 2) multilamellar vesicles consist of several bilayers. Cell membrane is a bilayer membrane, which is composed of two layers of mostly phospholipid molecules (see figure 11-11 in [1]). Each molecule is also composed of two parts of phosphate and long fatty acid hydrocarbon chains (see figure 10-2 in [2]). The phosphate group which is also recognized as the head of the phospholipid molecule carries the negative charge and acts as a hydrophilic (water attracted) component. On the other hand the lipid tails repel the water molecules and is hydrophobic. As a natural consequence of the bilayer membrane constituents and their behavior in regards to the water, two layers of

molecule chains form in a way that hydrophobic tails of two layers settle inside, along each other, forming the membrane with both hydrophilic heads facing the water. In other words, the hydrophilic heads shield the tails from the surrounding water inside and outside of the cell in a way that there is almost no water in the membrane and it also excludes molecules like sugars or salts that dissolve in water but not in oil (see figure 10-6 in [2]). In fact, the stable structure of cell membrane is due to the interaction of the hydrophilic heads and hydrophobic tails of the phospholipid molecules with the environment (see figure 10-5 in [2]).

Experiments on the biomembrane in order to determine the mechanical characteristics, begun in 1930s using sea urchin eggs [52] and then continued to study red blood cells [46]. The results of the experiments suggested that cell membrane as an enclosing and separating thin amphipathic (hydrophilic and hydrophobic) layer is a composite material and similar to the vesicle membrane with the total thickness around 5 nm. However cell membrane comprises embedding protein molecules through the membrane thickness (see figure 10-1 in [2]). In fact biomembrane structure is usually impermeable to most water-soluble (hydrophilic) molecules. The phospholipid chains as the dominant components of the membrane are closely held together by non-covalent interaction, they show the same behavior as a fluid when they freely move laterally and sideways through the membrane or even rarely diffuse transversely from one layer to another (see figure 10-8 in [2]). This behavior properly supports the idea for modeling the cell membrane as mosaic fluid suggested by Singer et al. [52] (see also [42]). The membrane is depicted as mosaic because it is composed of different kinds of macromolecules, such as integral proteins, peripheral proteins, glycoproteins, phospholipids, glycolipids, and in some cases cholesterol, lipoproteins. A biological membrane can be considered as a continuum material surface, in other words, membrane surface includes sufficient number of molecules which the fluctuations and effects due to behavior of one individual molecule are negligible [1,2]. It is worth noting that the continuum approach requires that any considered characteristic length must be sufficiently larger than the molecular distances and gaps, which means in continuum approach the analysis never studies the material behavior from molecular point of view. However membrane is discontinuous in the third direction along the thickness, which can be explained by the laminated structure of membrane as molecular strata.

1.1 Membrane deformation

Fung et al. [27] was among the first who analyzed the red blood cell deformation applying the classical membrane theory. They asserted that contribution of bending and curvature change in deformation of red blood cell is negligible compared to the effect of shear deformation. This was verified by the micropipette experiment for the case in which aspiration suction is below the one needed for sucking the vesicle up to a spherical configuration outside the pipette. In fact Evans et al. [16] showed that there is a large increase in suction pressure from 10^3 to 10^5 dyn/cm² after vesicle configuration outside the pipette becomes a sphere, where this rise in value, is attributed to the area dilation. Another work [17] categorized the unilamellar vesicles into three sizes as small unilamellar vesicle (SUV) with diameter less than $3 - 5 \times 10^{-6}$ cm, large unilamellar vesicle (LUV) for the diameter range 5×10^{-6} to 5×10^{-5} cm, and giant unilamellar vesicle (GUV) with size larger than 10^{-4} cm. This investigation claimed that volume change is energetically more expensive than area dilation for GUV, however it is reverse for LUV and SUV. Review of the literature shows the interest of researchers in giant vesicles with size of 2×10^{-3} cm [14, 18, 20, 22, 39].

Some of the previous studies on the red blood cell deformation pointed out that the majority of the membrane deformation is attributed to the distortion of membrane, while its area remains constant during distortion. That means, the membrane exhibits high resistance to change in area and low shear deformation rigidity [11, 13, 15, 19, 24, 25, 36, 37, 48]. Regarding the strong dependency of the membrane deformation on the Young's modulus, Skalak [53] and Evans [15] suggested to separate distortional deformation from dilatation in calculations. They neglected the influence of curvature variation for the vesicles with greater size than 10^{-4} cm because the curvature radius is much larger than the membrane thickness. However for the vesicle smaller than $3 - 5 \times 10^{-6}$ cm or regions with high curvature the membrane thickness is comparable with the curvature radius and elastic behavior of membrane is no longer independent of curvature [21]. Hence, size and shape of the vesicles and cells influence the deformation in a way that size significance can be adverted from two points of view 1) As a criterion for interference of membrane thickness and resistance against curvature change and 2) influence of size on fixity of volume and surface area of vesicle and cells.

Nadler [44] used a continuum approach to model the deformation of an inflated spherical membrane with fluid structure, under the contact pressure of two parallel

rigid plates. The membrane was assumed to behave as an isotropic nonlinear elastic material, where the neo-Hookean constitutive law was finally adopted for that. The membrane was treated as a two dimensional surface embedded in three dimensions and calculations were carried out based on the membrane theory. This implies that the thickness of the cell membrane and normal tractions were not considered in his work and membrane tractions only lied on the tangent plane to the surface at any points. In that work the referential configuration of the membrane was defined as a sphere through an injective immersion in polar coordinates. The deformed configuration was also defined by a different immersion in polar coordinates system and the deformation configuration was easily obtained. The principle stretches and directions in both undeformed and deformed configurations were achieved by comparison of the two representations of deformation gradient in curvilinear and decompositional forms. The equilibrium equation in referential form was used besides considering an isotropic strain energy function to find first order ordinary differential equations (ODEs) for the principle stretches and geometrical variable parameters. Finally the proper boundary conditions (BCs) were applied to the obtained system of ODEs as initial conditions (ICs), where the numerical method was employed to solve for the unknowns in contact and non-contact (free) regions satisfying the continuity condition for parameters associated to the point between the free zone and contact zone. It is worth mentioning that the membrane deformation was solved in that study by incompressibility consideration.

1.2 Membrane Adhesion

A receptor-ligand adhesion model was proposed by Bell et al. [6, 7] in which adhesion between two cells occurs as the result of attractive interaction, between mobile receptors and fixed ligands, and repulsive electrostatic interaction. Shenoy et al. [50] implemented a similar idea of receptor-ligand interaction to study the adhesion of a cell to a substrate. They considered the case in which the mean receptor density on the membrane is not sufficient such that, the receptor-ligand interaction cannot overcome the generic resistance to adhesion of the cell to the substrate. They explained that for the membrane to adhere, the receptors diffuse from the free region to the adhesion region in order to generate sufficient attractive force. They showed that the area of the contact region depends on the ratio of receptor density to ligand density, diffusivity of the receptors on the membrane and time. In another work, Gao

et al. [30] focused on the endocytosis of the extracellular particles, mediated by the receptors on the cell membrane. They considered a coated cell with mobile receptors and a spherical or cylindrical particle, containing ligands. Then they studied the mechanism in which the cell membrane engulfs the particle. The mobile receptors diffuse to the wrapping site and interact with the stationary ligands on the particle, which decreases the overall free energy of the membrane. A similar model was used by Liu et al. [40] for analyzing vesicle adhesion. They suggested a linear relation for the adhesion interaction while the vesicle membrane was modeled as a neo-Hookean hyperelastic membrane with negligible bending stiffness. The friction between the membrane and the substrate was neglected and Van der Waals force and other long-range, weak, repulsive forces were ignored. The adhesion mechanism in this study was based on the receptor-ligand interaction, where the receptors and ligands were initially uniformly distributed, however the receptors were allowed to diffuse on the vesicle membrane, while the ligands were fixed on the substrate. Previous experimental and numerical studies on the adhesion bonds confirmed the nonlinear behavior of the bonds, which should have significant influence on the cell adhesion [5, 34]. In another work Cheng et al. [10] considered two types of interactions between receptors and ligands. A long-ranged physical interaction was considered as the non-specific force, which was due to the van der Waals interaction. They suggested a relation for that non-specific force and claimed that the tangential component of the force (recruitment force) causes the recruitment of receptors. However, since the non-specific van der Waals force is weak it only leads to a shallow adhesion of cell to the substrate. Additionally, they introduced a chemically-induced covalent force as a short-ranged and strong force, which generated a deep adhesion between cell and substrate. According to the [2] binding of a receptor protein to a ligand with high affinity depends on the formation of a set of weak, noncovalent bonds and van der Waals attractions. Since each individual bond is weak, an effective and tight binding interaction requires that several weak bonds be formed simultaneously. Formation of a tight receptor-ligand bond as a set of weak noncovalent (physical) interaction, instead of one strong covalent (chemical) interaction, is consistent with the temporary behavior of the receptor-ligand bond, which allows the bond to break gradually.

Nadler et al. [45] focused on the adhesion and decohesion between a rigid flat punch and a biomembrane, considering two different initial cases of stress-free and prestressed membrane. In fact their work is distinguished from other researches by treating the membrane as an elastic material with nonlinear constitutive behavior and

nonlinear debonding process. First the local equilibrium equation in referential form was used to formulate the axisymmetric deformation of the initially flat and circular membrane. The polar and cylindrical coordinate systems were respectively used to define the undeformed and deformed configurations of the membrane. Then a problem of pull off of a flat rigid punch from a membrane was studied axisymmetrically by employing the Griffith fracture criterion. A nonlinear elastic constitutive behavior was assumed for the membrane besides the assumption of isotropy behavior of membrane to choose isotropic neo-Hookean material. The total strain energy of the membrane consists of strain energy of contact and non-contact (free) regions were into account and then energy release rate was obtained as the variation of strain energy respect to the contact area variation. Then based on the Griffith fracture criterion the obtained energy release rate must be greater or equal to the work of adhesion between the membrane and punch. Finally the membrane profile was obtained by solving for Griffith criterion relation besides the equilibrium equation.

Currently Sohail et al. [54] studied the adhesion of fluid-filled membrane under the influence of electrostatic forces. They studied the membrane deformation and adhesion of a vesicle, to a rigid and charged substrate, by modeling the vesicle as a flexible charged particle inflated by incompressible fluid. The vesicle is inside an electrolyte and its membrane can goes under a large nonlinear elastic deformation. In spite of incompressibility assumption for enclosed fluid, the membrane area was considered extensible. That work was constructed on membrane theory in which the bending stiffness of the membrane was negligible and all the tractions and stress tensor lied on the tangent plane to the membrane two dimensional manifold and do not have a normal component. Therefore the deformation and adhesion of the membrane to the substrate were controlled by the fixed-distributed charges on the membrane and substrate, under electrostatic force. They first started with the Debye-Huckel (D-H) equation which is a linearized form of the general Poisson-Boltzmann equation (where the nonlinear Poisson-Boltzmann equation is obtained by substituting the statistically gained Boltzmann law ,for charge density, into Gauss's law). Then an infinitesimal charged element of the membrane was considered as a point charge in the electrolyte, where the potential function was considered. The electrostatic field and consequently electrostatic forces applied by charges on membrane and substrate to that element of membrane were calculated and then the total electrostatic force was obtained by integration. Finally the same method as applied in [44] was implemented to obtain the principle stretches and deformed configuration of the adhered vesicle.

In another work Evans [18] studied the membrane-membrane adhesion of two spherical vesicles aspirated into pipettes by treating them as an elastic continuum material. The contour of the adhesion zone was modeled via construction of the equilibrium equations for free and adhesion zones and satisfaction of continuity at the connection point. In continuum model the energy released after adhesion is equal to the minimum energy required for detachment. This means the energy required to detach the membranes is much larger than adhesion energy, which is strongly in agreement with experimental observations. It is worth noting that in that research the binding force behavior was simplified as a linear behavior which followed the Hook's law and local bending stiffness of the membrane was contributed. The same force equilibrium method was applied by Martinez et al. [43] and they approximated the adhesion bond behavior by linear Hook's law same as Evans [18].

Biocellular adhesion can be more complicated than receptor-ligand link, in which the inner cellular constituent called cytoskeleton that acts as the cellular skeleton and strengthens the cell stability, is involved in adhesion by connecting to the receptors and supporting them from inside the cell. This type of adhesion usually induces receptors aggregation in a region called focal adhesion (FA) [4, 29, 43]. There are two models of cell detachment as peeling model in which the focal contact has no mechanical rigidity and thus adhesive bonds break gradually starting from the heading point. This model is associated with minimum detachment energy. On the other hand fracture model is completely rigid, so bond failure involves equal stress distribution among all bonds and abrupt rupture which this participation of all bonds together in detachment causes the highest detachment energy. Regarding the structure of linkage between intracellular constituent, cytoskeleton, and extracellular matrix (ECM), a serial connection of two springs was used by Schwarz et al. [49] to model the elastic behavior of intercellular component and ECM as a united structure.

According to the above review of literature the following report first attempts to present a detailed analysis of modeling of cell behavior in adhesion to a substrate. Regarding the previous discussion about the similar behavior of the phospholipid bilayer membrane of the cell to the isotropic fluid, in the present work the cell membrane is modeled as an isotropic fluid-like surface and a constitutive relation of a free energy is derived for a two dimensional isotropic continuum fluid membrane. Since one of the main objectives of the current work is to shed light on the significant role of presence of the receptors in adhesion and deformation of the cell, this idea is considered in the presented model for the isotropic fluid-like membrane, such that the developed strain

energy is sensitive to the presence of the receptors. Due to the previous studies about electrostatic characteristic of the integrin proteins, which carry positive charges and nonpolar characteristic of the ligand proteins, a nonlinear binding force is developed to model the receptor-ligand interaction as an ion-induced dipole interaction between mobile receptors on the membrane and fixed ligands on the substrate. In order to consider a continuum approach the binding force between receptors on an infinitesimal area of the membrane with a local receptor density and an infinitesimal area of substrate with a local ligand density is formulated. The tangential component of the receptor-ligand binding force is then used to formulate the diffusion of the receptors on the cell membrane, by deriving a constitutive relation for the flux of the receptors due to the receptor-ligand interactions. In addition to the influence of the receptor-ligand binding force, the interaction between receptors on the membrane is also engaged in the diffusion equation by using the Fick's law. In the second part the proposed models in earlier sections are implemented to a particular cell with axisymmetric configuration and adhesion and deformation of the cell is studied. The impacts of variety of material, binding and diffusion constitutive coefficients on membrane deformation and adhesion are finally discussed and compared together.

Chapter 2

Formulation and Application of the Model

2.1 Mathematical modeling of the cell

In this chapter we are concerned with the formulation of a comprehensive model, which approximates the adhesion and deformation of a biological cell (biocell) to a rigid substrate. The adhesion is mediated by means of two types of proteins exist on the cell membrane and substrate. The type of protein molecule on the membrane, which is involved in adhesion is integrin that is also called under the general name of receptor (see figure 19-64 in [2]). These integrins are mobile, transmembrane proteins on the cell membrane that link to the stationary fibronectin proteins (ligands) on the substrate and construct the adhesion of the cell to the substrate. Due to the electrostatic characteristics of integrin and ligand proteins, a charge-induced dipole bond is developed here to model the adhesion force of the cell to the substrate (see figure 3-37 in [2]). As another external force applied on the membrane, which has a considerable effect on adhesion and deformation of the cell, is the enclosed fluid inside the cell, which is taken as an incompressible fluid. The behavior of the cell in adhesion and deformation is strongly dependent on the material characteristic of the cell membrane. According to the observed experimental results in literature, the cell membrane behavior in dilation and distortion is mostly close to the behavior of a fluid and a biological membrane can be considered as a continuum material in two dimensions defined on the membrane surface. In other words membrane surface includes sufficient number of molecules which the fluctuations and effects due to

behavior of one individual molecule are negligible [1, 2]. It is worth noting that the continuum approach requires that any considered characteristic length must be sufficiently larger than the molecular distances and gaps, which means in continuum approach the analysis never studies the material behavior from molecular point of view. Therefore in the current work a fluid-like strain energy function is proposed to approximate the mechanical behavior of the cell membrane. This strain energy accounts for the resistance of the fluid-like membrane to the in-plane dilation, however neglects any distortion in the membrane. The thickness of the cell membrane with respect to its curvature radius plays a significant role in modeling the cell membrane by shell or membrane theory, such that if the membrane thickness of the cell is more than %10 of the curvature radius of the membrane, then the cell membrane is modeled by shell theory and bending stiffness of the cell membrane is considered, otherwise membrane theory is used for modeling [23]. However, in the current work, the membrane theory is used for modeling, since the membrane of the cell is considered to be comprised of phospholipid molecules and other components of the membrane plus the cytoskeleton underneath the membrane are ignored. Therefore, the behavior of the cell membrane is better modeled by using membrane theory. That means, the bending stiffness of the membrane is ignored and the normal forces to the membrane are tolerated as in-plane stresses. As a novelty and since the influence of the receptor presence on the adhesion and deformation of the cell has not been sufficiently studied, in the present work the effect of the presence of the receptors on the areal dilation of the membrane is addressed through the introduction of spontaneous areal dilation. The conception of spontaneous areal dilation affects the material behavior of the membrane through the proposed strain energy function. According to the mobility of the receptors on the membrane and the electrostatic characteristics of the receptors and ligands, the migration of the receptors on the membrane is considered to be under the influence of receptor-receptor and receptor-ligand interactions. Therefore, a diffusion model is developed, which governs the distribution of the receptors on the membrane. The notation and terminology used in the following are standard in differential geometry of surfaces (see [12, 31, 47]).

2.1.1 Constitutive equation of the cell membrane

Since the cell is deformable, the constitutive response of the material to the external loads influences the equilibrium condition of the body, therefore the constitutive

strain energy as the parameter, which determines the stress within the hyperelastic membrane material has a significant importance. As mentioned in chapter 1 the previous work in the literature shows that the phospholipid molecules as the dominant component of the membrane are closely held together by the non-covalent interaction, which grants sufficient lateral freedom to the molecules to possess a fluid-like behavior in the surface of the cell membrane. Therefore the characteristic behavior of the cell membrane in dilation and distortion is mostly close to the behavior of the fluid, which means that the areal dilation of the membrane is energetically expensive, however the membrane possesses a small resistance to the distortion. Therefore, a fluid-like strain energy function is proposed to approximate the mechanical behavior of the cell membrane. This strain energy accounts for the resistance of the fluid-like membrane to the in-plane dilation, however is insensitive to any distortion in the membrane. Additionally, since the deformation response of the cell membrane is modeled by membrane theory, the bending stiffness of the membrane is ignored and the normal forces to the membrane are tolerated by the in-plane stresses. The cell membrane is modeled as a compressible, isotropic fluid surface, where its symmetry group includes every rotation about an axis normal to the membrane surface.

As mentioned before, in the present work three different configurations are defined as reference, natural and spatial configurations to describe the geometry of the cell in various stress and deformation conditions. As a physical characteristic, a body in continuum mechanics occupies regions of Euclidean space at time t . The reference configuration is defined as a fixed region that a body occupies in the Euclidean space [9, 32]. The reference configuration is also referred to as undeformed configuration, which is associated with $\mathbf{F} = \mathbf{1}$, where \mathbf{F} denotes the deformation gradient and $\mathbf{1}$ is the surface identity tensor. Therefore the reference configuration roles like the origin for measurement of the deformation in the body. The spatial configuration is defined as the region that a body occupies in the Euclidean space at any time t , which is also named as deformed configuration [9, 32]. It is notable that, the reference configuration is not usually defined for the analysis of fluid, since in the case of an open system of a fluid in flow (control volume) there is no fixed amount of a fluid and we are more interested in the flow of a fluid in time and space. However, in the case of a closed system of a stationary fluid without flow, the reference configuration of the fluid is definable and useful [33]. Therefore a fluid-like cell membrane can be considered as a closed system of a fluid without flow, for which the reference configuration is defined here. Due to presence of the receptors on the cell membrane, in the current work

a third configuration is considered as natural configuration, which is defined as the configuration of the body in which the strain energy function is minimized. In other words, in natural configuration the stress tensor in all representation forms of Cauchy, first and second Piola stresses vanish and therefore this configuration is also referred to as the stress-free configuration [9, 32]. The natural configuration is considered as the origin for measurement of stresses in the body and usually coincides with the reference configuration, however this coincidence is not the case here.

According to the discussion above, consider a cell in the absence of receptors, the reference configuration of the cell is defined after consideration of the receptors on the membrane, such that the membrane is constrained to remain undeformed. The natural configuration as the stress-free configuration, is described after the constraint on the reference configuration is removed and therefore the cell deforms due to the presence of the receptors and releases the existing membrane stress. The cell is then inflated by an incompressible fluid to avoid any possible compressive stresses in the membrane. The discussed configurations are schematically shown in Fig.2.1, where χ , χ_{sp} and χ_e respectively denote the injective immersions of motions between every two configurations of the reference-spatial, reference-natural and natural-spatial.

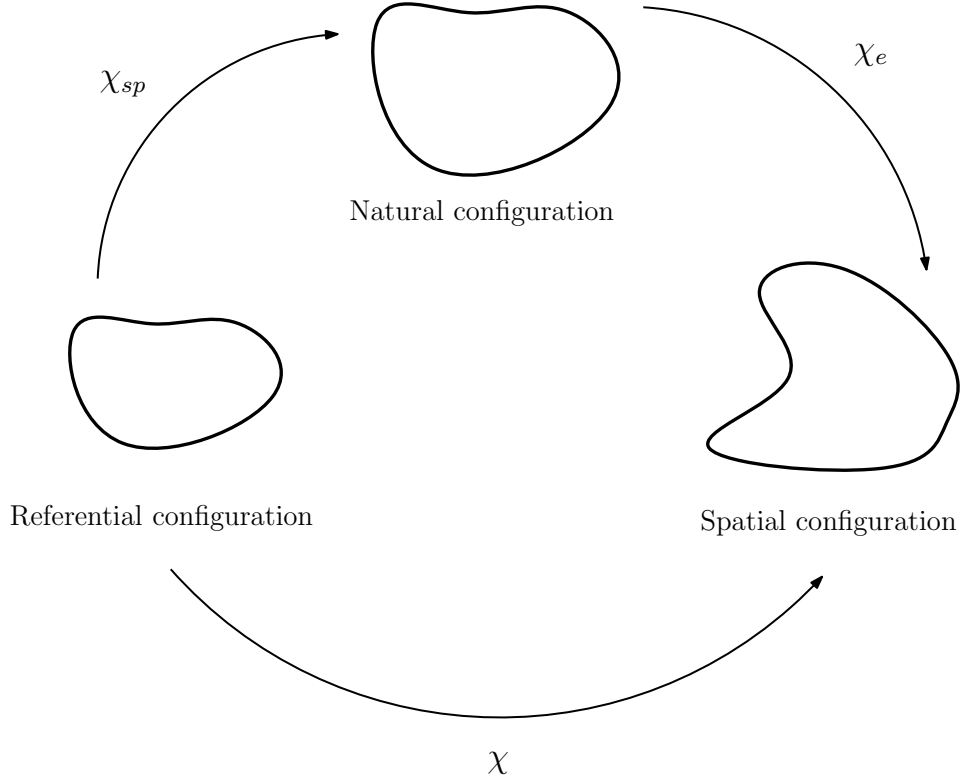


Figure 2.1: Referential (undeformed), natural (stress-free) and spatial (deformed) configurations and related deformation gradients.

In accordance to the definitions of three configurations and since in the theory of nonlinear elasticity the strain energy function depends on the elastic deformation gradient [33], here the fluid-like strain energy of the cell membrane is defined as $\psi = \tilde{\psi}(\mathbf{F}_e)$, where the elastic deformation gradient is $\mathbf{F}_e = \text{Grad}_s(\chi_e)$ and $\text{Grad}_s(\cdot)$ denotes the surface gradient operator in the referential form. By definitions of the referential, natural and spatial configurations three deformation gradients are related as

$$\mathbf{F}_{sp} = {}_o\mathbf{A}_\alpha \otimes \mathbf{A}^\alpha, \quad \mathbf{F}_e = \mathbf{a}_\beta \otimes {}_o\mathbf{A}^\beta \implies$$

$$\mathbf{F} = \mathbf{F}_e \mathbf{F}_{sp} = \mathbf{a}_\alpha \otimes \mathbf{A}^\alpha, \quad (2.1)$$

where the deformation gradient is $\mathbf{F} = \text{Grad}_s(\chi)$, the spontaneous deformation gradient is $\mathbf{F}_{sp} = \text{Grad}_s(\chi_{sp})$, ${}_o\mathbf{A}_\alpha$ and ${}_o\mathbf{A}^\beta$ are respectively covariant and contravariant bases of the natural configuration and \mathbf{a}_α is covariant basis of the spatial configuration. Since the constitutive equation of the strain energy $\tilde{\psi}$ is required to be invariant

under the change of frame

$$\psi = \tilde{\psi}(\mathbf{F}_e) \implies \psi^* = \tilde{\psi}(\mathbf{F}_e^*), \quad (2.2)$$

where according to the transformations of the scalar field of strain energy ψ and deformation gradient tensor \mathbf{F}_e under the change in frame, respectively as $\psi^* = \psi$ and $\mathbf{F}_e^* = \mathbf{Q}\mathbf{F}_e$, for all rotation tensors \mathbf{Q}

$$\psi^* = \tilde{\psi}(\mathbf{F}_e^*) \implies \psi = \tilde{\psi}(\mathbf{Q}\mathbf{F}_e). \quad (2.3)$$

Since the rotation tensor \mathbf{Q} is arbitrary we are at liberty to choose $\mathbf{Q} = \mathbf{R}_e^T$, where \mathbf{R}_e is the orthogonal tensor in polar decomposition of the elastic deformation gradient $\mathbf{F}_e = \mathbf{R}_e\mathbf{U}_e$, such that \mathbf{U}_e is the positive-definite symmetric tensor called elastic right stretch tensor that transforms a vector in natural configuration to a vector in the same configuration. It is notable that the orthogonal tensor \mathbf{R}_e acts between natural and spatial configurations such that $\mathbf{R}_e^T\mathbf{R}_e = \mathbf{R}_e\mathbf{R}_e^T = \mathbf{1}$. Therefore,

$$\psi = \tilde{\psi}(\mathbf{Q}\mathbf{F}_e) = \tilde{\psi}(\mathbf{R}_e^T\mathbf{R}_e\mathbf{U}_e) = \tilde{\psi}(\mathbf{U}_e) = \tilde{\psi}(\sqrt{\mathbf{C}_e}) = \check{\psi}(\mathbf{C}_e), \quad (2.4)$$

where $\mathbf{C}_e = \mathbf{U}_e^2 = \mathbf{F}_e^T\mathbf{F}_e$ is the elastic right Cauchy-Green deformation tensor that acts on a vector in natural configuration and maps it to a vector in the same configuration. Therefore, from (2.3), and (2.4), the consideration of the frame-indifference (objectivity) for the strain energy requires that $\tilde{\psi}$ is a function of elastic deformation gradient \mathbf{F}_e by means of the elastic right Cauchy-Green deformation gradient \mathbf{C}_e

$$\psi = \tilde{\psi}(\mathbf{F}_e) \implies \psi = \check{\psi}(\mathbf{C}_e). \quad (2.5)$$

From the representation theorem of an isotropic scalar function of a tensor [33], the strain energy of the membrane with isotropic fluid characteristic is dependent on only one principle invariant, $J_e^2 = \det \mathbf{C}_e$, where elastic areal dilation J_e governs the areal dilation of the membrane between spontaneous and spatial configurations, therefore

$$\psi = \check{\psi}(\mathbf{C}_e) = \check{\psi}(\det \mathbf{C}_e) = \check{\psi}(J_e^2) = \hat{\psi}(J_e). \quad (2.6)$$

Also from (2.1)₃, $J = J_e J_{sp}$, where $J = \sqrt{\det \mathbf{C}}$ is the areal dilation measures the dilation of the area between the reference and spatial configurations and $J_{sp} = \sqrt{\det \mathbf{C}_{sp}}$

denotes the spontaneous areal dilation, that relates the dilation of the area between the reference and natural configurations. Also $\mathbf{C} = \mathbf{U}^2 = \mathbf{F}^T \mathbf{F}$ and $\mathbf{C}_{sp} = \mathbf{U}_{sp}^2 = \mathbf{F}_{sp}^T \mathbf{F}_{sp}$ are respectively the right Cauchy-Green deformation and spontaneous right Cauchy-Green deformation tensors in reference configuration that act on a vector in that configuration and transfer it to a vector in the same configuration. Therefore for an isotropic fluid-like cell membrane the strain energy per unit volume of the natural configuration is

$$\psi = \hat{\psi}(J_e) = \hat{\psi}(JJ_{sp}^{-1}). \quad (2.7)$$

Since a continuous function can be represented in the form of a polynomial of order n when $n \rightarrow \infty$, here the strain energy function $\hat{\psi}$ is represented in that form. This constitutive function has to satisfy some constitutive restrictions, which are physically admissible and mathematically convenient as: 1) the constitutive relation of the strain energy must be frame-indifferent, 2) the strain energy must satisfy the dissipation inequality, 3) natural (stress free) configuration happens at $J_e = 1$ ($J = J_{sp}$), 4) an increase in a component of the strain should lead to an increase in the corresponding component of the stress and 5) extreme strain should be maintained by the infinite stress (see [3,41]). It is worth noting that the constitutive relation of the strain energy function $\hat{\psi}(J_e)$ as a constitutive relation for a scalar function of a scalar variable J_e satisfies the frame-indifference requirement as discussed in (2.5) and (2.6). The compatibility of the strain energy function $\hat{\psi}(J_e)$ with the physics laws are discussed later. The condition of $J_e = 1$ ($J = J_{sp}$) is associated with the fact that natural configuration is introduced separately here from reference configuration, such that the membrane in natural configuration is dilated due to the presence of the receptors as $J = J_{sp}$. According to the definition of the natural configuration as the configuration in which the strain energy is minimized and therefore the stress vanishes, the necessary and sufficient conditions for the first restriction are

$$\frac{\partial \hat{\psi}(J_e)}{\partial J_e} \Big|_{J_e=1} = 0, \quad \frac{\partial^2 \hat{\psi}(J_e)}{\partial J_e^2} \Big|_{J_e=1} \geq 0. \quad (2.8)$$

The second restriction means that the stress as a function of the strain tensor should be a monotonically increasing. For a hyperelastic material in which stress tensor function is obtained as the derivative of a scalar function with respect to the deformation gradient, the monotonic stress function requires the convexity of the strain energy function under any arbitrary deformation ($\forall J_e$). From the definition of the convexity,

it is obtained that scalar strain function is convex if and only if for all J_e

$$\frac{\partial^2 \hat{\psi}(J_e)}{\partial J_e^2} \geq 0. \quad \forall J_e \quad (2.9)$$

Considering the general form of the $\hat{\psi}$ as the polynomial of order n

$$\psi = \hat{\psi}(J_e) = \sum_{n=1}^{\infty} (\alpha_n + \beta_n J_e)^n. \quad (2.10)$$

Since the function $\hat{\psi}$ is a continuous function the polynomial terms in (2.10) are basis of the function $\hat{\psi}$, means that the terms are linearly independent. Therefore, the constitutive restrictions are applied to each term of (2.10) individually. In order to have the natural configuration at $J = J_e = 1$, from (2.8)₁ and (2.10)

$$\begin{aligned} \frac{\partial \hat{\psi}(J_e)}{\partial J_e} \Big|_{J_e=1} &= \frac{\partial}{\partial J_e} \Big|_{J_e=1} \sum_{n=1}^{\infty} (\alpha_n + \beta_n J_e)^n = \\ &= \sum_{n=1}^{\infty} \frac{\partial}{\partial J_e} \Big|_{J_e=1} (\alpha_n + \beta_n J_e)^n = 0. \end{aligned} \quad (2.11)$$

That means

$$\frac{\partial}{\partial J_e} \Big|_{J_e=1} (\alpha_n + \beta_n J_e)^n = n\beta_n (\alpha_n + \beta_n)^{n-1} = 0, \quad (2.12)$$

which results into $\alpha_n = -\beta_n$ and therefore, (2.10) becomes

$$\hat{\psi}(J_e) = \sum_{n=1}^{\infty} \beta_n (J_e - 1)^n. \quad (2.13)$$

Now with an analogous procedure, from (2.8)₂ and (2.13)

$$\begin{aligned} \frac{\partial^2}{\partial J_e^2} \Big|_{J_e=1} (\beta_n (J_e - 1)^n) &\geq 0 \implies \\ \beta_n n(n-1) (J_e - 1)^{n-2} \Big|_{J_e=1} &\geq 0. \end{aligned} \quad (2.14)$$

Therefore the strain energy function is obtained after application of first constitutive restriction as

$$\hat{\psi}(J_e) = \sum_{n=2}^{\infty} \beta_n (J_e - 1)^n. \quad (2.15)$$

The second constitutive restriction (2.9), which compels the strain energy function to

be convex under any arbitrary motion ($\forall J_e$) should now be applied to (2.15), therefore

$$\begin{aligned} \frac{\partial^2}{\partial J_e^2} (\beta_n (J_e - 1)^n) &\geq 0 \quad \forall J_e \implies \\ \beta_n n(n-1)(J_e - 1)^{n-2} &\geq 0 \quad \forall J_e \implies \\ n &= \{2, 4, 6, \dots\}, \beta_n > 0. \end{aligned} \tag{2.16}$$

Consequently, the convex strain energy function per unit volume of the natural configuration $\hat{\psi}$ is obtained from (2.16)

$$\boxed{\psi = \hat{\psi}(J_e) = \sum_{n=2,4,6,\dots}^{\infty} K_n (J_e - 1)^n,} \tag{2.17}$$

where $K_n > 0$ are material constitutive constants, defined as the energy per unit volume of the natural configuration. For simplicity, in the current work only the first term of the series is used to model the constitutive behavior of the cell membrane

$$\boxed{\hat{\psi}(J_e) = K_m (J_e - 1)^2,} \tag{2.18}$$

where $K_m > 0$ is the material constitutive constant representing the stiffness of membrane to area dilation and is defined as the energy per unit volume of the natural configuration.

2.1.2 Stress in the cell membrane

The strain energy ψ and Cauchy stress tensor \mathbf{T} of an isotropic, compressible, viscous fluid are governed by the constitutive equations of the form

$$\psi = \tilde{\psi}(\rho, \mathbf{L}), \quad \mathbf{T} = \tilde{\mathbf{T}}(\rho, \mathbf{L}), \tag{2.19}$$

where ρ is the density of the fluid, $\mathbf{L} = \text{grad}_s(\mathbf{v})$ is the velocity gradient tensor, \mathbf{v} is the velocity vector of the fluid and $\text{grad}_s(\cdot)$ denotes the surface gradient operator in spatial configuration. It is notable that strain energy $\tilde{\psi}$ is measured per unit mass and the Cauchy stress $\tilde{\mathbf{T}}$ and density ρ are successively measured per unit length and per unit area in spatial configuration. Since the constitutive equations are required to be invariant under the changes of the frame (frame-indifference), it is obtained by

the definition of the frame-indifference that

$$\tilde{\psi}(\rho, \mathbf{L}) = \tilde{\psi}(\rho, \mathbf{D}), \quad \tilde{\mathbf{T}}(\rho, \mathbf{L}) = \tilde{\mathbf{T}}(\rho, \mathbf{D}), \quad (2.20)$$

where the stretching tensor \mathbf{D} is $\mathbf{D} = \text{sym } \mathbf{L} = \frac{1}{2}(\mathbf{L} + \mathbf{L}^T)$. This means that due to the frame-indifference of the constitutive equation, the strain energy function $\tilde{\psi}$ and Cauchy stress $\tilde{\mathbf{T}}$ are dependent on the velocity gradient tensor \mathbf{L} through stretching tensor \mathbf{D}

$$\psi = \tilde{\psi}(\rho, \mathbf{D}), \quad \mathbf{T} = \tilde{\mathbf{T}}(\rho, \mathbf{D}). \quad (2.21)$$

The Cauchy stress tensor of a viscous fluid can be divided into static (equilibrium) stress tensor $\tilde{\mathbf{T}}_{eq}$ and the viscous stress tensor $\tilde{\mathbf{T}}_{vis}$

$$\tilde{\mathbf{T}}(\rho, \mathbf{D}) = \tilde{\mathbf{T}}_{eq}(\rho, \mathbf{0}) + \tilde{\mathbf{T}}_{vis}(\rho, \mathbf{D}), \quad (2.22)$$

where the static Cauchy stress $\tilde{\mathbf{T}}_{eq}$ is the stress in the fluid in the absence of flow, however the viscous Cauchy stress $\tilde{\mathbf{T}}_{vis}$ represents the stress in the fluid due to flow. It is notable that viscous stress tensor $\tilde{\mathbf{T}}_{vis}$ is a deviatoric (traceless) tensor. Since the constitutive equation of the equilibrium Cauchy stress should be frame-indifferent and from definition of the frame-indifference

$$\begin{aligned} \mathbf{T}_{eq} = \tilde{\mathbf{T}}_{eq}(\rho, \mathbf{0}) &\implies \mathbf{Q}\mathbf{T}_{eq}\mathbf{Q}^T = \tilde{\mathbf{T}}_{eq}(\rho, \mathbf{Q}\mathbf{0}\mathbf{Q}^T) \implies \\ \mathbf{Q}\mathbf{T}_{eq}\mathbf{Q}^T = \tilde{\mathbf{T}}_{eq}(\rho, \mathbf{Q}\mathbf{0}\mathbf{Q}^T) &= \tilde{\mathbf{T}}_{eq}(\rho, \mathbf{0}) = \mathbf{T}_{eq} \implies \\ \mathbf{Q}\mathbf{T}_{eq}\mathbf{Q}^T &= \mathbf{T}_{eq}. \end{aligned} \quad (2.23)$$

Therefore the static Cauchy stress tensor must have a specific form of

$$\tilde{\mathbf{T}}_{eq} = -\tilde{p}_{eq}(\rho)\mathbf{1}, \quad (2.24)$$

where $\mathbf{1} = \mathbb{P}\mathbf{I}$ is the identity tensor on the membrane tangent plane, \mathbf{I} denotes the identity tensor in three dimensional Euclidean space \mathbb{E}^3 , $\mathbb{P} = \mathbf{I} - \mathbf{n} \otimes \mathbf{n}$ is the projection tensor onto the membrane tangent plane, \mathbf{n} is the normal vector to the membrane tangent plane and \tilde{p}_{eq} is the equilibrium pressure function. This pressure always act inward and normal to any surface in fluid, which is represented as a negative sign in (2.24). Therefore, the Cauchy stress tensor of an isotropic, compressible and viscous

fluid can be expressed from (2.22) and (2.24) as

$$\tilde{\mathbf{T}}(\rho, \mathbf{D}) = -\tilde{p}_{eq}(\rho)\mathbf{1} + \tilde{\mathbf{T}}_{vis}(\rho, \mathbf{D}). \quad (2.25)$$

In addition the constitutive equation must satisfy the dissipation inequality

$$\rho \frac{D\psi}{Dt} - \mathbf{T} \cdot \mathbf{D} \leq 0, \quad (2.26)$$

where $D(\cdot)/Dt$ represents the material time derivative. It is notable that the strain energy in (2.26) is defined per unit mass and \mathbf{T} and ρ are respectively defined per unit length and area in spatial configuration. From substitution of (2.21)₁ and (2.25) into (2.26)

$$\rho \left(\frac{\partial \tilde{\psi}(\rho, \mathbf{D})}{\partial \rho} \dot{\rho} + \frac{\partial \tilde{\psi}(\rho, \mathbf{D})}{\partial \mathbf{D}} \cdot \dot{\mathbf{D}} \right) - \left(-\tilde{p}_{eq}(\rho)\mathbf{1} + \tilde{\mathbf{T}}_{vis}(\rho, \mathbf{D}) \right) \cdot \mathbf{D} \leq 0, \quad (2.27)$$

where $(\dot{\cdot})$ denotes the material time derivative. Using $\mathbf{1} \cdot \mathbf{D} = \text{tr } \mathbf{D} = \text{tr } \mathbf{L} = \text{div } \mathbf{v}$ and the continuity equation

$$\frac{D\rho}{Dt} + \rho \text{div } \mathbf{v} = 0, \quad (2.28)$$

where $\text{tr}(\cdot)$ is the trace operator and $\text{div}(\cdot)$ denotes the divergence operator in the spatial configuration, the dissipation inequality yields

$$\left(\tilde{p}_{eq}(\rho) - \rho^2 \frac{\partial \tilde{\psi}(\rho, \mathbf{D})}{\partial \rho} \right) \text{tr } \mathbf{D} + \rho \frac{\partial \tilde{\psi}(\rho, \mathbf{D})}{\partial \mathbf{D}} \cdot \dot{\mathbf{D}} - \tilde{\mathbf{T}}_{vis}(\rho, \mathbf{D}) \cdot \mathbf{D} \leq 0. \quad (2.29)$$

Since the inequality (2.29) must hold for all tensors $\dot{\mathbf{D}}$ therefore, its coefficient must be zero otherwise the inequality can be violated for different values of $\dot{\mathbf{D}}$ in different deformations. Hence $\partial \tilde{\psi}(\rho, \mathbf{D})/\partial \mathbf{D} = \mathbf{0}$, which results in $\psi = \tilde{\psi}(\rho)$. Also, the inequality must hold for all symmetric \mathbf{D} , therefore without loss in generality \mathbf{D} can be replaced by $a\mathbf{D}$ for $a > 0$. Dividing by a

$$\left(\tilde{p}_{eq}(\rho) - \rho^2 \frac{\partial \tilde{\psi}(\rho)}{\partial \rho} \right) \text{tr } \mathbf{D} - \tilde{\mathbf{T}}_{vis}(\rho, a\mathbf{D}) \cdot \mathbf{D} \leq 0. \quad (2.30)$$

If $a \rightarrow 0$, since $\tilde{\mathbf{T}}_{vis}(\rho, \mathbf{0}) = \mathbf{0}$, therefore

$$\left(\tilde{p}_{eq}(\rho) - \rho^2 \frac{\partial \tilde{\psi}(\rho)}{\partial \rho} \right) \text{tr } \mathbf{D} \leq 0. \quad (2.31)$$

Since (2.31) must hold for all symmetric stretching tensor \mathbf{D} , therefore

$$\left(\tilde{p}_{eq}(\rho) - \rho^2 \frac{\partial \tilde{\psi}(\rho)}{\partial \rho} \right) = 0. \quad (2.32)$$

The equilibrium fluid pressure is obtained as

$$\tilde{p}_{eq}(\rho) = \rho^2 \frac{\partial \tilde{\psi}(\rho)}{\partial \rho} \quad (2.33)$$

and from (2.30) and (2.32), the viscous Cauchy stress must satisfy

$$\tilde{\mathbf{T}}_{vis}(\rho, \mathbf{D}) \cdot \mathbf{D} \geq 0. \quad (2.34)$$

However, as mentioned above the fluid-like cell membrane is considered as a closed system of fluid without flow and therefore equilibrium pressure in (2.24) and (2.33) generates the only stress field in the membrane. Hence the viscous Cauchy stress in (2.34) is not applicable to this work

$$\mathbf{T} = \tilde{\mathbf{T}}_{eq}(\rho, \mathbf{0}) = -\tilde{p}_{eq}(\rho) \mathbf{1} = -\rho^2 \frac{d\tilde{\psi}(\rho)}{d\rho} \mathbf{1}. \quad (2.35)$$

The proposed strain energy in (2.18) is dependent on elastic areal dilation J_e , therefore (2.35) is required to be represented as a function of J_e . From local form of the conservation of mass law, the fluid-like membrane density in natural configuration ρ_N is related to the density of the membrane in spatial configuration ρ by

$$\rho = \frac{\rho_N}{J_e}, \quad (2.36)$$

where ρ_N and ρ are successively defined as the mass per unit volume in natural and spatial configurations. Hence the strain energy $\tilde{\psi}(\rho)$ can be represented as

$$\psi = \tilde{\psi}(\rho) = \tilde{\psi}(J_e^{-1}) = \tilde{\psi}(J_e), \quad (2.37)$$

where strain energy functions $\tilde{\psi}$ and $\check{\psi}$ are defined as the energy per unit mass. Also from (2.36)

$$d\rho = -\frac{\rho_N}{J_e^2} dJ_e. \quad (2.38)$$

Substitution of (2.37) and (2.38) into (2.35) yields

$$\mathbf{T} = -\rho^2 \frac{d\tilde{\psi}(\rho)}{d\rho} \mathbf{1} = \rho_N \frac{d\check{\psi}(J_e)}{dJ_e} \mathbf{1}. \quad (2.39)$$

Finally the Cauchy stress tensor of the fluid-like cell membrane is obtained as

$$\boxed{\begin{aligned} \mathbf{T} = \tilde{\mathbf{T}}_{eq}(\rho) &= -\rho^2 \frac{d\tilde{\psi}(\rho)}{d\rho} \mathbf{1} = \frac{d\check{\psi}(J_e)}{dJ_e} \mathbf{1} \implies \\ \mathbf{T} &= \hat{\mathbf{T}}(J_e) = \frac{d\hat{\psi}(J_e)}{dJ_e} \mathbf{1}, \end{aligned}} \quad (2.40)$$

where $\hat{\psi}(J_e)$ is the strain energy per unit volume of the natural configuration and $\hat{\mathbf{T}}$ is defined as the force per unit area of the spatial configuration. Now the proposed fluid-like strain energy in (2.18) can be substituted into (2.40) to obtain the relation for the Cauchy stress in the membrane

$$\boxed{\hat{\mathbf{T}}(J_e) = \hat{p}_m(J_e) \mathbf{1}, \quad \hat{p}_m(J_e) = \frac{d\hat{\psi}(J_e)}{dJ_e} = 2K_m (J_e - 1),} \quad (2.41)$$

where $\hat{p}_m(J_e)$ is the membrane pressure function per unit spatial area.

2.1.3 Spontaneous areal dilation

Unlike previous work which did not acknowledge the influence of the presence of receptors on area dilation, here an additional area dilation is introduced to consider extra role of receptors in deformation of the cell membrane. Considering an area A on the reference configuration in the absence of receptors, once N number of receptors are present on the same area and the area is permitted to expand, it dilates to $A_0 = A + \zeta N$ on natural configuration, where ζ denotes the additional area due to the area of a single receptor (see Fig.2.2).

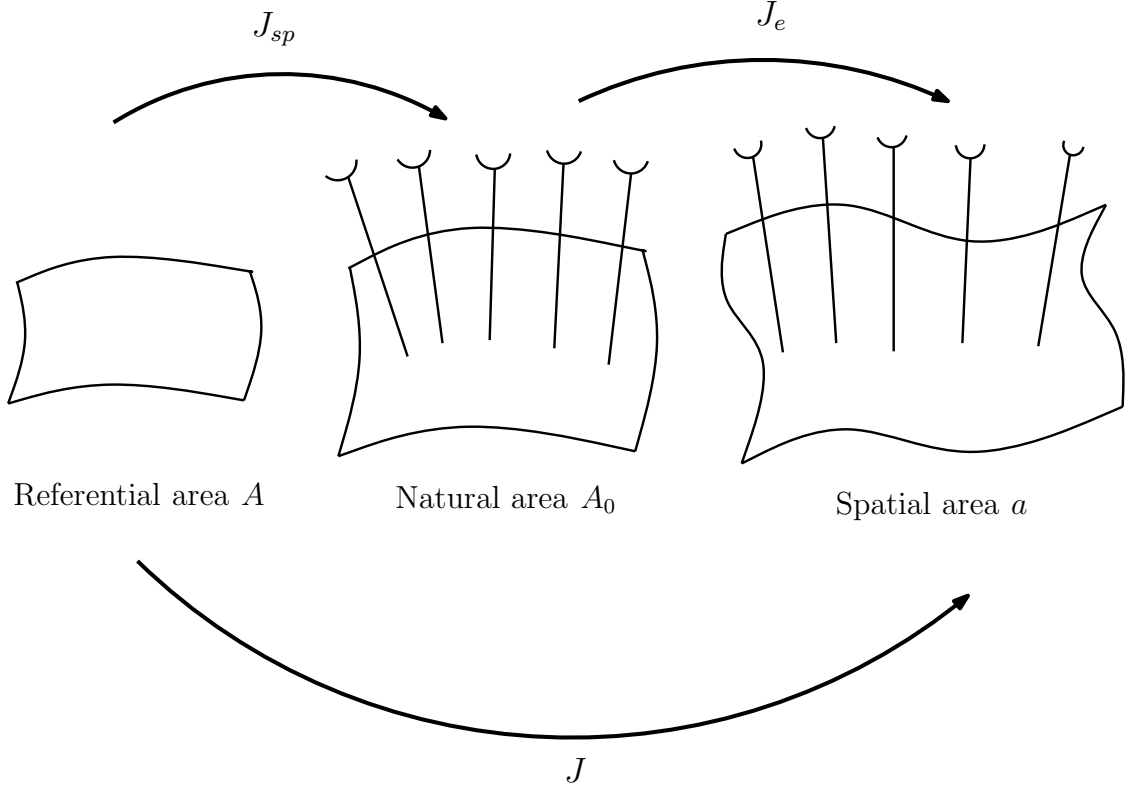


Figure 2.2: Referential (undeformed), natural (stress-free) and spatial (deformed) area elements and related area dilations [26].

The spontaneous area dilation is defined by the ratio of the two areas in natural and reference configurations

$$J_{sp} = \frac{dA_0}{dA}. \quad (2.42)$$

It follows that the spontaneous area dilation, J_{sp} due to the presence of receptors takes the form

$$J_{sp} = \frac{d(A + \zeta N)}{dA} = 1 + \zeta \frac{dN}{dA} = 1 + \zeta \rho_{r_0} = 1 + \zeta J \rho_r, \quad (2.43)$$

where ρ_{r_0} and ρ_r are respectively the receptor densities on the reference and spatial configurations. Therefore

$$\boxed{\hat{J}_{sp}(J, \rho_r) = 1 + \zeta J \rho_r.} \quad (2.44)$$

The product $J \rho_r$ is the pull-back receptor density to the reference configuration. It is notable that (2.44) preserves the global area of the cell membrane under diffusion of the receptors and in the absence of any elastic deformation.

2.1.4 Binding force

In the current work the adhesion and deformation of the cell to the substrate is studied by considering the equilibrium response of the membrane of the cell to the external loads. The response of the cell membrane in the equilibrium condition is governed by the constitutive behavior of the membrane material. A fluid-like constitutive equation was proposed in previous section to model the behavior of the membrane. That constitutive model was also improved by consideration of the newly introduced spontaneous areal dilation, which accounted the influence of the presence of receptors on the areal dilation of the membrane. A constitutive relation was then proposed for the spontaneous areal dilation, which depended on receptor density and local areal dilation. The membrane of the cell experiences three types of distributed forces on its surface. These three surface forces include 1) binding force, which is the interaction between mobile receptors on the membrane and fixed ligands on the substrate, 2) fluid pressure force, which is the normal force generated by the pressure of the enclosed fluid inside the cell and is applied to the cell membrane in outward normal direction, 3) surface reaction force, which is a surface force applied in inward normal direction to the membrane along the contact region and is induced by the reaction pressure of the substrate.

In the present work the adhesion between a cell membrane and a substrate is mediated by transmembrane integrin proteins (called also as receptors) and another type of proteins on the substrate called as fibronectins (or generally as ligands). Receptors the same as phospholipid molecules show a free lateral movement on the membrane, while ligands are fixed on the substrate. The electron micrograph shows that each receptor is comprised of two subsets, which in overall carries five divalent cations Ca^{+2} or Mg^{+2} on the head (see figure 19-64 in [2]). However ligands have a nonpolar structure, which means there is a weak, short-range noncovalent interaction between one receptor and one ligand. Therefore the reason that the mobile receptor proteins on the membrane interact, with high affinity, with the fixed ligand proteins on the substrate is due to the formation of a set of weak, noncovalent bonds and van der Waals attractions. Since each individual bond between one receptor and a ligand is weak, therefore many weak bonds must be formed simultaneously inside one bond in order to construct a strong interaction between a receptor and a ligand [1,2] (see figure 3-37 in [2]). Formation of a tight receptor-ligand bond as a set of weak noncovalent (physical) interaction, instead of one strong covalent (chemical) interaction, is consis-

tent with the temporary behavior of the receptor-ligand bond, which allows the bond to break gradually. This consideration of receptor-ligand interaction is also consistent with the microscopic observation in which a binding is established, when one ligand fits precisely into cavity of a receptor like a hand into a glove (see figure 3-37 in [2]). Therefore we adopt the proposed approach by Alberts et al. [1,2], which was used by Liu et al. [40] to model one strong receptor-ligand bond with high affinity, as a set of number of noncovalent weak sub-bonds. Regarding above discussion a binding force is associated to polarization of a nonpolar ligand molecule in the electrostatic field of a charged receptor. In other words a charge-induced dipole interaction is considered here to model a receptor-ligand binding.

It can be shown that the free energy function of an ion-induced dipole (ion-nonpolar molecule) interaction, between one ion, holding total charge of $Q = Ze$, (where Z is the ionic valency and $e = 1.602 \times 10^{-19}C$ is the elementary charge) and one nonpolar molecule is [38]

$$\tilde{W}(r) = -\frac{1}{2}u_{ind}E, \quad (2.45)$$

where $u_{ind} = \alpha E$ is the induced dipole in nonpolar molecule due to the external electrostatic field E of charges, $\alpha = \alpha_0 + u_{ind}^2/3kT$ is the total polarizability coefficient, α_0 denotes the polarizability of the nonpolar molecule, $k = 1.381 \times 10^{-23} JK^{-1}$ is the Boltzmann's constant and T represents the absolute temperature. The electrostatic field E of a charge Q in an electrolyte is obtained from the free energy for the Coulomb interaction given by [38]

$$\tilde{\phi}(r) = \frac{Qe^{-Kr}}{4\pi\epsilon_0\epsilon r}, \quad (2.46)$$

where ϵ denotes the dimensionless relative permittivity (static dielectric constant), $\epsilon_0 = 8.854 \times 10^{-12} C^2J^{-1}m^{-1}$ is the permittivity of free space, K represents the inverse of the Debye length and r is the distance. Therefore the electrostatic field $\tilde{E}(r)$ of the charge Q in the electrolyte is

$$\tilde{E}(r) = -\frac{d\tilde{\phi}(r)}{dr}. \quad (2.47)$$

From (2.46) and (2.47)

$$\tilde{E}(r) = \frac{Ze(Kr + 1)e^{-Kr}}{4\pi\epsilon_0\epsilon r^2}. \quad (2.48)$$

By substitution of (2.48) into (2.45), the free energy function of the ion-induced dipole

interaction becomes

$$\tilde{W}(r) = -\frac{1}{2}\alpha \frac{(Ze)^2(Kr + 1)^2 e^{-2Kr}}{(4\pi\epsilon_0\epsilon)^2 r^4}. \quad (2.49)$$

Now, if assume that the receptor-ligand interaction is always in vertical direction the derivative of the free energy function of the ion-induced dipole (2.49) with respect to the distance yields the binding force between one receptor and a ligand

$$\mathbf{F}_b = \frac{dW(r)}{dr}(-\mathbf{k}), \quad (2.50)$$

where \mathbf{k} is a unit vector in vertical direction. If N_b shows the number of weak noncovalent sub-bonds, which form in a receptor-ligand interaction, (2.49) and (2.50) yields

$$\mathbf{F}_b = -C(Kr + 1) \left((Kr + 1)^2 + 1 \right) \frac{e^{-2Kr}}{r^5} \mathbf{k}, \quad (2.51)$$

where distance $r = h + h_0$, such that h_0 is the gap between the cell and substrate, h is the vertical distance of any point on the membrane from the region of the membrane in contact with substrate, $C = \alpha N_b (Ze)^2 / (4\pi\epsilon_0\epsilon)^2$. Since this work is based on the continuum approach, therefore a similar concept is considered for the binding force, in which the number of receptors on any infinitesimal area element is assumed to be dense enough, such that there is always sufficient number of receptors on the area element regardless of tiny size of that. Hence an infinitesimal area element da with local receptor density as ρ_r is considered on the spatial configuration, where exist $\rho_r da$ number of receptors. Considering the continuum approach for the receptor-ligand interaction, if a one-to-one interaction is also assumed between a receptor and a ligand, then the binding force \mathbf{f}_b per unit spatial area is defined between the cell and substrate, using (2.51), as

$$\boxed{\mathbf{f}_b = \frac{d\mathbf{F}_b}{da} = -f_b \mathbf{k}, \quad f_b = C(Kr + 1) \left((Kr + 1)^2 + 1 \right) \frac{e^{-2Kr}}{r^5} \rho_{rl},} \quad (2.52)$$

where ρ_{rl} is the density of actively interacting receptors with ligands. In developed binding force model the receptors on the infinitesimal area with density ρ_r is treated as a point charge. Based on the assumption of one-to-one interaction between one receptor and a ligand, the density of actively interacting receptors with ligands is

determined by

$$\rho_{rl} = \begin{cases} \rho_r & \rho_r \leq \rho_l \\ \rho_l & \rho_r > \rho_l, \end{cases} \quad (2.53)$$

where ρ_l denotes the density of the ligands. That means only the receptors on the closest layer of the cell membrane interact with the ligands, while other receptors are shielded and do not participate in any interaction.

The projection tensor is now used to obtain the tangential and normal components of the binding force \mathbf{f}_b to the membrane surface. The tangential projection tensor is a linear mapping from a vector space to a vector space such that the mapping is defined by the tensor product of a unit vector by itself. Assume that \mathbf{u} is a unit vector, then the tangential projection tensor, $\mathbf{u} \otimes \mathbf{u}$ maps any arbitrary vector \mathbf{v} into the projection vector $(\mathbf{u} \cdot \mathbf{v})\mathbf{u}$ along the direction of \mathbf{u} . Similarly, normal projection tensor, $(\mathbf{I} - \mathbf{u} \otimes \mathbf{u})$, maps any arbitrary vector \mathbf{v} into the projection $\mathbf{v} - (\mathbf{v} \cdot \mathbf{u})\mathbf{u}$ onto the plane perpendicular to the unit vector \mathbf{u} . Consider \mathbf{a}_α and \mathbf{a}^α , where $\alpha = \{1, 2\}$, respectively as the covariant and contravariant basis of the cell membrane in spatial configuration. The tangential projection tensor \mathbb{P}_\parallel to the tangential plane of the membrane surface is defined as

$$\mathbb{P}_\parallel = \mathbf{a}_\alpha \otimes \mathbf{a}^\alpha \quad (2.54)$$

and therefore the projection of the binding force on the tangential plane to the membrane surface is

$$\mathbf{f}_b^t = \mathbb{P}_\parallel \mathbf{f}_b = (\mathbf{a}_\alpha \otimes \mathbf{a}^\alpha) \mathbf{f}_b. \quad (2.55)$$

The normal projection tensor \mathbb{P}_\perp to the perpendicular plane to the membrane surface is

$$\mathbb{P}_\perp = \mathbf{I} - (\mathbf{a}_\alpha \otimes \mathbf{a}^\alpha) = (\mathbf{n} \otimes \mathbf{n}) \quad (2.56)$$

and therefore the projection of the binding force in the normal direction to the membrane surface, \mathbf{n} , is

$$\mathbf{f}_b^n = \mathbb{P}_\perp \mathbf{f}_b = (\mathbf{I} - \mathbf{a}_\alpha \otimes \mathbf{a}^\alpha) \mathbf{f}_b = (\mathbf{n} \otimes \mathbf{n}) \mathbf{f}_b. \quad (2.57)$$

2.1.5 Diffusion of the receptors

As mentioned before, in the current work the adhesion of the cell to the substrate is mediated by interaction between the transmembrane integrin proteins and ligand proteins on the substrate. Receptors the same as phospholipid molecules show a free

lateral movement on the membrane, while ligands are fixed on the substrate. In order to study the migration of the receptors on the cell membrane, we consider the first law of the physics for the total number of receptors. Since the total number of receptors on the membrane is constant

$$\begin{aligned} \frac{D N}{D t} = 0 & \implies \\ \frac{D}{D t} \int d N &= \frac{D}{D t} \int_s \rho_r d a = \int_s \frac{D}{D t} (\rho_r d a) \\ &= \int_s \left(\frac{D \rho_r}{D t} + \rho_r \operatorname{div} \mathbf{v}_r \right) d a = 0, \end{aligned} \quad (2.58)$$

where \mathbf{v}_r denotes the velocity of receptor migration on the spatial configuration of the membrane. From localization theorem if (2.58) is valid for every surface s , then the continuity equation of the receptor density in spatial configuration is

$$\frac{D \rho_r}{D t} + \rho_r \operatorname{div}_s \mathbf{v}_r = \frac{\partial \rho_r}{\partial t} + \operatorname{div}_s (\rho_r \mathbf{v}_r) = 0, \quad (2.59)$$

where $\operatorname{div}_s(\cdot) = (\cdot)_{,\alpha} \cdot \mathbf{a}^\alpha$ is the spatial surface divergence operator. Considering a quasistatic process in which the time dependency of receptor density is ignored, the continuity equation of the receptor (2.59) becomes

$$\operatorname{div}_s (\rho_r \mathbf{v}_r) = 0, \quad (2.60)$$

where based on the definition of the flux, $\rho_r \mathbf{v}_r$ is the flux vector of the receptors in spatial configuration of the cell. In order to propose a constitutive equation for the flux vector of the receptors, the concept and logic of the receptor migration on the cell membrane should be studied in more details. As discussed the electron micrograph shows that each receptor is comprised of two subsets, which in overall carries five divalent cations Ca^{+2} or Mg^{+2} on the head [2]. The presence of the electrostatic charges on the integrins induces an electrostatic repulsive interaction between integrins, which attempts to push them to the farthest distance possible from others. The ligand proteins are nonpolar molecules, which are polarized within the electrostatic field of the charged integrins. This charge-induced dipole interaction between receptors and ligands also controls the migration of the receptors on the membrane by attracting the receptors toward the substrate. Consequently, the diffusion and final distribution of the receptors on the membrane are affected by the receptor-receptor

and receptor-ligand interactions.

In this work, the flux of receptors due to the receptor-receptor interaction is approximated by the Fick's law, which is a linear constitutive equation with respect to the gradient of receptor density

$$\mathbf{j}_r = -D \text{grad}_s(\rho_r), \quad (2.61)$$

where D denotes the Fick's law coefficient, which is taken to be a constant and $\text{grad}_s(\cdot) = (\cdot)_{,\alpha} \otimes \mathbf{a}^\alpha$ is the surface gradient operator on the spatial configuration. Fick's law asserts that the flux is proportional to the gradient of the receptor density, such that, receptors diffuse from high density to low density. The tangential component of the receptor-ligand interaction along the tangential plane to the membrane surface is considered to drive the receptors toward the substrate and consequently induce the diffusion of the receptors on the membrane. Therefore a constitutive equation is proposed based on the role of binding force in diffusion of the receptors, in which receptor flux is dependent on the tangential component of the binding force, \mathbf{f}_b^t (see (2.55)), as

$$\mathbf{j}_b = M\mathbb{P}_\parallel \mathbf{f}_b, \quad (2.62)$$

where M is the receptor mobility constitutive coefficient associated to the receptor-ligand binding traction. By presenting two constitutive equations, \mathbf{j}_r and \mathbf{j}_b , the flux filed of the receptors $\rho_r \mathbf{v}_r$ is described as

$$\rho_r \mathbf{v}_r = M\mathbb{P}_\parallel \mathbf{f}_b - D \text{grad}_s(\rho_r). \quad (2.63)$$

Since any constitutive equation has to satisfy the laws of physics, the proposed relation in (2.63) is required to satisfy the continuity equation in (2.60), which guarantees the conservation of receptors locally. Therefore the continuity equation of the receptor, (2.60), after substitution of the constitutive relation for receptor flux becomes

$$\text{div}_s(\rho_r \mathbf{v}_r) = \text{div}_s(M\mathbb{P}_\parallel \mathbf{f}_b - D \text{grad}_s(\rho_r)) = 0, \quad (2.64)$$

which implies

$$\boxed{M\mathbb{P}_\parallel \mathbf{f}_b - D \text{grad}_s(\rho_r) = \mathcal{C}}, \quad (2.65)$$

where \mathcal{C} is a constant vector. The proposed constitutive models are presented in Table 2.1 in summary.

Table 2.1: Summary of the developed models, which govern the deformation of the cell and diffusion of the receptors on the membrane.

Models	Constitutive equations	Equation
Full strain energy	$\psi = \hat{\psi}(J_e) = \sum_{n=2,4,6\dots}^{\infty} K_n (J_e - 1)^n$, $K_n > 0$	(2.17)
Strain energy (first term)	$\hat{\psi}(J_e) = K_m (J_e - 1)^2$, $K_m > 0$	(2.18)
Cauchy stress	$\hat{\mathbf{T}}(J_e) = 2K_m (J_e - 1) \mathbf{1}$	(2.41)
Spontaneous areal dilation	$\hat{J}_{sp}(J, \rho_r) = 1 + \zeta J \rho_r$	(2.44)
Binding force	$\mathbf{f}_b = C(Kr + 1) ((Kr + 1)^2 + 1) \frac{e^{-2Kr}}{r^5} \rho_{rl} \mathbf{k}$	(2.52)
Diffusion equation	$M\mathbb{P}_{\parallel} \mathbf{f}_b - D \text{grad}_s(\rho_r) = \mathcal{C}$	(2.65)

2.2 Implementation of the models

Now, the proposed models are used to study the constitutive behavior of a cell membrane under the application of the external loads in equilibrium condition, while the diffusion equation governs the migration of the receptors on the membrane. The implementation of the developed models in a symmetrical configuration is addressed in this section. The reference (undeformed) and spatial (deformed) configurations of a symmetrical cell are defined mathematically by introducing relative mappings to describe the geometry of the cell in various stress and deformation conditions. The curvilinear bases for both configurations are defined, using the introduced mappings and deformation gradients are obtained relatively. According to the nonlinear elasticity, the Cauchy stress tensor for the isotropic fluid membrane is dependent on an invariant of the elastic right Cauchy-Green deformation tensor (see (2.40) and (2.41)). This means that, the stress field of the cell membrane can be obtained by defining the the mappings of the configurations. Then the stress function and loading equations are used into the equilibrium equation of the cell membrane to predict its behavior. It is worth mentioning that, the referential representation of the equilibrium equation is chosen in this work.

2.2.1 Geometry and deformation of the cell

Here the cell membrane is modeled by membrane theory, considering only the in-plane dilation stiffness, while neglecting the bending stiffness. In other words the tractions in a membrane are lying in the tangent plane to the membrane and do not have any components normal to the tangent plane. Consider that Ω is an open subset of the real plane, $\Omega \subset \mathbb{R}^2$, and $\hat{\mathbf{X}}$ denotes an smooth enough, injective immersion $\hat{\mathbf{X}} : \Omega \rightarrow \omega$, where

$$\omega = \hat{\mathbf{X}}(\Omega) \quad (2.66)$$

is a two dimensional surface embedded into a three dimensional Euclidean space, $\omega \subset \mathbb{E}^3$ (see Fig.2.3). The injective characteristic of the immersion $\hat{\mathbf{X}}$ guarantees that each point $\mathbf{X} \in \omega$ can be unambiguously written as

$$\mathbf{X} = \hat{\mathbf{X}}(X), \quad X \in \Omega \quad (2.67)$$

where the two coordinates X_γ for $\gamma = \{1, 2\}$ of $X = (X_1, X_2)$ are called the convected coordinates of \mathbf{X} . The Greek indices in this work varies as the set $\{1, 2\}$ and the summation convention is applied.

Considering a cell membrane with spherical reference configuration of radius R , the polar coordinate system is used to define the mapping of the configuration, since the configuration is symmetric in both circumferential and meridional directions. Therefore, the reference configuration $\omega \subset \mathbb{E}^3$ is defined by the injective immersion $\hat{\mathbf{X}} : \Omega \rightarrow \omega$, which determines the position of any material point $X = (\phi, \theta)$ in the reference configuration as

$$\mathbf{X} = \hat{\mathbf{X}}(\phi, \theta) = R\mathbf{E}_R(\phi, \theta), \quad (2.68)$$

where the standard spherical coordinates $\{R, \phi, \theta\}$ are the curvilinear coordinates of the point $\mathbf{X} \in \omega \subset \mathbb{E}^3$, with the associate orthonormal spherical (polar) basis $\{\mathbf{E}_R(\phi, \theta), \mathbf{E}_\phi(\phi, \theta), \mathbf{E}_\theta(\theta)\}$ for $0 \leq \phi \leq \pi$ and $0 \leq \theta < 2\pi$. The gradient of the immersion $\hat{\mathbf{X}}$ in (2.68) generates a tensor of second order, which can be represented as a matrix of 3×2 .

$$\nabla \hat{\mathbf{X}}(\phi, \theta) = \left[\begin{array}{cc} \frac{\partial \hat{\mathbf{X}}}{\partial \phi} & \frac{\partial \hat{\mathbf{X}}}{\partial \theta} \end{array} \right], \quad (2.69)$$

where $\nabla(\cdot)$ denotes the gradient operator. The point $\mathbf{X} \in \omega$ represents a position in three dimensional Euclidean space, which is comprised of three components

$X_1(\phi, \theta)$, $X_2(\phi, \theta)$ and $X_3(\phi, \theta)$, while the immersion $\hat{\mathbf{X}}(\phi, \theta)$ is a mapping from the real plane \mathbb{R}^2 , which depends on two independent curvilinear coordinates ϕ and θ . Therefore, two columns of the gradient tensor in (2.69) present the partial derivatives of the injective immersion $\hat{\mathbf{X}}$ with respect to the independent curvilinear variables ϕ and θ , which are linearly independent due to the immersion characteristic of the mapping $\hat{\mathbf{X}}$.

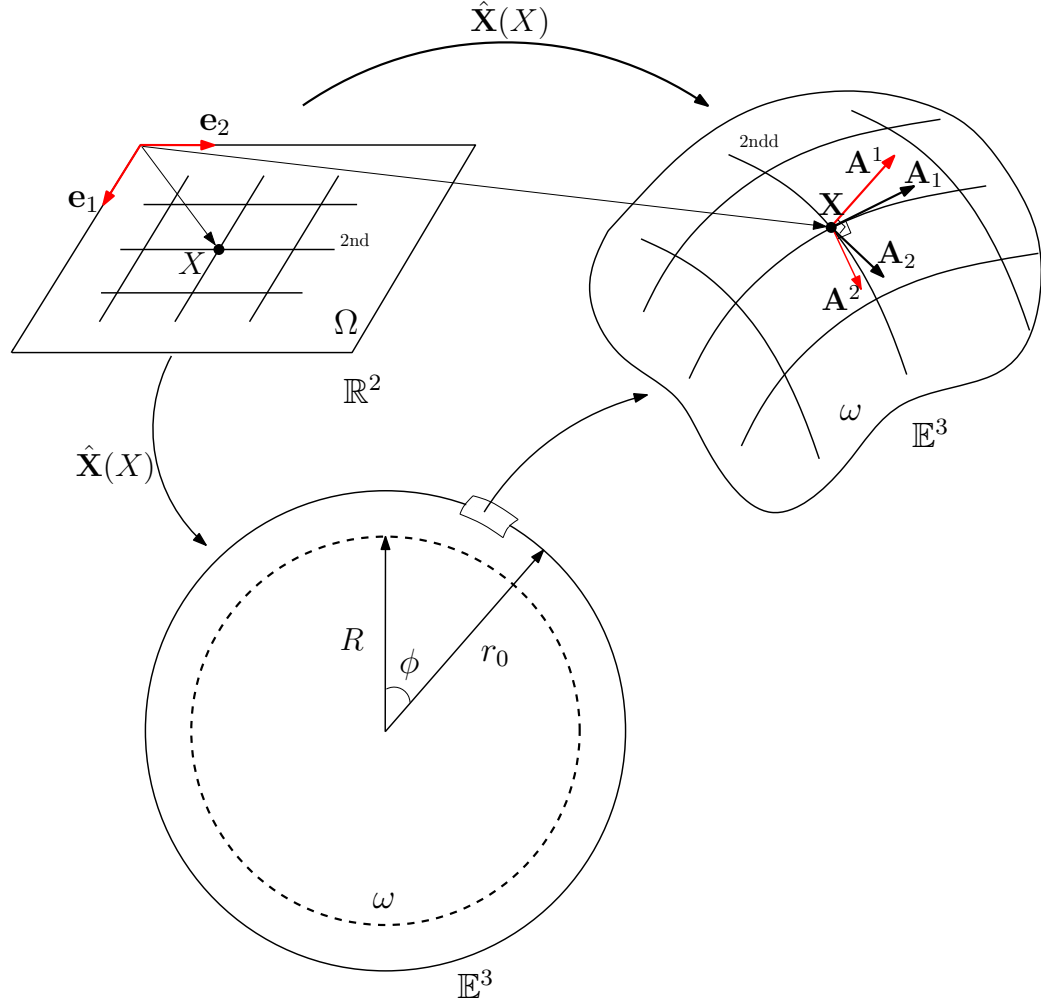


Figure 2.3: Reference (undeformed) configuration mapped by injective immersion $\hat{\mathbf{X}}$ and associated covariant and contravariant bases.

Since the partial derivatives of the immersion $\hat{\mathbf{X}}$ are linearly independent, they can be considered as the curvilinear basis of the tangential plane to the membrane

surface (See Fig.2.3), hence

$$\mathbf{A}_\alpha(\phi, \theta) = \frac{\partial \hat{\mathbf{X}}(\phi, \theta)}{\partial \theta_\alpha}, \quad (2.70)$$

where $\theta_1 = \phi$, $\theta_2 = \theta$ and \mathbf{A}_α denotes the covariant curvilinear basis of the tangential plane to the membrane surface at point $\mathbf{X} = \hat{\mathbf{X}}(\phi, \theta)$. From (2.68), (2.70) the two covariant basis are

$$\begin{aligned} \mathbf{A}_1(\phi, \theta) &= \frac{\partial \hat{\mathbf{X}}(\phi, \theta)}{\partial \phi} = \frac{\partial}{\partial \phi} (R\mathbf{E}_R(\phi, \theta)) = R \frac{\partial \mathbf{E}_R(\phi, \theta)}{\partial \phi} = R\mathbf{E}_\phi(\phi, \theta), \\ \mathbf{A}_2(\phi, \theta) &= \frac{\partial \hat{\mathbf{X}}(\phi, \theta)}{\partial \theta} = \frac{\partial}{\partial \theta} (R\mathbf{E}_R(\phi, \theta)) = R \frac{\partial \mathbf{E}_R(\phi, \theta)}{\partial \theta} = R \sin \phi \mathbf{E}_\theta(\theta), \end{aligned} \quad (2.71)$$

where $\partial \mathbf{E}_R / \partial \phi = \mathbf{E}_\phi(\phi, \theta)$ and $\partial \mathbf{E}_R / \partial \theta = \sin \phi \mathbf{E}_\theta(\theta)$. It is notable that, each covariant basis vector \mathbf{A}_α is tangent to the α -th coordinate line in ω , passing through point $\mathbf{X} = \hat{\mathbf{X}}(\phi, \theta)$, where the coordinate line in ω is defined as the image by $\hat{\mathbf{X}}$ of the points in Ω that located on the line parallel to the Cartesian basis \mathbf{e}_α passing through $(\phi, \theta) \in \mathbb{R}^2$ (See Fig.2.3). Therefore, the covariant basis \mathbf{A}_1 and \mathbf{A}_2 are not generally orthogonal. Considering the covariant basis \mathbf{A}_α defined in (2.70) and (2.71), the contravariant curvilinear basis of the tangential plane to the membrane surface at point $\mathbf{X} = \hat{\mathbf{X}}(\phi, \theta)$ are defined and denoted by \mathbf{A}^α such that

$$\mathbf{A}^\alpha \cdot \mathbf{A}_\beta = \delta_\beta^\alpha \quad (2.72)$$

where, δ_β^α is the Kronecker delta such that

$$\delta_\beta^\alpha = \begin{cases} 1 & \alpha = \beta \\ 0 & \alpha \neq \beta. \end{cases} \quad (2.73)$$

It is notable that according to the definition of the dot product of two vectors, the contravariant basis, (2.72), implies that contravariant basis \mathbf{A}^α and covariant basis \mathbf{A}_β are orthogonal if $\alpha \neq \beta$ (see Fig.2.3). In order to obtain the contravariant basis, we need first to define the metric tensor at point $\mathbf{X} = \hat{\mathbf{X}}(\phi, \theta)$ as a symmetric, positive definite tensor by $\nabla \hat{\mathbf{X}}^T(\phi, \theta) \nabla \hat{\mathbf{X}}(\phi, \theta)$. Therefore the covariant components of the metric tensor at point $\mathbf{X} = \hat{\mathbf{X}}(\phi, \theta)$ become

$$A_{\alpha\beta}(\phi, \theta) = \mathbf{A}_\alpha(\phi, \theta) \cdot \mathbf{A}_\beta(\phi, \theta). \quad (2.74)$$

Considering the covariant components of the metric tensor the contravariant components of the metric tensor at point $\mathbf{X} = \hat{\mathbf{X}}(\phi, \theta)$ is obtained as the components of the inverse matrix

$$[A^{\alpha\beta}(\phi, \theta)] = [A_{\alpha\beta}(\phi, \theta)]^{-1}, \quad (2.75)$$

where the contravariant components of the metric tensor is related to the dot product of the contravariant basis

$$A^{\alpha\beta}(\phi, \theta) = \mathbf{A}^\alpha(\phi, \theta) \cdot \mathbf{A}^\beta(\phi, \theta). \quad (2.76)$$

Now using (2.71) and (2.74), the covariant components of the metric tensor are

$$\left. \begin{aligned} A_{11} &= \mathbf{A}_1 \cdot \mathbf{A}_1 = R^2 \\ A_{12} &= A_{21} = \mathbf{A}_1 \cdot \mathbf{A}_2 = 0 \\ A_{22} &= \mathbf{A}_2 \cdot \mathbf{A}_2 = R^2 \sin^2(\phi) \end{aligned} \right\} \implies [A_{\alpha\beta}(\phi)] = \begin{bmatrix} R^2 & 0 \\ 0 & R^2 \sin^2(\phi) \end{bmatrix}. \quad (2.77)$$

From (2.75) and (2.77)

$$[A^{\alpha\beta}(\phi)] = \begin{bmatrix} R^2 & 0 \\ 0 & R^2 \sin^2(\phi) \end{bmatrix}^{-1} = \begin{bmatrix} R^{-2} & 0 \\ 0 & R^{-2} \sin^{-2}(\phi) \end{bmatrix}. \quad (2.78)$$

According to the role of contravariant component of the metric tensor $A^{\alpha\beta}$ in calculation of contravariant basis of the tangential plane to the membrane surface, the contravariant curvilinear basis of the membrane surface at point $\mathbf{X} = \hat{\mathbf{X}}(\phi, \theta)$ is obtained as

$$\mathbf{A}^\alpha(\phi, \theta) = A^{\alpha\beta}(\phi) \mathbf{A}_\beta(\phi, \theta). \quad (2.79)$$

Using (2.71), (2.78) and (2.79) the contravariant basis are

$$\begin{aligned} \mathbf{A}^1(\phi, \theta) &= A^{11} \mathbf{A}_1 + A^{12} \mathbf{A}_2 = R^{-1} \mathbf{E}_\phi(\phi, \theta), \\ \mathbf{A}^2(\phi, \theta) &= A^{21} \mathbf{A}_1 + A^{22} \mathbf{A}_2 = (R \sin \phi)^{-1} \mathbf{E}_\theta(\theta), \end{aligned} \quad (2.80)$$

Since $\hat{\mathbf{X}}(\phi, \theta)$ is an immersion from a flat two dimensional real plane $\Omega \subset \mathbb{R}^2$ to a two dimensional surface ω embedded in \mathbb{E}^3 , it is defined on only two independent variables ϕ and θ and therefore there exists two covariant and contravariant curvilinear bases respectively as $\mathbf{A}_1, \mathbf{A}_2$ and $\mathbf{A}^1, \mathbf{A}^2$, where the third covariant and contravariant bases

are defined via cross product $\mathbf{A}_3 = \mathbf{A}^3 = (\mathbf{A}_1 \times \mathbf{A}_2)/\|\mathbf{A}_1 \times \mathbf{A}_2\| = (\mathbf{A}^1 \times \mathbf{A}^2)/\|\mathbf{A}^1 \times \mathbf{A}^2\|$.

Considering the deformed configuration of the cell, the cylindrical coordinate system is used to define the mapping of the configuration, since it is symmetric in only meridional direction. Therefore, the spatial configuration $\kappa \subset \mathbf{E}^3$ is defined by the injective immersion $\hat{\mathbf{x}} : \Omega \rightarrow \kappa$, which determines the position of a material point in the spatial configuration as (see Fig.2.4)

$$\mathbf{x} = \hat{\mathbf{x}}(\phi, \theta) = u(\phi) \mathbf{i}(\theta) + h(\phi) \mathbf{k}, \quad (2.81)$$

where the standard spherical coordinates $\{\phi, \theta\}$ are the curvilinear coordinates of the point $\mathbf{x} \in \kappa \subset \mathbb{E}^3$, with the orthonormal cylindrical basis $\{\mathbf{i}(\theta), \mathbf{j}(\theta), \mathbf{k}\}$ of the spatial configuration for $0 \leq \phi \leq \pi$ and $0 \leq \theta < 2\pi$. The gradient of the immersion $\hat{\mathbf{x}}$ in (2.81) generates a tensor of second order, which can be represented as a matrix of 3×2

$$\nabla \hat{\mathbf{x}}(\phi, \theta) = \left[\begin{array}{cc} \frac{\partial \hat{\mathbf{x}}}{\partial \phi} & \frac{\partial \hat{\mathbf{x}}}{\partial \theta} \end{array} \right]. \quad (2.82)$$

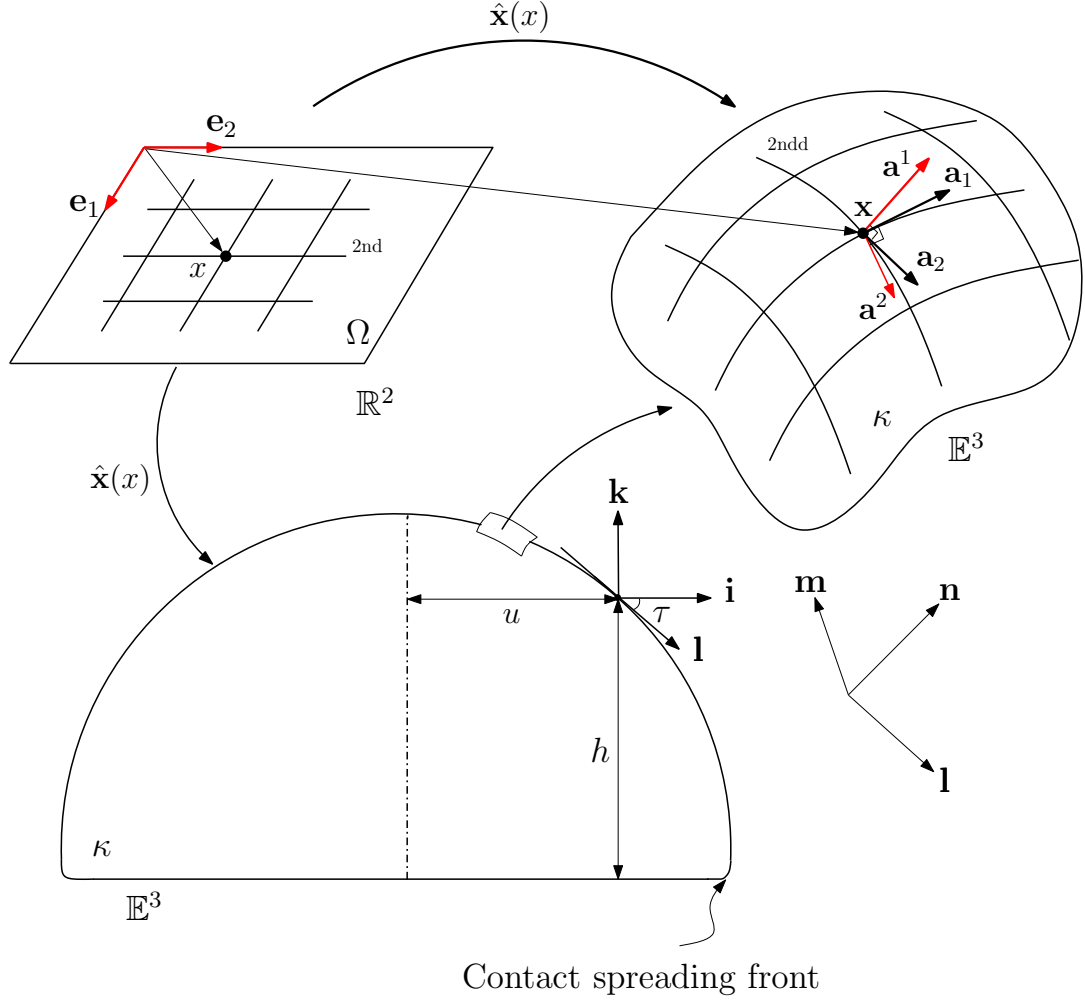
This is due to, the point $\mathbf{x} \in \kappa$ represents a position in three dimensional Euclidean space, which is comprised of three scalar components $x_1(\phi, \theta), x_2(\phi, \theta)$ and $x_3(\phi, \theta)$, while the immersion $\hat{\mathbf{x}}(\phi, \theta)$ is a mapping from a real plane \mathbb{R}^2 , which depends on two independent curvilinear variables $\theta_\alpha = \{\phi, \theta\}$ for $\alpha = \{1, 2\}$. Therefore, two columns of the gradient tensor in (2.82) present the partial derivatives of the injective immersion $\hat{\mathbf{x}}$ with respect to the independent curvilinear variables θ_α , which are linearly independent due to the immersion characteristic of the mapping $\hat{\mathbf{x}}$. Since the partial derivatives of the immersion $\hat{\mathbf{x}}$ are linearly independent, they can be considered as the curvilinear basis of the tangential plane to the membrane surface (See Fig.2.4), hence

$$\mathbf{a}_\alpha(\phi, \theta) = \frac{\partial \hat{\mathbf{x}}}{\partial \theta_\alpha}, \quad (2.83)$$

where \mathbf{a}_α denotes the covariant curvilinear basis of the tangential plane to the membrane surface at point $\mathbf{x} = \hat{\mathbf{x}}(\phi, \theta)$. From (2.81), (2.83) and by remembering that $\theta_\alpha = \{\phi, \theta\}$ for $\alpha = \{1, 2\}$, the two covariant basis are

$$\begin{aligned} \mathbf{a}_1(\phi, \theta) &= \frac{\partial \hat{\mathbf{x}}(\phi, \theta)}{\partial \phi} = \frac{\partial}{\partial \phi} (u(\phi) \mathbf{i}(\theta) + h(\phi) \mathbf{k}) = u'(\phi) \mathbf{i}(\theta) + h'(\phi) \mathbf{k}, \\ \mathbf{a}_2(\phi, \theta) &= \frac{\partial \hat{\mathbf{x}}(\phi, \theta)}{\partial \theta} = \frac{\partial}{\partial \theta} (u(\phi) \mathbf{i}(\theta) + h(\phi) \mathbf{k}) = u(\phi) \frac{\partial \mathbf{i}(\theta)}{\partial \theta} = u(\phi) \mathbf{j}(\theta), \end{aligned} \quad (2.84)$$

where $()' = d()/d\phi$ and $\partial \mathbf{i}/\partial \theta = \mathbf{j}(\theta)$.



Contact spreading front

Figure 2.4: Spatial (deformed) configuration mapped by injective immersion $\hat{\mathbf{x}}$ and associated covariant and contravariant bases.

It is notable that, each covariant basis vector \mathbf{a}_α is tangent to the α -th coordinate line in κ , passing through point $\mathbf{x} = \hat{\mathbf{x}}(\phi, \theta)$, where the coordinate line in κ is defined as the image by $\hat{\mathbf{x}}$ of the points in Ω that located on the line parallel to the Cartesian basis \mathbf{e}_α passing through (ϕ, θ) (See Fig.2.4). Therefore, the covariant basis \mathbf{a}_1 and \mathbf{a}_2 are not generally orthogonal. Considering the covariant basis \mathbf{a}_α defined in (2.83) and (2.84), the contravariant curvilinear basis of the tangential plane to the membrane surface at point $\mathbf{x} = \hat{\mathbf{x}}(\phi, \theta)$ are defined and denoted by \mathbf{a}^α such that

$$\mathbf{a}^\alpha \cdot \mathbf{a}_\beta = \delta_\beta^\alpha. \quad (2.85)$$

It is notable that according to the definition of the dot product of two vectors, the definition of the contravariant basis, (2.85), implies that contravariant basis \mathbf{a}^α and covariant basis \mathbf{a}_β are orthogonal where, $\alpha \neq \beta$ (see Fig.2.4). Also the covariant and contravariant basis are identical, $\mathbf{a}^\alpha = \mathbf{a}_\alpha$, if the coordinate lines are perpendicular. In order to obtain the contravariant basis, we need to define the metric tensor at point $\mathbf{x} = \hat{\mathbf{x}}(\phi, \theta)$ as a symmetric, positive definite tensor by $\nabla \hat{\mathbf{x}}^T(\phi, \theta) \nabla \hat{\mathbf{x}}(\phi, \theta)$. Therefore the covariant components of the metric tensor at point $\mathbf{x} = \hat{\mathbf{X}}(\phi, \theta)$ become

$$a_{\alpha\beta}(\phi, \theta) = \mathbf{a}_\alpha(\phi, \theta) \cdot \mathbf{a}_\beta(\phi, \theta). \quad (2.86)$$

Considering the covariant components of the metric tensor the contravariant components of the metric tensor at point $\mathbf{x} = \hat{\mathbf{x}}(\phi, \theta)$ is obtained as the components of the inverse matrix

$$[a^{\alpha\beta}(\phi, \theta)] = [a_{\alpha\beta}(\phi, \theta)]^{-1}, \quad (2.87)$$

where the contravariant components of the metric tensor is related to the dot product of the contravariant basis

$$a^{\alpha\beta}(\phi, \theta) = \mathbf{a}^\alpha(\phi, \theta) \cdot \mathbf{a}^\beta(\phi, \theta). \quad (2.88)$$

Now using (2.84) and (2.86), the covariant components of the metric tensor are

$$\left. \begin{aligned} a_{11} &= \mathbf{a}_1 \cdot \mathbf{a}_1 = u'^2 + h'^2 \\ a_{12} &= a_{21} = \mathbf{a}_1 \cdot \mathbf{a}_2 = 0 \\ a_{22} &= \mathbf{a}_2 \cdot \mathbf{a}_2 = u^2 \end{aligned} \right\} \implies [a_{\alpha\beta}(\phi)] = \begin{bmatrix} u'^2 + h'^2 & 0 \\ 0 & u^2 \end{bmatrix}. \quad (2.89)$$

From (2.87) and (2.89)

$$[a^{\alpha\beta}(\phi)] = \begin{bmatrix} u'^2 + h'^2 & 0 \\ 0 & u^2 \end{bmatrix}^{-1} = \begin{bmatrix} (u'^2 + h'^2)^{-1} & 0 \\ 0 & u^{-2} \end{bmatrix}. \quad (2.90)$$

According to the role of contravariant component of the metric tensor $a^{\alpha\beta}$ in calculation of contravariant basis of the tangential plane to the membrane surface, the contravariant curvilinear basis of the membrane surface at point $\mathbf{x} = \hat{\mathbf{x}}(\phi, \theta)$ is obtained as

$$\mathbf{a}^\alpha(\phi, \theta) = a^{\alpha\beta}(\phi) \mathbf{a}_\beta(\phi, \theta). \quad (2.91)$$

Using (2.84), (2.90) and (2.91) the contravariant basis are

$$\begin{aligned}\mathbf{a}^1(\phi, \theta) &= a^{11}\mathbf{a}_1 + a^{12}\mathbf{a}_2 = \frac{u'\mathbf{i} + h'\mathbf{k}}{u'^2 + h'^2}, \\ \mathbf{a}^2(\phi, \theta) &= a^{21}\mathbf{a}_1 + a^{22}\mathbf{a}_2 = \frac{\mathbf{j}}{u}.\end{aligned}\tag{2.92}$$

Since $\hat{\mathbf{x}}(\phi, \theta)$ is an immersion from a flat two dimensional real plane $\Omega \subset \mathbb{R}^2$ to a two dimensional surface κ embedded in \mathbb{E}^3 , it is defined on only two independent variables ϕ and θ and therefore there exists two covariant and contravariant curvilinear bases respectively as $\mathbf{a}_1, \mathbf{a}_2$ and $\mathbf{a}^1, \mathbf{a}^2$, where the third covariant and contravariant bases are defined via cross product $\mathbf{a}_3 = \mathbf{a}^3 = (\mathbf{a}_1 \times \mathbf{a}_2) / \|\mathbf{a}_1 \times \mathbf{a}_2\| = (\mathbf{a}^1 \times \mathbf{a}^2) / \|\mathbf{a}^1 \times \mathbf{a}^2\|$.

Since the injective immersions of reference and spatial configuration $\hat{\mathbf{X}}(\phi, \theta)$ and $\hat{\mathbf{x}}(\phi, \theta)$ are both differentiable at any points $(\phi, \theta) \in \Omega$, the deformation gradient \mathbf{F} is defined between the reference and spatial configurations as (see Fig.2.5)

$$d\hat{\mathbf{x}}(\phi, \theta) = \mathbf{F}(\phi, \theta) d\hat{\mathbf{X}}(\phi, \theta) \implies \mathbf{F}(\phi, \theta) = \text{Grad } \hat{\mathbf{x}}(\phi, \theta).\tag{2.93}$$

From definitions of the immersion (2.68) of the reference configuration and covariant basis related to the same configuration (2.70)

$$d\hat{\mathbf{X}}(\phi, \theta) = \frac{\partial \hat{\mathbf{X}}(\phi, \theta)}{\partial \theta_\alpha} d\theta_\alpha = \mathbf{A}_\alpha(\phi, \theta) d\theta_\alpha.\tag{2.94}$$

Similarly, from the defined immersion for spatial configuration (2.81) and the covariant basis (2.83)

$$d\hat{\mathbf{x}}(\phi, \theta) = \frac{\partial \hat{\mathbf{x}}(\phi, \theta)}{\partial \theta_\alpha} d\theta_\alpha = \mathbf{a}_\alpha(\phi, \theta) d\theta_\alpha.\tag{2.95}$$

The deformation gradient is obtained from (2.93), (2.94) and (2.95) as

$$\begin{aligned}\mathbf{a}_\alpha(\phi, \theta) d\theta_\alpha &= \mathbf{F}(\phi, \theta) \mathbf{A}_\alpha(\phi, \theta) d\theta_\alpha \implies \\ \mathbf{a}_\alpha(\phi, \theta) &= \mathbf{F}(\phi, \theta) \mathbf{A}_\alpha(\phi, \theta).\end{aligned}\tag{2.96}$$

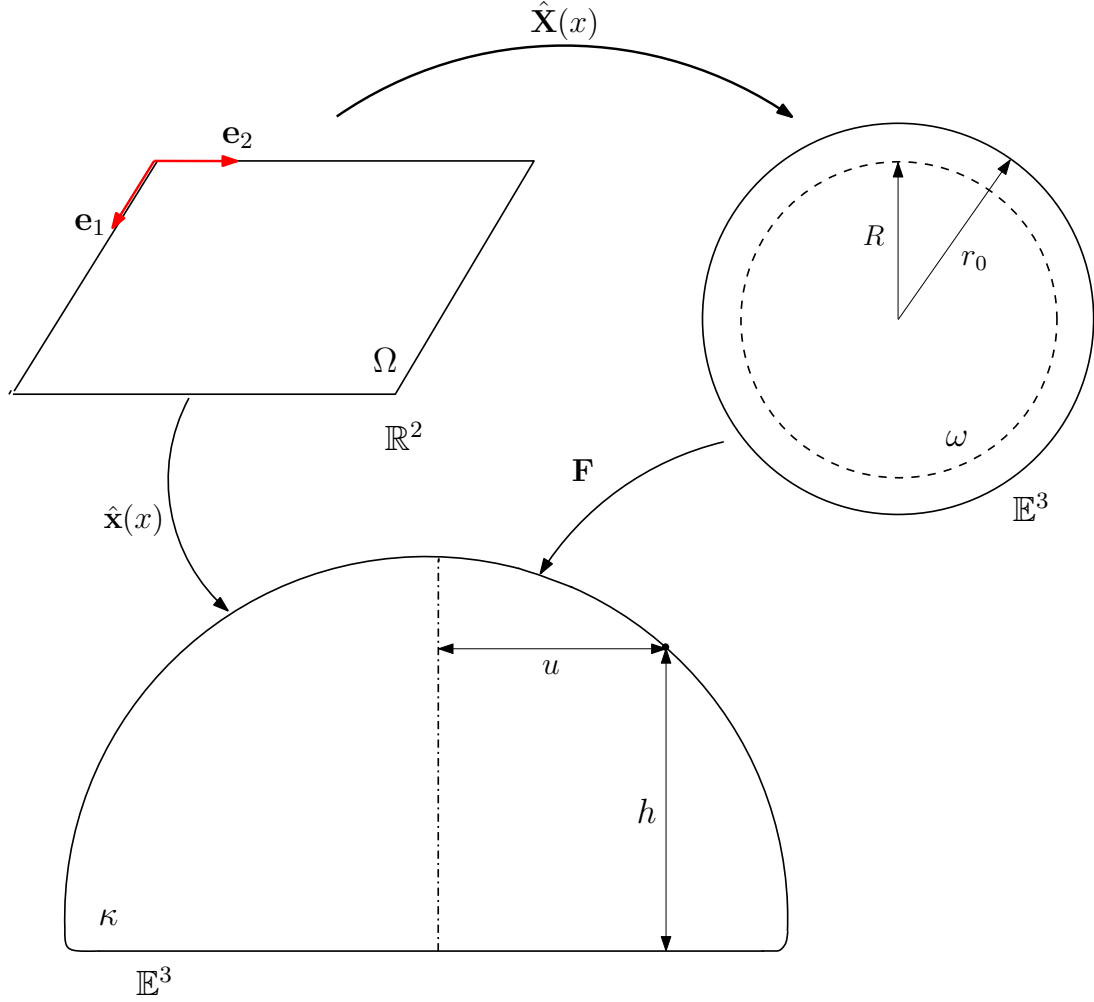


Figure 2.5: Reference (undeformed) and spatial (deformed) configurations mapped by injective immersions and the deformation gradient \mathbf{F} between them.

Now in order to extract the deformation gradient \mathbf{F} , do tensor product of both sides of (2.96) by contravariant basis of reference configuration \mathbf{A}^α

$$\begin{aligned} \mathbf{a}_\alpha(\phi, \theta) \otimes \mathbf{A}^\alpha(\phi, \theta) &= \mathbf{F}(\phi, \theta) \mathbf{A}_\alpha(\phi, \theta) \otimes \mathbf{A}^\alpha(\phi, \theta) \implies \\ \mathbf{F}(\phi, \theta) &= \mathbf{a}_\alpha(\phi, \theta) \otimes \mathbf{A}^\alpha(\phi, \theta), \end{aligned} \quad (2.97)$$

where $\mathbf{A}_\alpha \otimes \mathbf{A}^\alpha = \mathbf{1}$. By substituting the curvilinear basis, (2.80) and (2.84), the deformation gradient becomes as:

$$\mathbf{F} = (u'(\phi) \mathbf{i}(\theta) + h'(\phi) \mathbf{k}) \otimes \frac{1}{R} \mathbf{E}_\phi(\phi, \theta) + u(\phi) \mathbf{j}(\theta) \otimes \frac{1}{R \sin(\phi)} \mathbf{E}_\theta(\theta). \quad (2.98)$$

The relations between bases of spherical coordinate and cylindrical coordinate systems are obtained from Fig.2.6 as

$$\begin{aligned}\mathbf{E}_R(\phi, \theta) &= \sin(\phi)\mathbf{E}_1(\theta) + \cos(\phi)\mathbf{E}_3, \\ \mathbf{E}_\phi(\phi, \theta) &= \cos(\phi)\mathbf{E}_1(\theta) - \sin(\phi)\mathbf{E}_3, \\ \mathbf{E}_\theta(\theta) &= \mathbf{E}_2(\theta),\end{aligned}\tag{2.99}$$

where $\{\mathbf{E}_1(\theta), \mathbf{E}_2(\theta), \mathbf{E}_3\}$ are the orthonormal cylindrical basis of the reference configuration. Use the relation between polar and cylindrical coordinate systems, (2.99), as the substitution for polar basis in (2.98), the deformation gradient tensor \mathbf{F} becomes

$$\mathbf{F} = (u'\mathbf{i} + h'\mathbf{k}) \otimes \frac{1}{R} (\cos(\phi)\mathbf{E}_1 - \sin(\phi)\mathbf{E}_3) + u\mathbf{j} \otimes \frac{1}{R\sin(\phi)}\mathbf{E}_2.\tag{2.100}$$

Consider the representation of the deformation gradient tensor \mathbf{F} in terms of the meridional and hoop (circumferential) principle stretches denoted respectively by $\lambda(\phi)$ and $\mu(\phi)$, yields

$$\mathbf{F}(\phi, \theta) = \lambda(\phi)\mathbf{l}(\phi, \theta) \otimes \mathbf{L}(\phi, \theta) + \mu(\phi)\mathbf{m}(\theta) \otimes \mathbf{M}(\theta),\tag{2.101}$$

where orthonormal vectors $\{\mathbf{l}(\phi, \theta), \mathbf{m}(\theta)\}$ and $\{\mathbf{L}(\phi, \theta), \mathbf{M}(\theta)\}$ successively denote the principle directions at point $\mathbf{x} = \hat{\mathbf{x}}(\phi, \theta)$ on tangential plane to spatial κ and at point $\mathbf{X} = \hat{\mathbf{X}}(\phi, \theta)$ on the tangential plane to the referential ω configurations, such that normal vector to spatial configuration becomes $\mathbf{n}(\phi, \theta) = \mathbf{l}(\phi, \theta) \times \mathbf{m}(\theta)$ (see Fig.2.4) and to the referential configuration is $\mathbf{N}(\phi, \theta) = \mathbf{L}(\phi, \theta) \times \mathbf{M}(\theta)$ (see Fig.2.6).

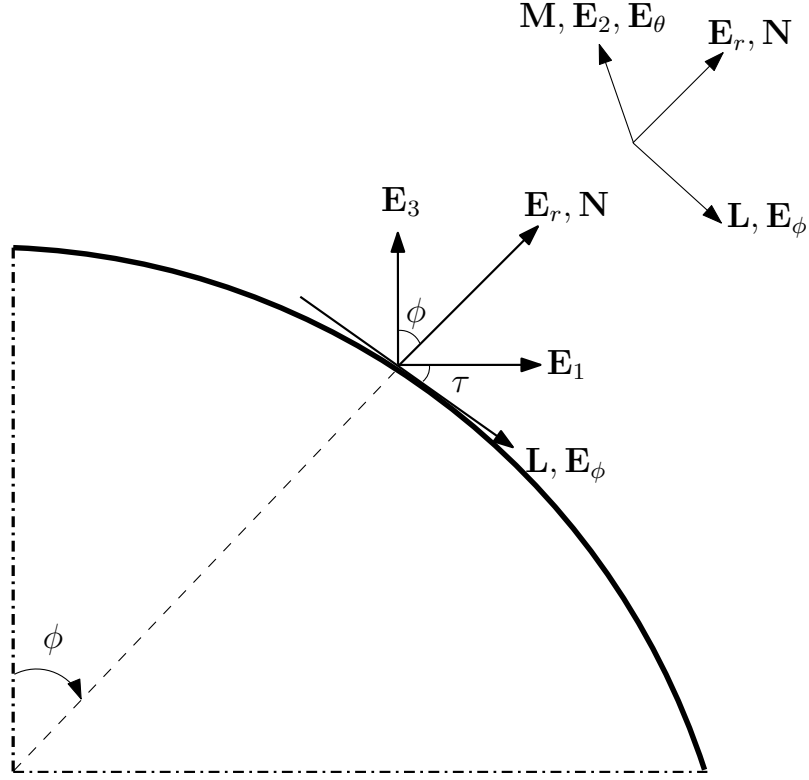


Figure 2.6: The relation between bases in different coordinate systems.

From comparison of (2.100) and (2.101) and by using (2.84)₁ and (2.99)_{2,3}

$$\lambda = \frac{\sqrt{(u')^2 + (h')^2}}{R}, \quad \mu = \frac{u}{R \sin \phi}, \quad \mathbf{l} = \frac{u' \mathbf{i} + h' \mathbf{k}}{\lambda R} = \frac{\mathbf{a}_1}{\lambda R}, \quad (2.102)$$

$$\mathbf{m} = \mathbf{j}, \quad \mathbf{L} = \cos(\phi) \mathbf{E}_1 - \sin(\phi) \mathbf{E}_3 = \mathbf{E}_\phi, \quad \mathbf{M} = \mathbf{E}_2 = \mathbf{E}_\theta.$$

The meridional principle direction, \mathbf{l} , can be represented by the angle $\tau(\phi)$ as illustrated in Fig.2.4

$$\mathbf{l}(\phi, \theta) = \cos(\tau) \mathbf{i} - \sin(\tau) \mathbf{k}. \quad (2.103)$$

The normal unit vector \mathbf{n} is represented in terms of the cylindrical unit vectors \mathbf{i} and \mathbf{j} using the definition of \mathbf{n} as the cross product of tangential unit vectors \mathbf{l} and \mathbf{m} (see Fig.2.4), therefore from (2.102)₄ and (2.103)

$$\mathbf{n}(\phi, \theta) = \mathbf{l} \times \mathbf{m} = (\cos(\tau) \mathbf{i} - \sin(\tau) \mathbf{k}) \times \mathbf{j} \implies$$

$$\mathbf{n}(\phi, \theta) = \sin(\tau) \mathbf{i} + \cos \tau \mathbf{k}. \quad (2.104)$$

The first order nonlinear ordinary differential equations (ODEs), which govern the

geometry of the cell membrane are established by comparison of (2.102)₃ and (2.103) as

$$\boxed{\begin{aligned} u'(\phi) &= \lambda(\phi)R \cos(\tau), \\ h'(\phi) &= -\lambda(\phi)R \sin(\tau). \end{aligned}} \quad (2.105)$$

Before closing this subsection it is worth it to find another representation of the contravariant basis of the spatial configuration. From (2.92) and (2.102)_(1,3,4)

$$\mathbf{a}^1(\phi, \theta) = \frac{\mathbf{1}}{R\lambda}, \quad \mathbf{a}^2(\phi, \theta) = \frac{\mathbf{m}}{u}. \quad (2.106)$$

Considering the developed constitutive equation for the spontaneous areal dilation (2.44), the partial derivatives of the strain energy function (2.18) are obtained as

$$\begin{aligned} \hat{\psi}_{,J_e} &= 2K_m(JJ_{sp}^{-1} - 1), & \hat{\psi}_{,J_e\lambda} &= 2K_m \left(\frac{\mu J_{sp} - \lambda \mu^2 \zeta \rho_r}{J_{sp}^2} \right), \\ \hat{\psi}_{,J_e\mu} &= 2K_m \left(\frac{\lambda J_{sp} - \lambda^2 \mu \zeta \rho_r}{J_{sp}^2} \right), & \hat{\psi}_{,J_e\rho_r} &= -2K_m (JJ_{sp}^{-1})^2 \zeta. \end{aligned} \quad (2.107)$$

2.2.2 Equilibrium condition of the cell

It is notable that, the reference configuration is not usually defined for the analysis of the fluid control volume, since in the case of an open system of a fluid in flow (control volume) there is no fixed amount of a fluid and we are more interested in the flow of a fluid in time and space. However, in the case of a closed system of a stationary fluid without flow, the reference configuration of the fluid is definable and useful [33]. Therefore a fluid-like cell membrane can be considered as a closed system of a fluid without flow, for which the reference configuration is defined here. Due to presence of the receptors on the cell membrane, in the current work a third configuration is considered as natural configuration, which is defined as the configuration of the body in which the strain energy function is minimized. In other words, in natural configuration the stress tensor in all representation forms of Cauchy, first and second Piola stresses vanish and therefore this configuration is also referred to as the stress-free configuration [9, 32]. The natural configuration is considered as the origin for measurement of stresses in the body and usually coincides with the reference configuration, however this coincidence is not the case in here.

The physical quantities and relations can be represented in the form of any defined

configuration, for instance the derived Cauchy stress tensor in (2.40) and (2.41) is a representation of the stress distribution, defined as the force per unit area of the spatial configuration, which generates a traction vector \mathbf{t} as the force per unit area of spatial configuration by acting on unit normal vector \mathbf{n} to the spatial configuration, such that the infinitesimal force $d\mathbf{f}$ becomes

$$d\mathbf{f} = \mathbf{t} da = \hat{\mathbf{T}}\mathbf{n} da, \quad (2.108)$$

where da is an infinitesimal area of spatial configuration. The same infinitesimal force $d\mathbf{f}$ can also be represented by the first Piola stress tensor $\hat{\mathbf{P}}$ as

$$d\mathbf{f} = \mathbf{t} da = \hat{\mathbf{P}}\mathbf{N} dA, \quad (2.109)$$

where dA denotes the infinitesimal area in reference configuration and the first Piola stress \mathbf{P} is defined as the force per unit area of the reference configuration, such that acts on the normal unit vector \mathbf{N} to the reference configuration and generates a traction force \mathbf{t} as the force per area of spatial configuration. In the current work, since the spatial configuration is well-defined by the injective immersion (2.81) and curvilinear bases (2.84) and (2.92), therefore we can represent the stress tensor in spacial form as the Cauchy stress \mathbf{T} in order to use the equilibrium equation in spatial form

$$\operatorname{div}_s \hat{\mathbf{T}} + \rho \mathbf{b}_m = \mathbf{0}, \quad (2.110)$$

where the spatial surface divergence operator is well-defined by the contravariant curvilinear basis of spatial configuration (2.92) as $\operatorname{div}_s = (\cdot)_{,\alpha} \cdot \mathbf{a}^\alpha$, such that $(\cdot)_{,\alpha}$ denotes the partial derivative with respect to the independent variable θ^α and \mathbf{b}_m represents the body force and lateral traction per unit mass. However, we can neither define the stress tensor as the force per unit area of the natural configuration, nor express the equilibrium equation in natural form, since we did not introduce any immersion, which geometrically defines the natural configuration and the corresponding curvilinear basis. This means that the deformation gradient \mathbf{F}_e is not geometrically defined between natural and deformed configuration to express the stress tensor in terms of the force per unit natural area. It is worth noting that based on the definition of the natural configuration in where strain energy is minimized and consequently the stress field vanishes, this configuration is the origin of stress measurements. Finally, since in this work the reference configuration is defined for fluid-like cell membrane

by (2.68) the referential representation of the equilibrium equation associated with the first Piola stress \mathbf{P} is used to study the deformation and equilibrium condition of the cell membrane

$$\boxed{\text{Div}_s \hat{\mathbf{P}} + J\mathbf{b} = \mathbf{0}}, \quad (2.111)$$

where Div_s denotes the referential surface divergence operator, defined by contravariant curvilinear basis of the reference configuration (2.80) as $\text{Div}_s = (\cdot)_{,\alpha} \cdot \mathbf{A}^\alpha$ and \mathbf{b} represents the body force and lateral traction per unit spatial area.

In order to use the referential representation of the equilibrium equation (2.111), the first Piola stress tensor $\hat{\mathbf{P}}$ should be derived from Cauchy stress tensor (2.40)

$$\hat{\mathbf{P}} = \hat{\mathbf{T}}\mathbf{F}^* = J\hat{\mathbf{T}}\mathbf{F}^{-T}, \quad (2.112)$$

where $\mathbf{F}^* = J\mathbf{F}^{-T}$ is called the cofactor of deformation gradient tensor \mathbf{F} . Now, from equation of deformation gradient (2.97)

$$\mathbf{F}^{-T}(\phi, \theta) = \mathbf{a}^\alpha(\phi, \theta) \otimes \mathbf{A}_\alpha(\phi, \theta). \quad (2.113)$$

Now, from (2.71), (2.92) and (2.113) in accordance to the (2.102)₂

$$\begin{aligned} \mathbf{F}^{-T} &= \frac{u'\mathbf{i} + h'\mathbf{k}}{u'^2 + h'^2} \otimes (u'\mathbf{i} + h'\mathbf{k}) + \frac{\mathbf{j}}{u} \otimes u\mathbf{j} = \\ &= \frac{\mathbf{l}}{\lambda R} \otimes R\mathbf{L} + \frac{\mathbf{m}}{u} \otimes R \sin(\phi)\mathbf{M} \implies \\ &\mathbf{F}^{-T} = \lambda^{-1}\mathbf{l} \otimes \mathbf{L} + \mu^{-1}\mathbf{m} \otimes \mathbf{M}. \end{aligned} \quad (2.114)$$

Also the areal dilation J is defined as the ratio of the infinitesimal area in spatial configuration da , to the one in reference configuration dA

$$J(\phi) = \frac{da}{dA}. \quad (2.115)$$

By the definition of the determinant operator, $da/dA = \sqrt{\det \mathbf{C}}$, where according to the definition of the right Cauchy-Green deformation tensor $\mathbf{C} = \mathbf{F}^T\mathbf{F}$. Considering the representation of the deformation gradient \mathbf{F} in terms of the principle stretches

and principle directions (2.101)

$$\mathbf{F}^T = \lambda \mathbf{L} \otimes \mathbf{l} + \mu \mathbf{M} \otimes \mathbf{m}. \quad (2.116)$$

Therefore, the right Cauchy-Green deformation tensor \mathbf{C} can be represented by principle stretches and directions, using (2.101) and (2.116)

$$\begin{aligned} \mathbf{C} &= (\lambda \mathbf{L} \otimes \mathbf{l} + \mu \mathbf{M} \otimes \mathbf{m})(\lambda \mathbf{l} \otimes \mathbf{L} + \mu \mathbf{m} \otimes \mathbf{M}) \implies \\ \mathbf{C} &= \lambda^2 \mathbf{L} \otimes \mathbf{L} + \mu^2 \mathbf{M} \otimes \mathbf{M}. \end{aligned} \quad (2.117)$$

From (2.115), (2.117) and $da/dA = \sqrt{\det \mathbf{C}}$ the areal dilation J becomes

$$\begin{aligned} J(\phi) &= \sqrt{\det \mathbf{C}} = \sqrt{\lambda^2(\phi)\mu^2(\phi)} \implies \\ J(\phi) &= \lambda(\phi)\mu(\phi). \end{aligned} \quad (2.118)$$

Therefore, by substitution for Cauchy stress $\hat{\mathbf{T}}$, \mathbf{F}^{-T} and areal dilation J from (2.40), (2.114) and (2.118) into (2.112), the relation for the first Piola stress tensor of an isotropic fluid-like membrane cell is obtained as

$$\begin{aligned} \hat{\mathbf{P}} &= \lambda \mu \frac{d\hat{\psi}(J_e)}{dJ_e} (\lambda^{-1} \mathbf{l} \otimes \mathbf{L} + \mu^{-1} \mathbf{m} \otimes \mathbf{M}) \implies \\ &\boxed{\hat{\mathbf{P}}(\phi, \theta) = \hat{\psi}_{,J_e}(\mu \mathbf{l} \otimes \mathbf{L} + \lambda \mathbf{m} \otimes \mathbf{M})}. \end{aligned} \quad (2.119)$$

where comma in subscript $(\cdot)_{,\alpha}$, represents partial derivative with respect to the subscript term.

The constitutive relation of first Piola stress, (2.119), must satisfy every physical law, including the balance of linear momentum (2.111). The referential surface divergence operator is well-defined by the contravariant curvilinear basis of reference configuration (2.80) as $\text{Div}_s = (\cdot)_{,\alpha} \cdot \mathbf{A}^\alpha$, such that $(\cdot)_{,\alpha}$ denotes the partial derivative with respect to the independent variable $\theta^\alpha = \{\phi, \theta\}$ for $\alpha = \{1, 2\}$. Therefore, from definition of referential surface divergence operator

$$\text{Div}_s \hat{\mathbf{P}}(\phi, \theta) = \left(\hat{\mathbf{P}}(\phi, \theta) \right)_{,\alpha} \cdot \mathbf{A}^\alpha = \hat{\mathbf{P}}_{,\phi} \cdot \mathbf{A}^1 + \hat{\mathbf{P}}_{,\theta} \cdot \mathbf{A}^2. \quad (2.120)$$

By using the constitutive equation of first Piola stress (2.119) and contravariant curvi-

linear basis of reference configuration (2.80)

$$\text{Div}_s \hat{\mathbf{P}}(\phi, \theta) = \left((\mu \hat{\psi}_{,J_e})' + \mu \hat{\psi}_{,J_e} \frac{\cos \phi}{\sin \phi} \right) \frac{\mathbf{1}}{R} + \mu \hat{\psi}_{,J_e} \frac{\mathbf{l}'}{R} - \frac{\lambda}{R \sin \phi} \hat{\psi}_{,J_e} \mathbf{i}. \quad (2.121)$$

In calculation of $\text{Div}_s \hat{\mathbf{P}}$ in (2.121) the following relations were noted

$$\begin{aligned} \mathbf{M}'(\theta), \mathbf{m}'(\theta), (\mu(\phi) \hat{\psi}_{,J_e}(\phi))_{,\theta}, (\lambda(\phi) \hat{\psi}_{,J_e}(\phi))_{,\theta} &= 0, \\ \mathbf{M}_{,\theta}(\theta) = \mathbf{E}_{2,\theta}(\theta) &= -\mathbf{E}_1(\theta), \\ \mathbf{m}_{,\theta}(\theta) = \mathbf{j}_{,\theta}(\theta) &= -\mathbf{i}(\theta). \end{aligned} \quad (2.122)$$

Now, from (2.7), (2.18) and (2.44)

$$\psi = \hat{\psi}(J_e) = \hat{\psi}(J J_{sp}^{-1}) = \hat{\psi}(\lambda(\phi), \mu(\phi), \rho_r(\phi)) = \hat{\psi}(\phi). \quad (2.123)$$

Therefore we can show from chain rule that

$$\hat{\psi}'_{,J_e}(\lambda, \mu, \rho_r) = \hat{\psi}_{,J_e \lambda} \lambda' + \hat{\psi}_{,J_e \mu} \mu' + \hat{\psi}_{,J_e \rho_r} \rho_r'. \quad (2.124)$$

From (2.121) and (2.124)

$$\begin{aligned} \text{Div}_s \hat{\mathbf{P}}(\phi, \theta) = & \quad (2.125) \\ & \left[\mu \hat{\psi}_{,J_e \lambda} \lambda' + (\hat{\psi}_{,J_e} + \mu \hat{\psi}_{,J_e \mu}) \mu' + \left(\hat{\psi}_{,J_e \rho_r} \rho_r' + \hat{\psi}_{,J_e} \frac{\cos(\phi)}{\sin(\phi)} \right) \mu \right] \frac{\mathbf{1}}{R} \\ & + \mu \hat{\psi}_{,J_e} \frac{\mathbf{l}'}{R} - \hat{\psi}_{,J_e} \frac{\lambda}{R \sin(\phi)} \mathbf{i}. \end{aligned}$$

Considering the obtained relation for the divergence of first Piola stress (2.125), the various types of external body force is addressed here. The membrane of the cell experiences three types of distributed forces (body force and lateral traction) on its surface. These three forces include 1) binding force, which is the interaction between mobile receptors on the membrane and fixed ligands on the substrate, 2) fluid pressure force, which is the normal force generated by the pressure of the enclosed fluid inside the cell and is applied to the cell membrane in outward normal direction and 3) surface reaction force, which is a surface force applied in inward normal direction to the membrane along the contact region and is induced by the reaction pressure

of the substrate. One of the external forces applied to the membrane of the cell is the surface traction exerted by the enclosed fluid inside the cell. Since the fluid is enclosed it is considered as a closed system in rest in which the Cauchy stress only includes the static stress and the viscous stress of the fluid vanishes. The static stress of the enclosed fluid is related to the temperature and density of the fluid through some type of equation of state. Since any constitutive equation is required to satisfy the frame-indifference condition, the same calculation process as in (2.23) shows that the static Cauchy stress of the enclosed fluid has a scalar form, which only depends on the spatial density of the fluid as

$$\hat{\mathbf{T}}(\rho_f) = \hat{\mathbf{T}}_{eq}(\rho_f) = p_f(\rho_f)\mathbf{1}, \quad (2.126)$$

where p_f is fluid pressure and ρ_f denotes spatial density of enclosed fluid inside cell. Therefore the associated traction applied by the fluid pressure to the membrane becomes:

$$\mathbf{f}_f(\rho) = p_f(\rho_f)\mathbf{n}. \quad (2.127)$$

Since the weight of the enclosed fluid is ignored then the equilibrium condition of the fluid yields (see (2.110))

$$\text{div } \hat{\mathbf{T}}(\rho_f) = \text{grad } p_f(\rho_f) = \mathbf{0}, \quad (2.128)$$

which means the pressure of the fluid inside the cell is homogeneous. For compressible fluid the pressure, p_f , is a function of the fluid volume dilation J_f , however in the present work we assume that the bulk stiffness of the enclosed fluid is much higher than the membrane stiffness and the incompressibility assumption is appropriate for the enclosed fluid inside the cell. The assumption of incompressibility of the enclosed fluid implies that the pressure function becomes a constant Lagrange multiplier and is not a constitutive quantity of the fluid.

The binding force caused by the interaction between receptors and ligands is one of the distributed forces applied to the surface of the cell membrane. This force can be resolved into two orthogonal components, along the tangential direction \mathbf{l} on the tangential plane to the membrane surface and in the normal direction. The tangential component of this interaction along the tangential plane to the membrane surface drives the receptors toward the substrate and consequently induces the diffusion of the receptors on the membrane. Therefore, the tangential component of the binding

force was considered into diffusion equation of the receptors, (2.65), through introduction of a constitutive equation for the flux vector of the receptors, caused by the receptor-ligand interaction. The normal component of the binding force (receptor-ligand) interaction \mathbf{f}_b^n in (2.57) is directly subjected to the cell membrane and therefore is involved in the deformation of the membrane for which is considered into the equilibrium equation of the membrane (2.111). The normal component of binding force is obtained using (2.52) and (2.57)

$$\begin{aligned}\mathbf{f}_b^n &= (\mathbf{n} \otimes \mathbf{n})\mathbf{f}_b = (\mathbf{f}_b \cdot \mathbf{n})\mathbf{n} = (-f_b \mathbf{k} \cdot \mathbf{n})\mathbf{n} \implies \\ \mathbf{f}_b^n &= -f_b \cos(\tau)\mathbf{n}.\end{aligned}\tag{2.129}$$

The cell is supported by the substrate, which is assumed to be a rigid solid and frictionless, hence the contact traction (force per unit area of the cell spatial configuration) \mathbf{f}_c is normal to the substrate and in the direction opposite to the normal of the membrane surface. Therefore this traction is obtained as

$$\mathbf{f}_c = -p_c \mathbf{n},\tag{2.130}$$

where p_c denotes the contact pressure defined as the force per unit area of the cell spatial configuration. The resultant of body force and lateral tractions exerted on the membrane due to receptor-ligand interaction, enclosed fluid pressure and contact traction is

$$\mathbf{b} = (f_b^n + p_f - p_c) \mathbf{n}\tag{2.131}$$

defined in (2.127), (2.129) and (2.130). Note that the angle τ in (2.129), between the tangential direction \mathbf{l} and horizontal direction (see Fig.2.4), becomes $\tau = \pi$.

Now, by placing (2.125) and (2.131) into referential form of the equilibrium equation, (2.111),

$$\begin{aligned}\left[\mu \hat{\psi}_{,J_e \lambda} \lambda' + (\hat{\psi}_{,J_e} + \mu \hat{\psi}_{,J_e \mu}) \mu' + \left(\hat{\psi}_{,J_e \rho_r} \rho_r' + \hat{\psi}_{,J_e} \cos(\phi) \sin^{-1}(\phi) \right) \mu \right] \frac{\mathbf{l}}{R} \\ + R^{-1} \mu \hat{\psi}_{,J_e} \mathbf{l}' - R^{-1} \sin^{-1}(\phi) \hat{\psi}_{,J_e} \lambda \mathbf{i} + \lambda \mu (p_f - f_b \cos \tau - p_c) \mathbf{n} = \mathbf{0}.\end{aligned}\tag{2.132}$$

Considering the equation of equilibrium (2.132), we are now interested in projections of the equation onto the tangential plane of the membrane surface and also normal to that plane. The projection of the (2.132) onto the tangential plane is obtained by

applying the projection tensor (2.54) to (2.132). It is notable that, since the reference and spatial configurations, respectively defined by injective immersions (2.68) and (2.81), are symmetric in hoop (circumferential) direction, the projection tensor \mathbb{P}_{\parallel} on the membrane surface is only limited to the meridional direction. Hence, by using the covariant and contravariant curvilinear bases of the tangent plane of spatial configuration in (2.102)₃ and (2.106)₁

$$\mathbb{P}_{\parallel} = \mathbf{a}_1 \otimes \mathbf{a}^1 = R\lambda \mathbf{l} \otimes \frac{\mathbf{l}}{R\lambda} = \mathbf{l} \otimes \mathbf{l}. \quad (2.133)$$

The projection of the equilibrium equation (2.132) in the normal direction to the membrane surface is obtained by applying the projection tensor (2.56) to the equilibrium equation. However, we will first find the results of some dot products between unit vectors, which are useful for the rest of calculations. From (2.103)

$$\mathbf{l}'(\phi, \theta) = -\tau' \sin(\tau) \mathbf{i} - \tau' \cos(\tau) \mathbf{k}. \quad (2.134)$$

Therefore

$$\mathbf{l} \cdot \mathbf{l}' = (\cos(\tau) \mathbf{i} - \sin(\tau) \mathbf{k}) \cdot (-\tau' \sin(\tau) \mathbf{i} - \tau' \cos(\tau) \mathbf{k}) = 0. \quad (2.135)$$

From (2.103) and (2.104)

$$\begin{aligned} \mathbf{l} \cdot \mathbf{i} &= \cos(\tau) \mathbf{i} - \sin(\tau) \mathbf{k} \cdot \mathbf{i} = \cos(\tau), \\ \mathbf{l} \cdot \mathbf{k} &= \cos(\tau) \mathbf{i} - \sin(\tau) \mathbf{k} \cdot \mathbf{k} = -\sin \tau, \end{aligned} \quad (2.136)$$

$$\mathbf{l} \cdot \mathbf{n} = \mathbf{l} \cdot (\mathbf{l} \times \mathbf{m}) = 0.$$

Also, from (2.104) and (2.134)

$$\begin{aligned} \mathbf{n} \cdot \mathbf{i} &= (\sin(\tau) \mathbf{i} + \cos \tau \mathbf{k}) \cdot \mathbf{i} = \sin(\tau), \\ \mathbf{n} \cdot \mathbf{k} &= (\sin(\tau) \mathbf{i} + \cos \tau \mathbf{k}) \cdot \mathbf{k} = \cos(\tau), \\ \mathbf{n} \cdot \mathbf{l}' &= (\sin(\tau) \mathbf{i} + \cos \tau \mathbf{k}) \cdot (-\tau' \sin(\tau) \mathbf{i} - \tau' \cos(\tau) \mathbf{k}) = -\tau'. \end{aligned} \quad (2.137)$$

Now, the projection of the equilibrium equation (2.132) into tangential direction of the membrane is obtained using the projection tensor (2.133) in accordance to the

(2.135), (2.136) and (2.137)

$$\begin{aligned} & \left[\mu \hat{\psi}_{,J_e} \lambda' + (\hat{\psi}_{,J_e} + \mu \hat{\psi}_{,J_e \mu}) \mu' + \left(\hat{\psi}_{,J_e \rho_r} \rho_r' + \hat{\psi}_{,J_e} \cos(\phi) \sin^{-1}(\phi) \right) \mu \right. \\ & \quad \left. - \lambda \hat{\psi}_{,J_e} \cos(\tau) \sin^{-1}(\phi) \right] R^{-1} = 0, \end{aligned} \quad (2.138)$$

where by (2.102)₂ and (2.105)₁

$$\mu'(\phi) = \frac{\lambda \cos(\tau) - \mu \cos(\phi)}{\sin(\tau)}. \quad (2.139)$$

Hence, another first order nonlinear ODE (see (2.105)) is obtained from (2.138) and (2.139), which governs the variation of meridional principle stretch λ in the cell membrane

$$\begin{aligned} \lambda'(\phi) &= (\mu \hat{\psi}_{,J_e} \lambda)^{-1} \\ & \left[\lambda \hat{\psi}_{,J_e} \cos(\tau) \sin^{-1}(\phi) - \sin^{-1}(\phi) (\hat{\psi}_{,J_e} + \mu \hat{\psi}_{,J_e \mu}) (\lambda \cos(\tau) - \mu \cos(\phi)) \right. \\ & \quad \left. - \mu (\hat{\psi}_{,J_e \rho_r} \rho_r' + \hat{\psi}_{,J_e} \cos(\phi) \sin^{-1}(\phi)) \right]. \end{aligned} \quad (2.140)$$

The projection of the equilibrium equation (2.132) in the normal direction \mathbf{n} to the membrane surface is obtained by applying the projection tensor (2.56) to the equilibrium equation

$$\boxed{\tau'(\phi) = (\mu \hat{\psi}_{,J_e}) \left[R \lambda \mu (p_f - p_c - f_b \cos(\tau)) - \lambda \hat{\psi}_{,J_e} \sin(\tau) \sin^{-1}(\phi) \right]}. \quad (2.141)$$

2.2.3 Initial fluid pressure

The resistance of the cell membrane to the change in the curvature is negligible, which supports the application of the membrane theory in analysis of the membrane equilibrium. In this case, the role of the fluid pressure enclosed within the cell in bending resistance of the membrane is significant. This means that, the pressure of the enclosed fluid in the form of a surface traction exerts on the membrane and controls the deformation of the cell. Additionally, the fluid pressure plays a significant role in avoiding the wrinkles in cell membrane. Since the wrinkling of the cell membrane is not of interest, it is required first to make sure that the fluid pressure inside the

cell is high enough to prevent any wrinkles. In order to control the pressure of the enclosed fluid, cell is inflated from the referential radius of R to the spatial radius of $r_o \geq R$ (see Figs.2.3 and 2.5). Since the inflation of the reference configuration of the cell is a motion without any distortion in which the spherical shape of the cell preserves, the inflated cell is axisymmetric such that the two meridional λ and hoop (circumferential) μ principle stretches are equal, $\lambda = \mu$, at every point, and therefore from (2.102)₂

$$\begin{aligned} \mu &= \frac{u}{R \sin(\phi)} = \frac{r_0 \sin(\phi)}{R \sin(\phi)} = \frac{r_0}{R} \implies \\ \mu &= \lambda = \frac{r_0}{R}, \end{aligned} \tag{2.142}$$

which means the only requirement to guarantee positive stretches and avoid wrinkles in a spherical membrane is to inflate the cell to a high enough radius. In the absence of the body forces and due to the axisymmetry, at any point

$$\phi = \tau(\phi) \implies \tau'(\phi) = 1. \tag{2.143}$$

Now fluid pressure of the inflated cell is obtained in the absence of the body forces from application of (2.141) to the free region (non-adhesion region) under the conditions of (2.142) and (2.143), where the contact pressure p_c vanishes from (2.141) in free region. Hence

$$p_{f_0}(\phi) = \frac{2}{R\lambda} \hat{\psi}_{,J_e}. \tag{2.144}$$

Since for the inflated, spherical cell the principle stretches $\lambda = \mu = r_0/R$, the fluid pressure of the inflated cell p_{f_0} is obtained by using (2.44) and (2.107)₁

$$\boxed{p_{f_0}(\phi) = \frac{4K_m}{r_0} \left(\frac{r_0^2}{R^2 + \zeta \rho_r r_0^2} - 1 \right)}. \tag{2.145}$$

2.2.4 Initial contact pressure

The contact force between the cell and substrate is the reaction of the substrate to the cell membrane, which is applied in adhesion region (contact region) of the cell. Contact force as one of the external forces applied to the cell membrane is involved in deformation and final equilibrium configuration of the cell. The contact traction \mathbf{f}_c , in (2.130), as the force per unit area of the cell spatial configuration, is defined via contact pressure p_c . The contact pressure p_c is the reaction force of the substrate to the cell, per unit area of the spatial configuration. The contact pressure is obtained

by application of the (2.141) to the contact region (adhesion region) of the cell, where $\tau = \pi$ and $\tau'(\phi) = 0$ for $\phi_c \leq \phi \leq \pi$ (ϕ_c is the contact spreading front in Fig.2.4)

$$p_c = p_f + f_b. \quad (2.146)$$

As (2.146) shows the influences of both pressures of enclosed fluid and receptor-ligand interaction balance the contact pressure induced by the reaction of the substrate. If consider the reference configuration of the spherical cell in the absence of the body forces, then the binding traction f_b vanishes and (2.146) yields

$$p_{c0} = p_{f0}, \quad (2.147)$$

which means the fluid and contact pressures are equal for the reference configuration of the spherical cell in the absence of the body forces.

2.2.5 Receptor diffusion on the cell

As discussed before, the presence of the electrostatic charges on the integrins induces an electrostatic repulsive interaction between integrins, which attempts to push them to the farthest distance possible from others. The ligand proteins are nonpolar molecules, which are polarized within the electrostatic field of the charged integrins. This charge-induced dipole interaction between receptors and ligands also controls the migration of the receptors on the membrane by attracting the receptors toward the substrate. Consequently, the diffusion and final distribution of the receptors on the membrane are affected by the receptor-receptor and receptor-ligand interactions.

In this work, the flux of receptors due to the receptor-receptor interaction is approximated by the Fick's law, which is a linear constitutive equation with respect to the gradient of receptor density (see (2.61)). The tangential component of the receptor-ligand interaction along the tangential plane to the membrane surface is considered to drive the receptors toward the substrate and consequently induce the diffusion of the receptors on the membrane. Therefore a constitutive equation was proposed based on the role of binding force in diffusion of the receptors, in which receptor flux is dependent on the tangential component of the binding force (see (2.62)). Since any constitutive equation has to satisfy the laws of physics, the proposed relation in (2.63) is required to satisfy the continuity equation in (2.60), which guarantees the conservation of receptors locally. Therefore the continuity equation of the receptor,

(2.60), after substitution of the constitutive relation for receptor flux yielded (2.65). Now, since the reference and spatial configurations, respectively defined by injective immersions (2.68) and (2.81), are symmetric in hoop (circumferential) direction, the projection tensor \mathbb{P}_{\parallel} on the membrane surface is only limited to the meridional direction. Hence, by using the obtained projection tensor (2.133) for the cell membrane with hoop (circumferential) symmetry, the receptor diffusion equation becomes

$$\begin{aligned} M(\mathbf{1} \otimes \mathbf{1})\mathbf{f}_b - D \operatorname{grad}_s(\rho_r) &= \mathcal{C} \quad \implies \\ M(\mathbf{f}_b \cdot \mathbf{1})\mathbf{1} - D \operatorname{grad}_s(\rho_r) &= \mathcal{C}. \end{aligned} \tag{2.148}$$

Due to the axisymmetry of the geometry of the cell the diffusion of the receptors vanishes at $\phi = 0$ and $\phi = \pi$. Therefore $\mathcal{C} = 0$ at any point on the cell such that

$$M(\mathbf{f}_b \cdot \mathbf{1})\mathbf{1} = D \operatorname{grad}_s(\rho_r). \tag{2.149}$$

Now considering the definition of the spatial surface gradient operator $\operatorname{grad}_s(\cdot) = (\cdot)_{,\alpha} \otimes \mathbf{a}^\alpha$ and (2.52) and (2.136)₂

$$\begin{aligned} D(\rho_{r,\phi}(\phi)\mathbf{a}^1 + \rho_{r,\theta}(\phi)\mathbf{a}^2) &= -Mf_b(\mathbf{k} \cdot \mathbf{1}) \quad \implies \\ D\rho'_r \mathbf{a}^1 &= Mf_b \sin(\tau)\mathbf{1}. \end{aligned} \tag{2.150}$$

Now from (2.106), a first order nonlinear ODE is obtained, which governs the diffusion of the receptors on the cell membrane

$$\boxed{\rho'_r(\phi) = \frac{MR}{D}\lambda f_b \sin \tau.} \tag{2.151}$$

In the current work, a system of five coupled nonlinear first order ordinary differential equations comprises of (2.105), (2.140), (2.141) and (2.151) governs the equilibrium behaviors of the membrane configuration and receptor diffusion. This system of governing equations is first nondimensionalized in the next section, before it is solved numerically for the adhesion and deformation responses of the cell.

2.2.6 Nondimensionalized formulation

Dimensionless quantities are widely used in science and engineering to eliminate the dependency of the relations and results on a particular choice of units. Nondimensionalization leads to extensive applications of relations disregard of any units. Next, by a systematic nondimensionalization process all the quantities and equations are made dimensionless. Here, the over bar denotes nondimensionalized quantities. In order to nondimensionalize, recall that a spherical cell of radius R was considered as the referential configuration and then this cell was inflated to a sphere of radius $r_0 \geq R$, yielding the principle stretches $\lambda = \mu = r_0/R$ to the cell membrane (see (2.142)). The dimensionless inflation radius is defined as

$$\bar{r}_0 = \frac{2r_0}{R}. \quad (2.152)$$

It is convenient to nondimensionalize the lengths in relations by the length $2r_0$, which is the diameter of the inflated cell, such that

$$\bar{u}(\phi) = \frac{u}{2r_0}, \quad \bar{h}(\phi) = \frac{h}{2r_0}. \quad (2.153)$$

Therefore the dimensionless form of (2.105) is

$$\bar{u}' = \frac{\lambda}{\bar{r}_0} \cos(\tau), \quad \bar{h}' = -\frac{\lambda}{\bar{r}_0} \sin(\tau). \quad (2.154)$$

Although the meridional and circumferential principle stretches λ and μ , are naturally dimensionless by their definitions, the principle stretches in (2.102)_{1,2} can now be represented using the dimensionless terms as

$$\lambda = \bar{r}_0 \sqrt{(\bar{u}')^2 + (\bar{h}')^2}, \quad \mu = \frac{\bar{r}_0 \bar{u}}{\sin(\phi)}. \quad (2.155)$$

The strain energy function (2.18) and its partial derivatives (2.107) are nondimensionalized as

$$\bar{\psi}(J_e) = \frac{\hat{\psi}(J_e)}{K_m} = (J_e - 1)^2, \quad (2.156)$$

$$\begin{aligned} \bar{\psi}_{,J_e} &= \frac{\psi_{,J_e}}{K_m} = 2(JJ_{sp}^{-1} - 1), & \bar{\psi}_{,J_e\lambda} &= \frac{\psi_{,J_e\lambda}}{K_m} = 2 \left(\frac{\mu J_{sp}^{-\lambda} \mu^2 \bar{\zeta} \bar{\rho}_r}{J_{sp}^2} \right), \\ \bar{\psi}_{,J_e\mu} &= \frac{\psi_{,J_e\mu}}{K_m} = 2 \left(\frac{\lambda J_{sp}^{-\lambda^2} \mu \bar{\zeta} \bar{\rho}_r}{J_{sp}^2} \right), & \bar{\psi}_{,J_e\bar{\rho}_r} &= \frac{\psi_{,J_e\bar{\rho}_r}}{K_m} = -2 (JJ_{sp}^{-1})^2 \bar{\zeta}, \end{aligned} \quad (2.157)$$

The Cauchy stress tensor of the membrane (2.41) is nondimensionalized as

$$\bar{\mathbf{T}}(J_e) = \bar{p}_m(J_e)\mathbf{1}, \quad \bar{p}_m(J_e) = \frac{\hat{p}_m(J_e)}{K_m} = 2(J_e - 1). \quad (2.158)$$

The dimensionless receptor density is defined as

$$\bar{\rho}_r = \frac{\rho_r}{\rho_{r_0}}, \quad (2.159)$$

where ρ_{r_0} is the homogeneous initial receptor density on the inflated membrane, such that

$$\rho_{r_0} = \frac{N_r}{4\pi r_0^2}, \quad (2.160)$$

and N_r is the total number of receptors. The spontaneous area dilation in (2.44) can be expressed in terms of the dimensionless parameters

$$J_{sp}(\bar{\rho}_r) = 1 + \bar{\zeta}J\bar{\rho}_r, \quad (2.161)$$

where $\bar{\zeta} = \zeta\rho_{r_0}$ is the dimensionless coefficient of spontaneous area dilation. The fluid pressure of the inflated spherical cell (2.145) is represented in terms of the dimensionless parameters by using (2.144), (2.157)₁ and the representation of the principle stretches for inflated, spherical cell in terms of the dimensionless radius $\lambda = \mu = r_0/R = \bar{r}_0/2$ (see (2.152))

$$p_{f_0} = \frac{8\gamma_1}{\bar{r}_0} \left(\frac{\bar{r}_0^2}{4 + \bar{\zeta}\bar{r}_0^2} - 1 \right), \quad (2.162)$$

where $\gamma_1 = K_m/R$ is a material parameter of the membrane. The fluid pressure p_f is nondimensionalized by the fluid pressure of the spherical inflated cell (2.162)

$$\bar{p}_f = \frac{p_f}{p_{f_0}}, \quad (2.163)$$

The receptor-ligand binding force (2.52) is nondimensionalized by introducing the binding parameter $\gamma_2 = C\rho_{r_0}/(2r_0)^5$

$$\bar{f}_b = \frac{f_b}{\gamma_2} = (\bar{K}\bar{r} + 1) \left((\bar{K}\bar{r} + 1)^2 + 1 \right) \bar{\rho}_{rl} \frac{e^{-2\bar{K}\bar{r}}}{\bar{r}^5}, \quad (2.164)$$

where $\bar{K} = 2r_0K$ and $\bar{\rho}_{rl} = \rho_{rl}/\rho_{r_0}$ are respectively dimensionless Debye length and density of actively interacting receptors with ligands in (2.53). The dimensionless distance $\bar{r} = \bar{h} + \bar{h}_0$ is defined by using (2.153)₂. It is notable that the dimension of the binding parameter γ_2 can be verified by

$$[\gamma_2] = \frac{[C][\rho_{r_0}]}{[r_0]^5} = \frac{[N_b\alpha(Ze)^2/(\epsilon\epsilon_0)^2][\rho_{r_0}]}{[r_0]^5}. \quad (2.165)$$

Considering the dimension of each term in (2.165) [38]

$$\begin{aligned} [\alpha] &= [Coul]^2[L]^2[J]^{-1}, & [e] &= [Coul], & [\rho_r] &= [L]^{-2}, \\ [\epsilon_0] &= [Coul]^2[L]^{-1}[J]^{-1}, & [r_0] &= [L], & [N_b], [Z], [\epsilon] &: \text{Dimensionless}, \end{aligned} \quad (2.166)$$

where $[Coul]$, $[L]$ and $[J]$ respectively denote the dimensions of the Coulomb, length and Joule. According to the dimension of each term in (2.166) the dimension of the binding parameter γ_2 in (2.165) is identical to the dimension of the binding force \mathbf{f}_b in (2.52) and body force \mathbf{b} in equilibrium equation (2.111), as force per unit spatial area

$$[\gamma_2] = [FL^{-2}], \quad (2.167)$$

where $[F]$ denotes the dimension of the force. Finally, the dimensionless forms of the equilibrium equation in (2.140),(2.141) and the diffusion equation (2.38) can be similarly obtained as

$$\begin{aligned} \lambda' &= \frac{\lambda\bar{\psi}_{,J_e} \cos \tau - (\bar{\psi}_{,J_e} + \mu\bar{\psi}_{,J_e\mu}) (\lambda \cos \tau - \mu \cos \phi) - \mu (\bar{\psi}_{,J_e\bar{\rho}_r}\bar{\rho}'_r \sin \phi + \bar{\psi}_{,J_e} \cos \phi)}{\mu\bar{\psi}_{,J_e\lambda} \sin \phi}, \\ \tau' &= \frac{\lambda}{\mu\bar{\psi}_{,J_e}} \left(\frac{8}{\bar{r}_0} \mu \left(\frac{\bar{r}_0^2}{4 + \bar{\zeta}\bar{r}_0^2} - 1 \right) (\bar{p}_f - \bar{p}_c) - \bar{\gamma}\mu\bar{f}_b \cos \tau - \bar{\psi}_{,J_e} \frac{\sin \tau}{\sin \phi} \right), \\ \bar{\rho}'_r &= \gamma_3\lambda\bar{f}_b \sin \tau, \end{aligned} \quad (2.168)$$

where

$$\bar{\gamma} = \frac{\gamma_2}{\gamma_1} = \frac{RC\rho_{r_0}}{K_m(2r_0)^5}, \quad \gamma_3 = \frac{MRC}{D(2r_0)^5} \quad (2.169)$$

are dimensionless parameters such that the former one is the ratio of binding and membrane characteristics and the latter relation is the reciprocal diffusion parameter. The same procedure as for (2.146) is applied to the dimensionless representation

of τ' , (2.168)₂, in contact region (adhesion region) of the cell, where $\tau = \pi$ and $\tau'(\phi) = 0$ for $\phi_c \leq \phi \leq \pi$ (ϕ_c is the contact spreading front in Fig.2.4), to obtain the nondimensionalized contact pressure \bar{p}_c

$$\bar{p}_c = \bar{p}_f + \frac{\bar{r}_0 \bar{\gamma}}{8} \left(\frac{\bar{r}_0^2}{4 + \bar{r}_0^2 \bar{\zeta}} - 1 \right)^{-1} \bar{f}_b. \quad (2.170)$$

Based on the previous calculations, equations (2.154), (2.168) present the dimensionless form of a system of five coupled nonlinear first order ODEs. These equations are simplified at contact and free regions of the membrane in accordance with the specific conditions in those regions. The flatness of contact region parametrized by $\phi_c < \phi < \pi$ (where ϕ_c denotes the contact spreading front in Fig.2.4) rationalizes that $\tau(\phi) = \pi$, $h'(\phi) = 0$ and according to (2.168)₃, $\bar{\rho}'_r(\phi) = 0$, which implies that the receptor density is homogenous in the contact region. It is notable that the resultant nondimensionalized adhesion force, \bar{F}_{ad} , which is an upper bound of the required force for detaching the cell from substrate, is

$$\bar{F}_{ad} = \int_{s_l} \bar{f}_b da, \quad (2.171)$$

where s_l denotes the lower region of the membrane that ligand-receptor interaction occurs. The global equilibrium of the cell implies that the adhesion force is balanced by the contact force. Hence, the resultant adhesion force can be conveniently obtained by

$$\bar{F}_{ad} = \int_{s_c} \bar{p}_c da, \quad (2.172)$$

where the right hand side represents the resultant contact force (see (2.170)) and s_c is the contact region of the membrane. Then, since the contact pressure, \bar{p}_c , is homogenous in contact region, the adhesion force is obtained from (2.172) and (2.170) as

$$\bar{F}_{ad} = \bar{p}_c \pi \bar{u}_c^2, \quad (2.173)$$

where $\bar{u}_c = u_c/2r_0$. It is worth noting that the contact pressure vanishes from equation (2.168)₂ within free region.

2.2.7 Numerical Solution

The system of five coupled nonlinear first order ODEs, (2.154) and (2.168), is solved by consideration of following boundary conditions (BCs)

$$\bar{u}(0) = 0, \quad \tau(0) = 0, \quad \bar{u}(\pi) = 0, \quad \tau(\pi) = \pi, \quad \bar{h}(\pi) = 0 \quad (2.174)$$

as a boundary value problem (BVP). Since the BCs are known at either beginning or end points of the domain, the BVP can be solved numerically using the Shooting method. In this method a BVP is converted to an initial value problem (IVP) in which the known (BCs) at the beginning points are considered as the initial values for numerical method and the rest of unknown initial values are guessed. Then the system is solved and the solutions obtained at the end point of domain are compared with the known values of BCs there. An accurate solution is achieved by sufficiently repeating the process until the numerical solutions agree with the boundary conditions at the end point of the domain. In this work fourth order Runge-Kutta method, which is a single-step, explicit technique, is applied to the multiple shooting method to find the solutions for every point of membrane. To use multiple shooting method the domain of convected coordinate ϕ is meshed into $(n + 1)$ points $\{\phi_1 = 0, \phi_2, \dots, \phi_i = \frac{\pi}{2}, \dots, \phi_{n+1} = \pi\}$ and then the known values of BCs at both top pole $\phi = 0$ and bottom pole $\phi = \pi$ are considered as the initial values of the multiple shooting method. As mentioned before 4th order Runge-Kutta technique is implemented to start from both top and bottom poles and solve the system of ODEs finding the values at next points. Since there is not any transition in material and physical conditions at the midpoint of the membrane $\phi = \frac{\pi}{2}$, the behavior of the motion $\mathbf{x}(\mathbf{X})$ and fields $u(\phi)$, $h(\phi)$, $\lambda(\phi)$, $\tau(\phi)$ and $\rho_r(\phi)$ are smooth. Therefore to prevent any jump discontinuity the jump conditions must satisfy $[[u(\pi/2)]] = [[h(\pi/2)]] = [[\lambda(\pi/2)]] = [[\tau(\pi/2)]] = [[\rho_r(\pi/2)]] = 0$ where $[[f]] = f^+ - f^-$.

Furthermore, the incompressibility assumption of the enclosed fluid compels the constancy of volume, which imposes a constraint on the solution. The initial volume of the cell related to the reference configuration (undeformed cell) is

$$V_0 = \frac{4}{3}\pi r_0^3. \quad (2.175)$$

Using the same length of $2r_0$ as in (2.153) to nondimensionalized the initial volume

$$\bar{V}_0 = \frac{V_0}{(2r_0)^3} = \frac{\pi}{6}. \quad (2.176)$$

The volume of the deformed cell is obtained using the equation for volume of a conical frustum. The volume of a conical frustum of the height h and radius $r(z)$, where z is measured along the height is

$$V = \pi \int_0^h r^2(z) dz, \quad r(z) = R_1 + (R_2 - R_1) \frac{z}{h}, \quad (2.177)$$

where R_1 and R_2 are respectively the radius of the larger and smaller basis of frustum. Using the formula of conical frustum, (2.177), the volume of an infinitesimal frustum at height $0 < h(\phi_i) < h(0)$, where $0 < \phi_i < \pi$, becomes

$$V = \pi \int_{h_{i+1}}^{h_i} \left[u_i + (u_{i+1} - u_i) \frac{z}{h_i - h_{i+1}} \right] dz = \frac{\pi(h_i - h_{i+1})}{3} (u_i^2 + u_i u_{i+1} + u_{i+1}^2), \quad (2.178)$$

where $u_i = u(\phi_i)$ and $h_i = h(\phi_i)$. Considering (2.178), the volume of the deformed cell is

$$V = \frac{\pi}{3} \sum_{i=1}^m (u_{i+1}^2 + u_{i+1} u_i + u_i^2) (h_i - h_{i+1}), \quad (2.179)$$

where m denotes the number of infinitesimal conical frustum. According to (2.153), the dimensionless volume of enclosed fluid \bar{V} can be evaluated numerically by

$$\bar{V} = \frac{V}{(2r_0)^3} = \frac{\pi}{3} \sum_{i=1}^m (\bar{u}_{i+1}^2 + \bar{u}_{i+1} \bar{u}_i + \bar{u}_i^2) (\bar{h}_i - \bar{h}_{i+1}). \quad (2.180)$$

In addition, since the cell membrane is a closed system with constant number of receptors the total receptor numbers must be preserved. According to the spherical shape of the cell reference configuration, the initial number of the receptors is

$$N_0 = 4\pi r_0^2 \rho_{r_0}. \quad (2.181)$$

The number of receptors on the spatial (deformed) configuration is calculated through the lateral surface of the conical frustum. Consider a infinitesimal lateral surface of

the deformed cell membrane as dS at the height of $h(\phi)$ such that $0 < \phi < \pi$, then

$$S = \int_{\kappa} dS, \quad dS \approx 2\pi u \sqrt{(du)^2 + (dh)^2}. \quad (2.182)$$

Since $du(\phi) = \partial u(\phi)/\partial \phi d\phi$ and $dh(\phi) = \partial h(\phi)/\partial \phi d\phi$

$$S = \int_0^\pi 2\pi u \sqrt{(u')^2 + (h')^2} d\phi. \quad (2.183)$$

The infinitesimal lateral surface dS_i at $0 < \phi_i < \pi$ is approximated using the finite difference method as

$$dS_i = \pi(u_i + u_{i+1}) \sqrt{(u_{i+1} - u_i)^2 + (h_i - h_{i+1})^2}, \quad (2.184)$$

where the subscript i shows the associated parameter to $0 < \phi_i < \pi$. Therefore, the lateral surface of the cell, (2.182) and (2.183), is approximated using the finite difference method as

$$S = \sum_{i=1}^m \pi(u_i + u_{i+1}) \sqrt{(u_{i+1} - u_i)^2 + (h_i - h_{i+1})^2}. \quad (2.185)$$

Total number of receptors on deformed configuration N is calculated as

$$N = \sum_{i=1}^m \pi \rho_{r_i} (u_i + u_{i+1}) \sqrt{(u_{i+1} - u_i)^2 + (h_i - h_{i+1})^2}, \quad (2.186)$$

which can be represented in terms of the dimensionless parameters as

$$N = (2r_0)^2 \pi \rho_{r_0} \sum_{i=1}^m \bar{\rho}_{r_i} (\bar{u}_{i+1} + \bar{u}_i) \sqrt{(\bar{u}_i - \bar{u}_{i+1})^2 + (\bar{h}_i - \bar{h}_{i+1})^2}. \quad (2.187)$$

According to the above discussion, in order to use the multiple shooting method eight numbers of unknowns λ_B , ρ_{r_B} , h_T , λ_T , ρ_{r_T} , ϕ_c , p_f and ϕ_s are required to be initially guessed, where subscripts B and T are respectively associated to the $\phi = \pi$ and $\phi = 0$. The numerically obtained solutions for u , h , λ , τ and ρ_r are checked for discontinuity at $\phi = \pi/2$ as $[[u(\pi/2)]] = [[h(\pi/2)]] = [[\lambda(\pi/2)]] = [[\tau(\pi/2)]] = [[\rho_r(\pi/2)]] = 0$. Additionally, due to the incompressibility of the enclosed fluid within

cell, the volume of the cell should be preserved

$$\left| 1 - \frac{\bar{V}}{V_0} \right| \approx 0, \quad (2.188)$$

where $|\cdot|$ generates the absolute value. The conservation of number of receptors is checked as the seventh criterion in shooting method for the accuracy of the results

$$\left| 1 - \frac{N}{N_0} \right| \approx 0. \quad (2.189)$$

As the eighth checking criterion for shooting method, u_{max} should always occur at ϕ in which $\tau(\phi) = \pi/2$ (see (2.154)). Table 2.2 presents the summary of the BVP, which is solved numerically. The numerical results of the cell adhesion and deformation studied by the developed models will be presented in next chapter.

Table 2.2: Summary of the five nonlinear first order ODEs and the boundary conditions, which govern the deformation of the cell and diffusion of the receptors on the membrane.

ODEs	Equations
$\bar{u}' = \frac{\lambda}{\bar{r}_0} \cos(\tau)$	(2.154)
$\bar{h}' = -\frac{\lambda}{\bar{r}_0} \sin(\tau)$	(2.154)
$\lambda' = \frac{\lambda \bar{\psi}_{,J_e} \cos \tau - (\bar{\psi}_{,J_e} + \mu \bar{\psi}_{,J_e} \mu) (\lambda \cos \tau - \mu \cos \phi) - \mu (\bar{\psi}_{,J_e} \bar{\rho}'_r \sin \phi + \bar{\psi}_{,J_e} \cos \phi)}{\mu \bar{\psi}_{,J_e} \lambda \sin \phi}$	(2.168)
$\tau' = \frac{\lambda}{\mu \bar{\psi}_{,J_e}} \left(\frac{8}{\bar{r}_0} \mu \left(\frac{\bar{r}_0^2}{4 + \zeta \bar{r}_0^2} - 1 \right) (\bar{p}_f - \bar{p}_c) - \bar{\gamma} \mu \bar{f}_b \cos \tau - \bar{\psi}_{,J_e} \frac{\sin \tau}{\sin \phi} \right)$	(2.168)
$\bar{\rho}'_r = \gamma_3 \lambda \bar{f}_b \sin \tau$	(2.168)
BCs	Equations
$\bar{u}(0) = 0, \quad \tau(0) = 0, \quad \bar{u}(\pi) = 0, \quad \tau(\pi) = \pi, \quad h(\pi) = 0$	(2.174)
Constraints	Equations
$[[u(\pi/2)]] = [[h(\pi/2)]] = [[\lambda(\pi/2)]] = [[\tau(\pi/2)]] = [[\rho_r(\pi/2)]] = 0$	
$\frac{\bar{V}}{V_0} = 1$	(2.188)
$\frac{N}{N_0} = 1$	(2.189)
$u(\phi_m) = u_{max} \quad \text{at} \quad \tau(\phi_m) = \pi/2$	

Chapter 3

Results and Discussion

Given the vast range of data on cell characteristics and size, available in the literature, a small inflated cell with radius of $r_0 = 12.5 \text{ nm}$ [2], inflation of $r_0 = 1.5R$ and contact distance of $h_0 = 9 \text{ nm}$ [54] from the substrate is considered to investigate the suggested model. The following parameters are used $K_m = 0.1 \text{ N/m}$ [38, 56], receptor diffusivity $D = 10^{-14} \text{ m}^2/\text{sec}$ [35, 40] and mobility of receptors $M = 10^3 \text{ m/Nsec}$. In accordance with the molecular structure of the fibronectin proteins ($\text{C}_{47}\text{H}_{74}\text{N}_{16}\text{O}_{10}$), the electronic polarizability α_0 of the nonpolar atoms and bonds, tabulated in [38] and the relation between total polarizability α with α_0 , the constitutive parameter $C = 1.17 \times 10^{-52} \text{ Nm}^5$ is obtained for the electrolyte of water at room temperature with assumed $N_b = 20$ for the number of weak noncovalent sub-bonds between one receptor and a ligand. The coefficient of spontaneous areal dilation, ζ , is taken to be the cross-section area of a single receptor. The cross-sectional area of a single receptor is $\zeta = 5.0 \times 10^{-18} \text{ m}^2$ [2], density of the receptors on inflated cell membrane is taken as $\rho_{r_0} = 10^{17} \text{ m}^{-2}$ [54] and Debye length for the electrolyte of water is about $1 \mu\text{m}$ [38]. Note that in the current work the set of sizes and characteristics described above is addressed as the "original state" of the cell, when no receptor-ligand interactions exist. Considering such a cell, Fig.3.1 shows the equilibrium configurations of the cell for various ligand densities on the substrate. In the absence of binding force, the membrane only undergoes homogenous expansion, due to the enclosed fluid pressure, which sustains the cell spherical configuration. The presence of ligands on the substrate leads to the interaction between receptors and ligands that alters the receptor distribution on the membrane by driving them toward the substrate (see Fig.3.2). As the density of ligands on the substrate increases the receptor-ligand interaction grows accordingly (see (2.52)), which escalates the deformation of the cell, decrease

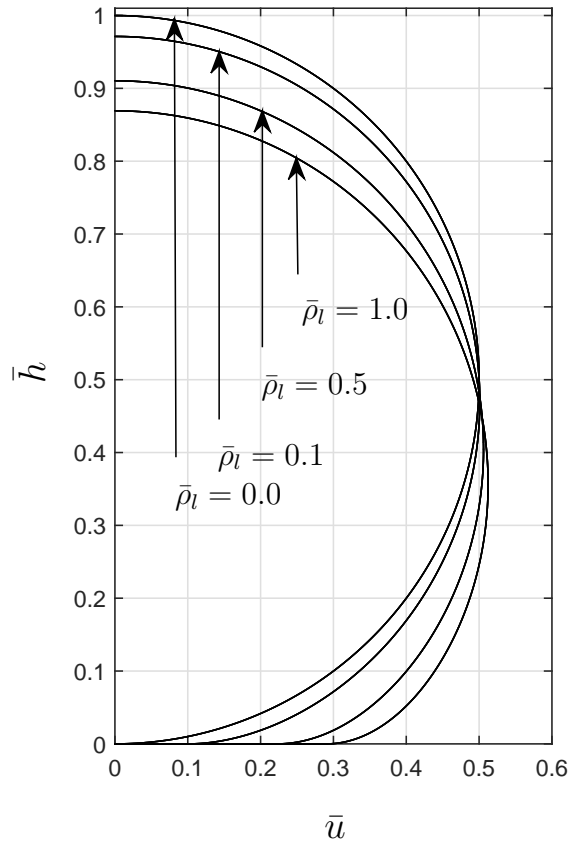


Figure 3.1: Cell configurations for different nondimensionalized ligand densities $\bar{\rho}_l = \{0.0, 0.1, 0.5, 1.0\}$ and $\{\bar{r}_0 = 3, \bar{\gamma} = 10^{-4}, \gamma_3 = 10^{-5}, \bar{K} = 0.025, \bar{\zeta} = 0.5, \bar{h}_0 = 0.35\}$ [26].

in the cell height and extension of contact region. Since the distance between receptors and ligands decreases, the interaction grows (see Fig.3.3) that leads to expansion of the contact region and increase in deformation. This demonstrate the coupling between receptor-ligand interaction and the cell deformation. The result of these coupled phenomena are noticeable in Fig.3.1, where the dimensionless cell heights are $\{1.00, 0.97, 0.91, 0.87\}$ for substrate ligand densities of $\{0, 0.1, 0.5, 1\}$, respectively.

Fig.3.1 shows that the height of the cell as a measure of cell deformation, decreases by more than 9%, when ligand density varies from zero to $\bar{\rho}_l = 0.5$, however variation in cell height drops by only 4% as ligand density rises from $\bar{\rho}_l = 0.5$ to $\bar{\rho}_l = 1$. This behavior can be attributed to the pressure of the enclosed fluid (see Fig.3.4), developed due to presence of ligands and consequent deformation. Although the cell membrane does not possess any bending stiffness, the enclosed fluid pressure yields the overall stiffness to the cell structure, which increases with the growth in ligand density. Additionally, the rate of receptor diffusion toward the substrate decreases as

ligand density grows, due to receptor saturation. Therefore, for high ligand density the rate of cell deformation diminishes such that further increase in ligand density does not yield any significant additional deformation.

Distributions of receptors on the cell membrane are depicted in Fig.3.2 for various nondimensionalized ligand densities. As previously explained, the receptor density was nondimensionalized with respect to the initial receptor density, ρ_{r_0} , (see (2.159) and (2.160)), where the value of $\rho_{r_0} = 10^{17} \text{ m}^{-2}$ [54] was used. Fig.3.2 shows a significant variation in receptor density.

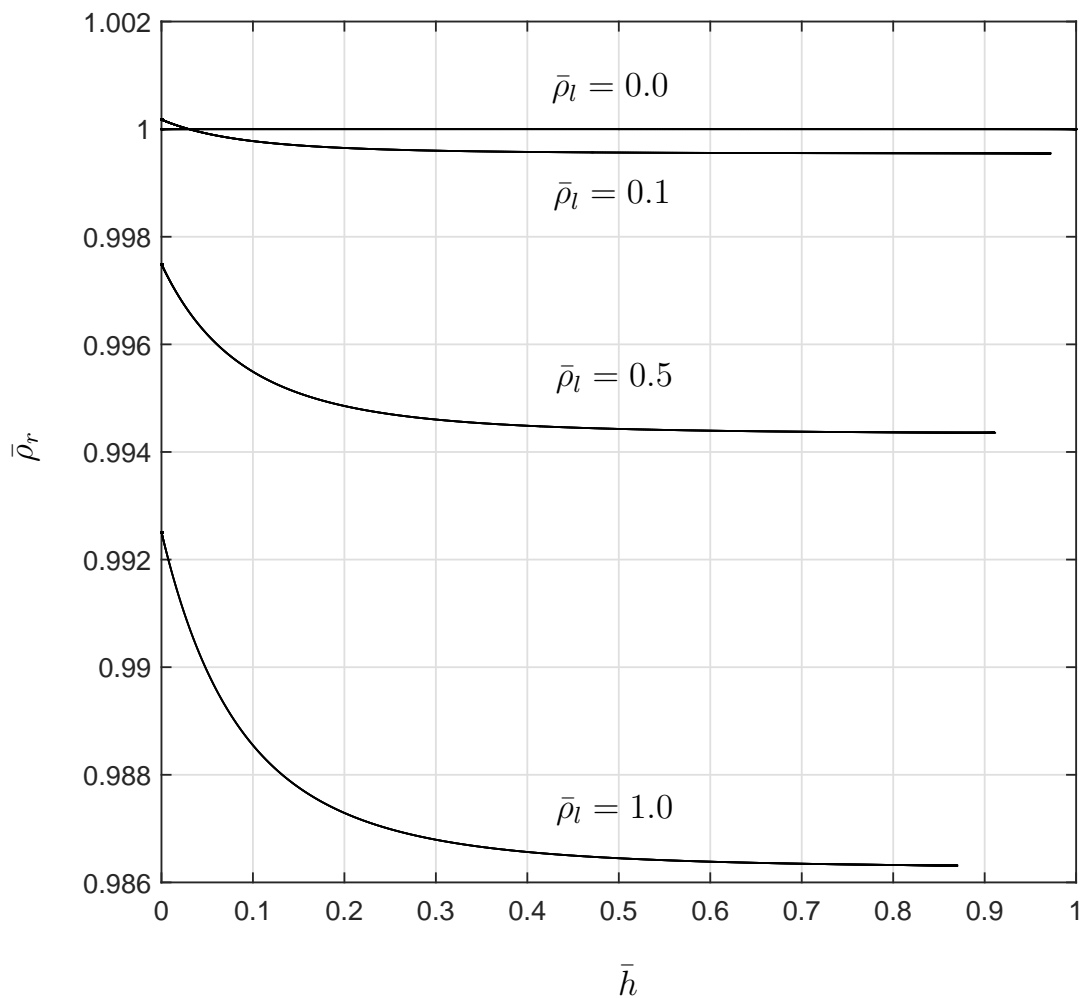


Figure 3.2: Nondimensionalized receptor density $\bar{\rho}_r$ versus dimensionless vertical distance \bar{h} for different nondimensionalized ligand densities $\bar{\rho}_l = \{0.0, 0.1, 0.5, 1.0\}$ and $\{\bar{r}_0 = 3, \bar{\gamma} = 10^{-4}, \bar{\gamma}_3 = 10^{-5}, \bar{K} = 0.025, \bar{\zeta} = 0.5, \bar{h}_0 = 0.35\}$ [26].

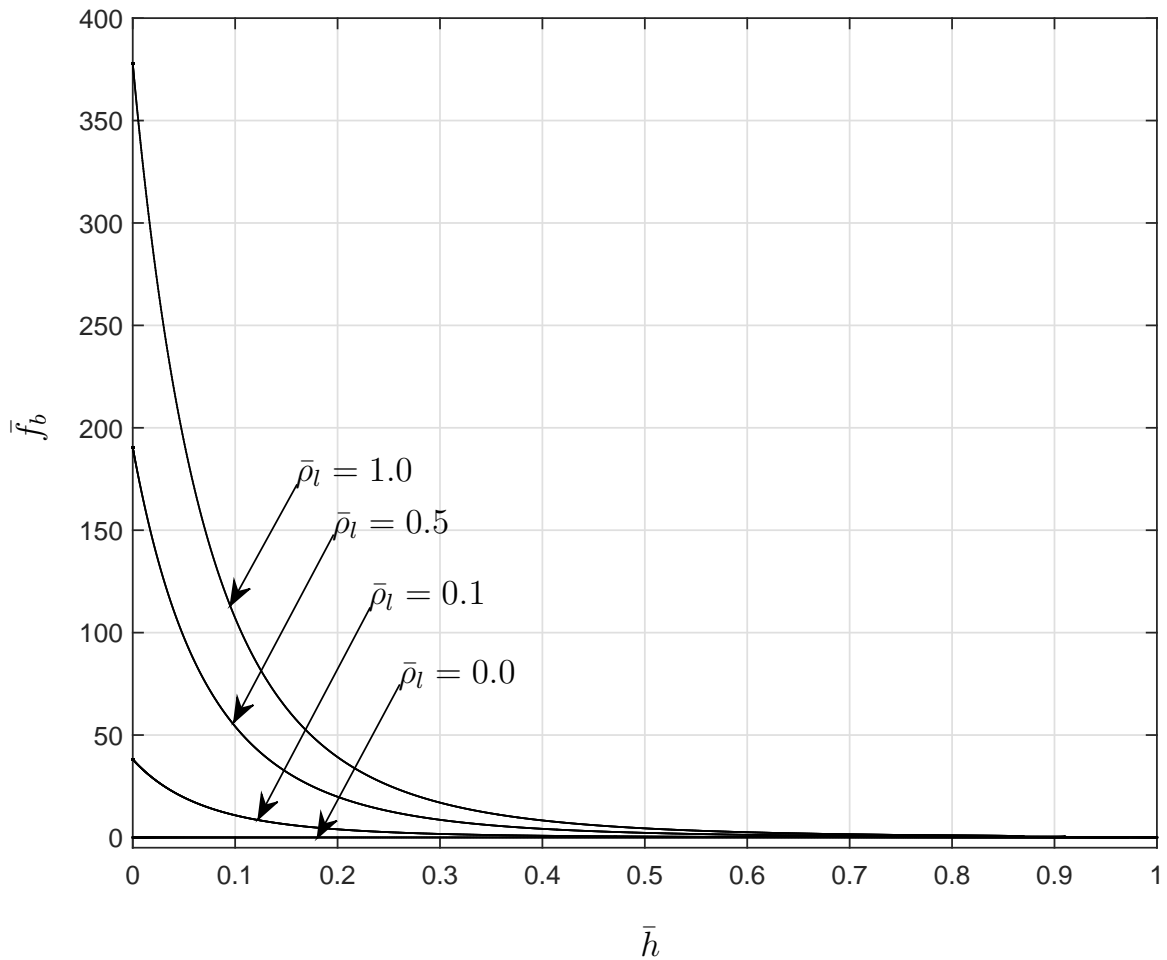


Figure 3.3: Distribution of the nondimensionalized binding force \bar{f}_b on the membrane versus dimensionless vertical distance \bar{h} for different nondimensionalized ligand densities $\bar{\rho}_l = \{0.0, 0.1, 0.5, 1.0\}$ and $\{\bar{r}_0 = 3, \bar{\gamma} = 10^{-4}, \gamma_3 = 10^{-5}, \bar{K} = 0.025, \bar{\zeta} = 0.5, \bar{h}_0 = 0.35\}$ [26].

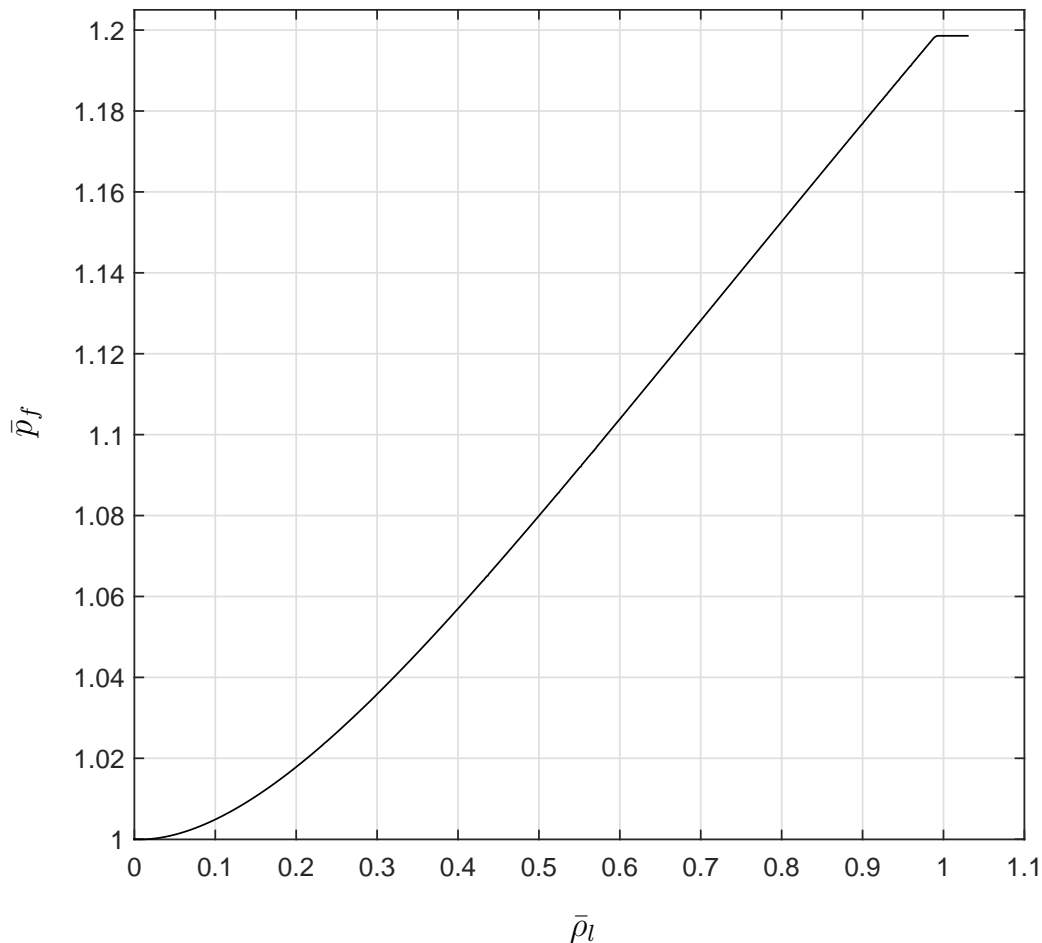


Figure 3.4: The nondimensionalized pressure of the enclosed fluid, \bar{p}_f , versus dimensionless ligand density, $\bar{\rho}_l$, and $\{\bar{r}_0 = 3, \bar{\gamma} = 10^{-4}, \gamma_3 = 10^{-5}, \bar{K} = 0.025, \bar{\zeta} = 0.5, \bar{h}_0 = 0.35\}$ [26].

Since the upper region of the membrane is shielded from ligands attractions, the distribution of receptors in this region is only governed by repelling interactions between receptors, which establish a homogeneous distribution in the upper region of the membrane. Similarly, in the contact region of the membrane with the substrate, the receptor distribution is also homogenous, since the tangential component of the receptor-ligand interactions vanishes (see (2.168)₃) and the receptor distribution is only due to the receptor-receptor interactions, governed by the Fick's law. However, in the lower region of the membrane, which is not in contact with the substrate, the receptor distribution is inhomogeneous due to the non-vanishing tangential component of the receptor-ligand interactions and the repulsion between receptors. The

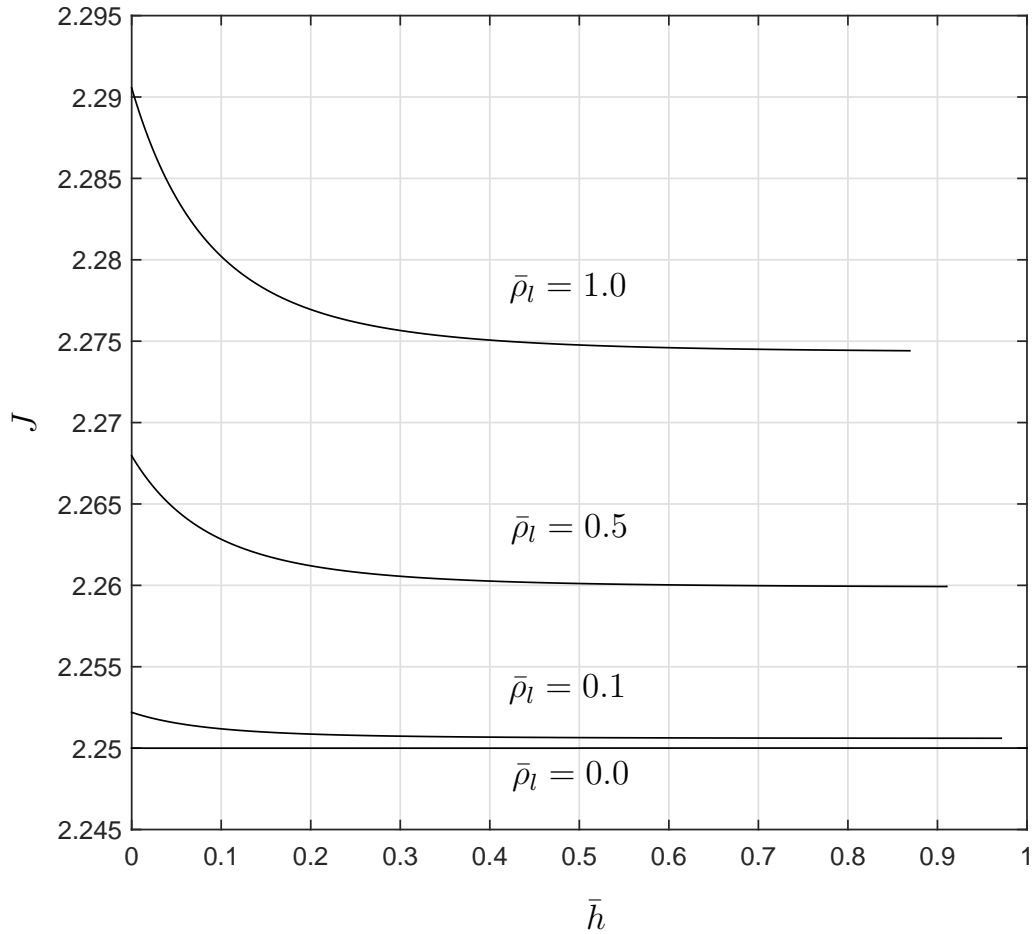


Figure 3.5: The membrane area dilation, J , versus the dimensionless vertical distance, \bar{h} , for different nondimensionalized ligand densities $\bar{\rho}_l = \{0.0, 0.1, 0.5, 1.0\}$ and $\{\bar{r}_0 = 3, \bar{\gamma} = 10^{-4}, \gamma_3 = 10^{-5}, \bar{K} = 0.025, \bar{\zeta} = 0.5, \bar{h}_0 = 0.35\}$ [26].

results depicted in Fig.3.2 show the diffusion of receptors toward the ligands on the substrate, where the receptor density reaches its maximum value at the contact region and minimum value at the upper region. It is worth noting that, increase in the ligand density on the substrate engages more receptors in the adhesion process, which leads to accumulation of receptors in the lower region of the membrane specially in the contact region. Simultaneously the receptors density in the shielded region of the membrane reduces as a consequence of conservation of receptors. Additionally, the diffusion of more receptors toward the ligands increases the local deformations of the membrane.

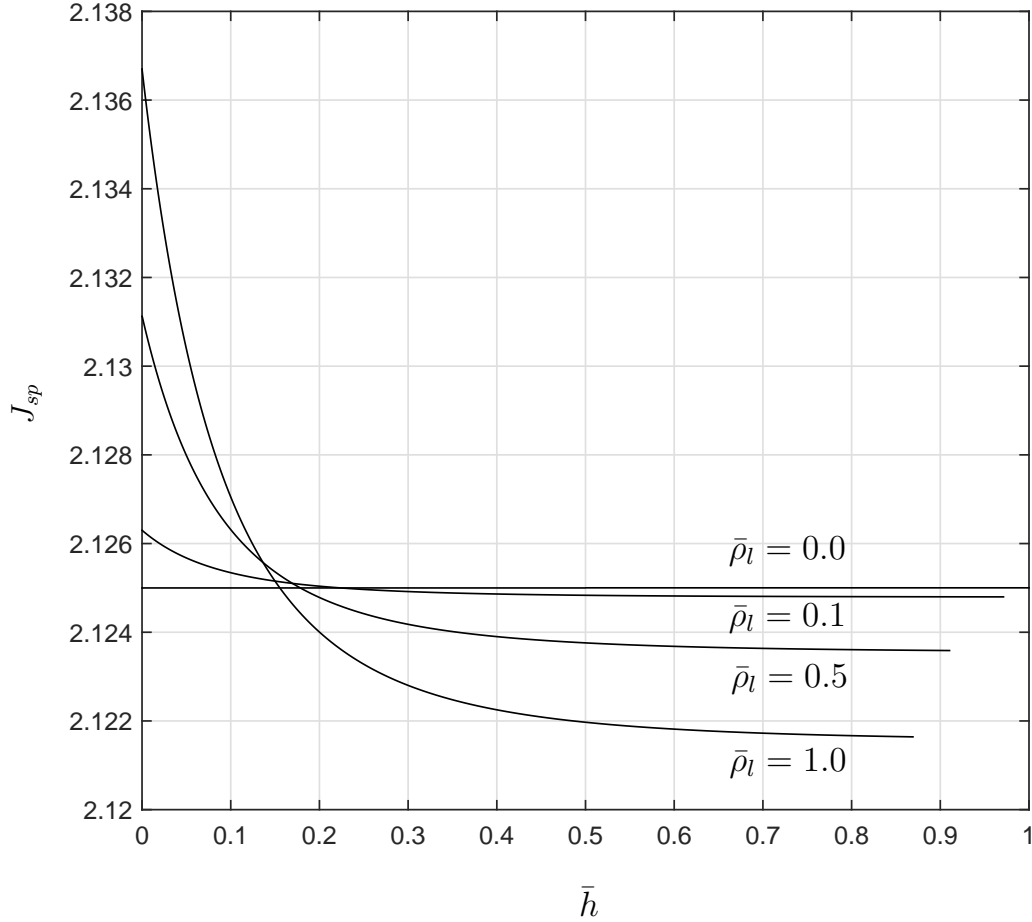


Figure 3.6: The spontaneous area dilation, J_{sp} , on the membrane versus the dimensionless vertical distance, \bar{h} , for different nondimensionalized ligand densities $\bar{\rho}_l = \{0.0, 0.1, 0.5, 1.0\}$ and $\{\bar{r}_0 = 3, \bar{\gamma} = 10^{-4}, \gamma_3 = 10^{-5}, \bar{K} = 0.025, \bar{\zeta} = 0.5, \bar{h}_0 = 0.35\}$ [26].

The measurement of the local area dilation of the membrane, J , is the product of the spontaneous area dilation, J_{sp} , and the elastic area dilation, J_e , as $J = J_e J_{sp}$. Figs.3.5 and 3.6 show that both local area dilations J and J_{sp} grow in the contact region for larger ligand density on the substrate. Therefore, the presence of more ligands on the substrate entails two consequences as accumulation of more receptors in contact region and simultaneously larger area dilation of the membrane, which yields the receptor density distributions as shown in Fig.3.2 for various ligand densities. Fig.3.5 depicts the membrane area dilation, J , of the deformed configurations for different densities of ligands on the substrate. Area dilation is homogeneous in the upper shielded region of the membrane since this region does not interact with ligands on the substrate (see Fig.3.3) and therefore the distribution of receptors in this region is only governed by receptor-receptor repelling interactions (see Fig.3.2). Dilation of

membrane area increase in the lower region of the membrane and attains its maximum value at the contact region, where it is also homogeneous, that is in accordance with the receptor density distribution. This increase in area dilation is attributed to both the receptor-ligand interactions and the presence of higher receptor density. Fig.3.6 shows the variation of spontaneous area dilation J_{sp} , which is defined in (2.44). Since the receptor density (see Fig.3.2)) and area dilation (see Fig.3.5)) are directly related to J_{sp} (see (2.161)), it shows a very similar behavior.

Returning to Fig.3.3, the binding force distribution is analogous to the receptors distribution on the lower region of the membrane. This similarity in distribution is attributed to the proportional relation, (2.52) and (2.53), between the binding force and the receptor density. However, there exists a discrepancy between receptor density and binding force in upper region of membrane, where binding force vanishes despite non-zero density of receptors. This inconsistency refers to the fact that the upper region of membrane is shielded from the effects of ligands.

The nondimensionalized adhesion force \bar{F}_{ad} between the cell and the substrate is of immense importance since it represents the required force to detach the cell. According to the obtained results for the nondimensionalized binding force and pressure of enclosed fluid depicted respectively in Figs.3.3 and 3.4 the adhesion force \bar{F}_{ad} grows for larger density of ligands on substrate (see Fig.3.7). However dimensionless adhesion force attains its maximum at 0.72 and then remains unaltered for sufficiently large density of ligands, which is a consequent response upon cessation of receptor diffusion and membrane deformation. In summery, the system of five coupled nonlinear ODEs ((2.154) and (2.168)) models the adhesion and deformation behaviors of the membrane as the resultant roles of surface tractions like binding force, strain energy function of membrane, receptor and ligand densities, electrolytic and diffusion characteristics. Consideration of the impact of one parameter on adhesion and deformation, needs precise understanding of its relation with other factors. The area dilation as the change in areal size of a membrane element, alters the receptor density on that element, which according to the Ficks law ((2.61)) induces a receptor diffusion (see (2.64) and (2.61)). In addition, the induced variation in receptor density due to the area dilation affects the number of formed receptor-ligand interactions ((2.52) and (2.53) or (2.164)), which is the driving force for adhesion of the cell to the membrane (see (2.171), (2.172), (2.170) and (2.173)).

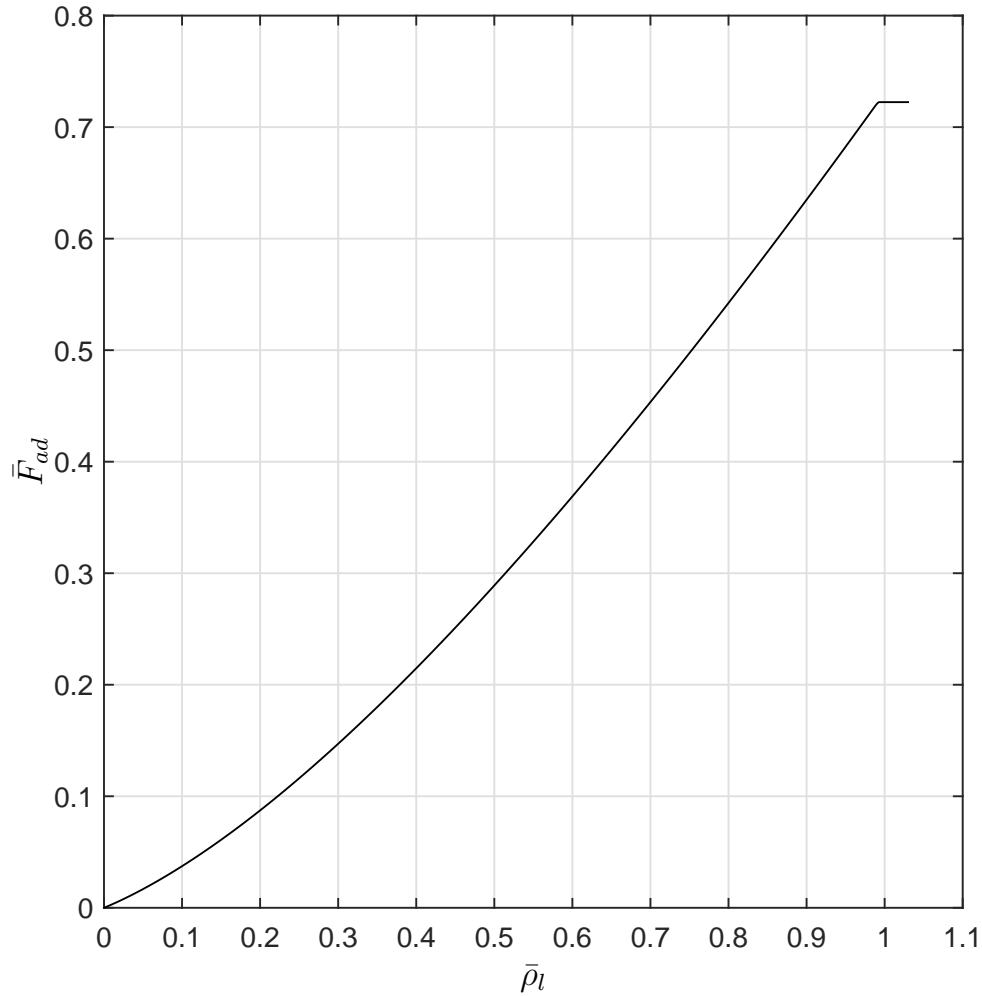


Figure 3.7: The nondimensionalized resultant adhesion force of the cell, \bar{F}_{ad} , versus the dimensionless ligand density $\bar{\rho}_l$ and $\{\bar{r}_0 = 3, \bar{\gamma} = 10^{-4}, \gamma_3 = 10^{-5}, \bar{K} = 0.025, \bar{\zeta} = 0.5, \bar{h}_0 = 0.35\}$ [26].

Besides that increase or decrease in binding force has a direct impact on deformation of the cell and area of contact zone, which the contact area itself plays a significant role in adhesion force of the cell (see (2.173)). Also since the tangential component of the binding force ((2.52) and (2.53) or (2.164)) is involved in diffusion of the receptors on the membrane ((2.62) and (2.65)), the induced variation in binding force influences the diffusion of the receptors and the receptor density. In other words as the matter of coupling influences of different factors, the area dilation has an impact on local receptor density on the membrane, then the induced variation in re-

ceptor density and the resultant receptor diffusion influence the binding force between receptors and ligands and therefore affect the adhesion force of the cell. The change in binding force also generates some diffusion of the receptors and causes alteration in receptor density. It is worth noting that increase in the density of ligands on the substrate increases the membrane pressure (see Fig.3.8), which is a direct result of the proposed constitutive relation (2.158) and variations of area dilations J and J_{sp} .

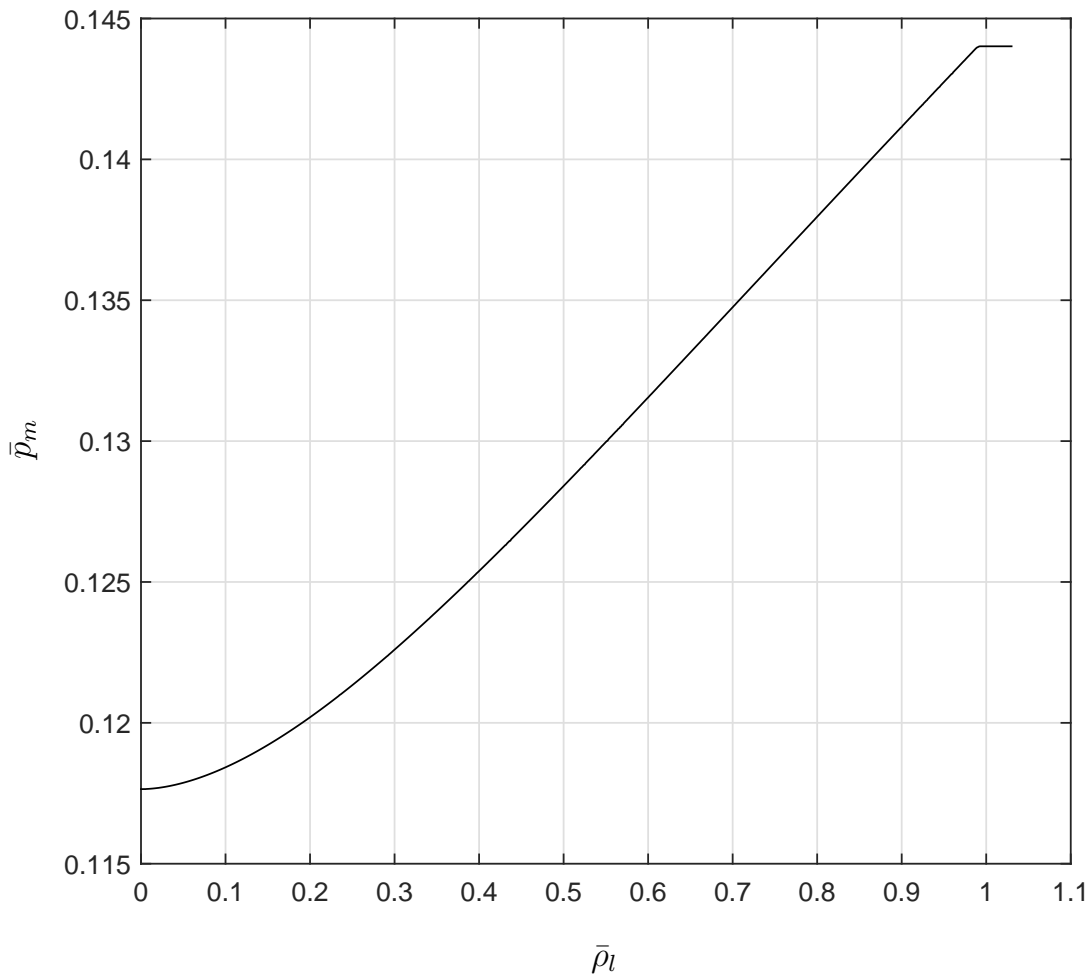


Figure 3.8: The nondimensionalized pressure, \bar{p}_m , in the membrane versus the dimensionless ligand density, $\bar{\rho}_l$, and $\{\bar{r}_0 = 3, \bar{\gamma} = 10^{-4}, \gamma_3 = 10^{-5}, \bar{K} = 0.025, \bar{\zeta} = 0.5, \bar{h}_0 = 0.35\}$ [26].

As previously discussed, by increasing the density of the ligands on the substrate the magnitudes of the fluid pressure \bar{p}_f , adhesion force \bar{F}_{ad} and membrane pressure \bar{p}_m increase (see Figs.3.4, 3.7 and 3.8 respectively). That is because by increasing

the ligand density on the substrate binding force increases (see (2.164) and Fig.3.3), which drags more receptors toward the substrate. By diffusion of the receptors toward the substrate the distance between receptors and ligands decreases, which results in additional growth in binding force and consequently growth in fluid pressure, adhesion force and membrane pressure. However, for sufficiently large density of ligands on the substrate the diffusion of the receptors to the lower segment of the membrane stops due to the fixed number of receptors on the cell and therefore, binding force remains constant and consequently the deformation of the cell ceases and fluid pressure, adhesion force and membrane pressure remain constant. It is notable that, the continuous behavior of these functions are expected. However, due to the dependency of the proposed equation for the binding force on the smaller density of receptors and ligands (see (2.164) and (2.53)), the plotted functions of fluid pressure, adhesion force and membrane pressure, respectively in Figs.3.4, 3.3 and 3.8, do not have a continuous derivatives at the large ligand density for that growth in functions ceases. In other words, although the functions of \bar{P}_f , \bar{F}_b and \bar{P}_m are continuous, their derivatives contain a discontinuity at the value of ligand density for which the functions begin to remain constant.

To this point, the direct and indirect roles of the receptors on the deformation and adhesion of the cell were discussed, however one of the main interest of the present work is to shed new light on another effect of the receptors on the cell membrane behavior. To our knowledge, previous work did not acknowledge the influence of presence of receptors on the area dilation of the membrane, which is recognized here through the introduction of spontaneous area dilation J_{sp} . The following results compare the deformation and adhesion behaviors of a small cell in original state. Here, the cross-sectional area of a single receptor varies as $0.0 \leq \zeta \leq 0.5 \times 10^{-18} \text{ m}^2$ with consequent nondimensionalized values $0.0 \leq \bar{\zeta} \leq 0.5$ and the density of ligands on the substrate is $\bar{\rho}_l = 1.0$. It is worth noting that values of the coefficient $\bar{\zeta}$ is restricted to the range $0.0 \leq \bar{\zeta} \bar{\rho}_r < 1.0$ which is imposed by stress free condition where $J = J_{sp}$. Based on our previous discussions on the distributions of area dilations J and J_{sp} (see Figs. 3.5, 3.6), receptor density (see Fig.3.2) and binding force (see Fig.3.3), the maxima and minima values of the distributions are attained at the contact region and shielded region of membrane, respectively. Thus the following discussion focuses on these two regions. Comparison of the maximum heights of the cell for $\bar{\zeta} = 0.0$ and $\bar{\zeta} = 0.5$ in Fig.3.9 indicates a 11.60% reduction, which demonstrates the important role of the spontaneous areal dilation due to the receptors presence on the membrane

deformation. As stated in (2.43) and (2.161) the coefficient of the spontaneous area dilation, $\bar{\zeta}$, constitutes the sensitivity of membrane dilation to the presence of receptors. When $\bar{\zeta} = 0.0$ is the case in which the cell membrane does not yield area dilation due to presence of receptors and $J_{sp} = 1.0$. However increase in the coefficient $\bar{\zeta}$ enhances the effect of the spontaneous area dilation due to the receptor presence. Additionally, area dilation associated with $\zeta > 0$ effects the receptor density in a way that reduces the density gradient of receptors, which, in turn, reduces the flux governed by the Fick's law. This allows larger diffusion of receptors toward the substrate, and hence yields larger adhesion force (see Fig.3.10) and cell deformation (see Fig.3.9). The adhesion force depicted in Fig.3.10 demonstrates convincingly the significant effect of the area dilation due to the presence of receptors on the cell adhesion force, which dramatically rises for coefficients $\bar{\zeta} > 0.35$. Although intuitively the influence of the spontaneous areal dilation is expected to be insignificant, the results obtained in this work show that it is significant.

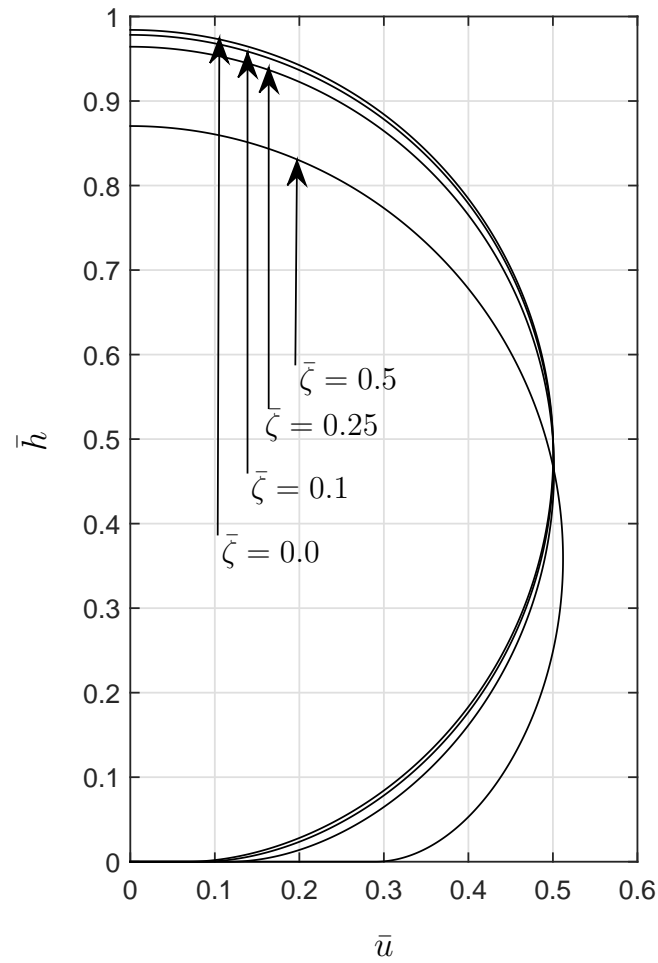


Figure 3.9: Deformed configurations of the cell for different values of the dimensionless coefficient of spontaneous area dilation $\bar{\zeta} = \{0.0, 0.1, 0.25, 0.5\}$ and $\{\bar{r}_0 = 3, \bar{\gamma} = 10^{-4}, \gamma_3 = 10^{-5}, \bar{K} = 0.025, \bar{h}_0 = 0.35, \bar{\rho}_l = 1.0\}$ [26].

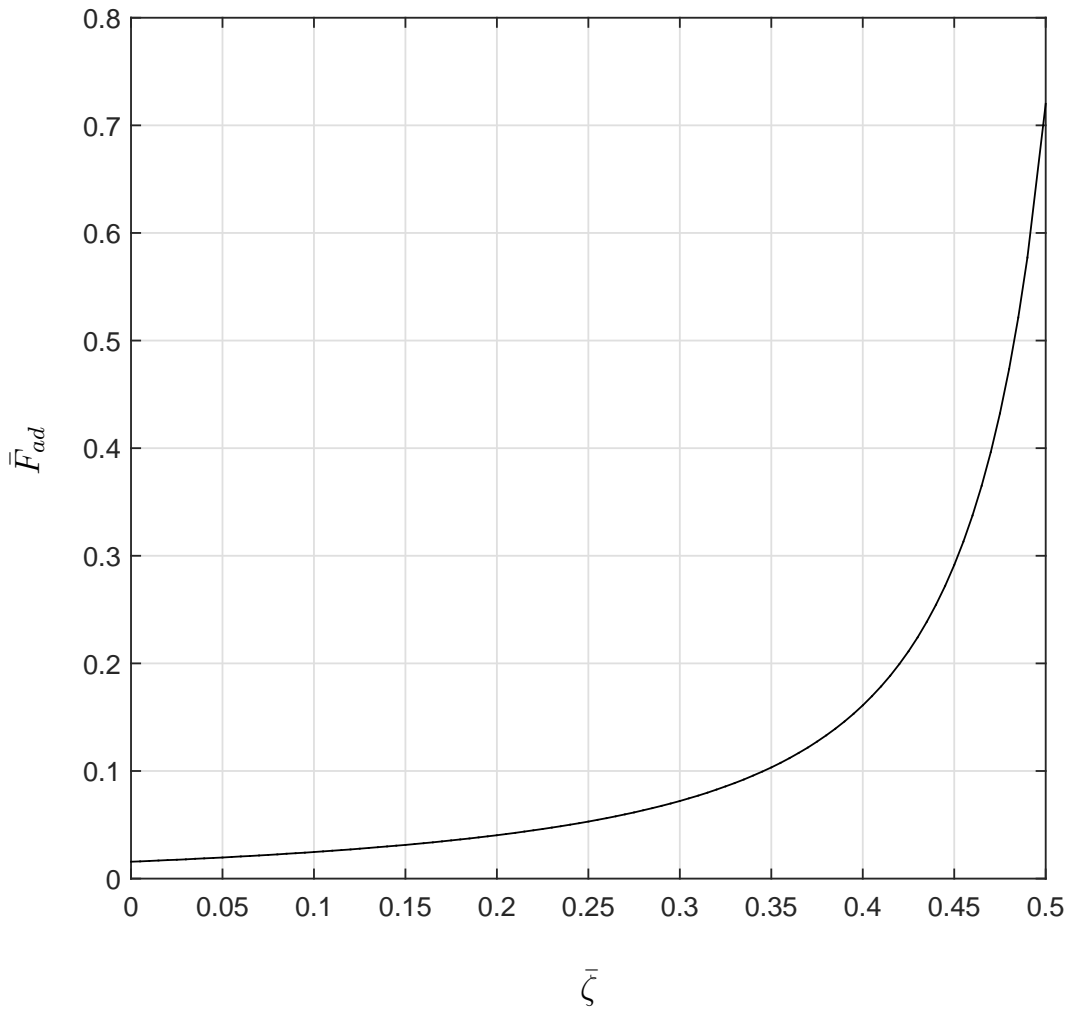


Figure 3.10: The nondimensionalized adhesion force of the cell \bar{F}_{ad} versus dimensionless coefficient of spontaneous area dilation $\bar{\zeta}$ and $\{\bar{r}_0 = 3, \bar{\gamma} = 10^{-4}, \gamma_3 = 10^{-5}, \bar{K} = 0.025, \bar{h}_0 = 0.35, \bar{\rho}_l = 1.0\}$ [26].

The results associated with the influence of electrolytic characteristic of the extracellular environment on the deformation and adhesion behaviors of cells are presented in Figs.3.11 and 3.12 in terms of the nondimensionalized Debye length inverse \bar{K} . The cell is in the original state, while the Debye length of the electrolytic environment outside of the cell alters from 1 nm to 1 μ m with associated dimensionless values $\bar{K} = \{25.0, 2.5, 0.25, 0.025\}$ and the ligand density on the substrate is $\bar{\rho}_l = 1.0$. Debye length characterizes the sphere of influence of the electrostatic field generated by a charge in an electrolyte. Hence the results in Fig.3.11 show admissible consistency with the Debye length characteristic in a way that deformation of the cell increases,

for larger Debye length. These results indicate that the height of the cell reduces by 13.0% when Debye length of the electrolyte varies from 1 nm to 1 μm . For an electrolytic environment with large Debye length the distance in which electrostatic interactions between charges and induced dipoles occur, increases and therefore the binding force (see (2.164)) increases which results in larger diffusion of receptors and cell deformation. By increasing the Debye length, the electrostatic effect of the charges within the electrolyte is enhanced, which strengthens the receptor-ligand interactions (2.164) and thus increases the deformation of the cell.

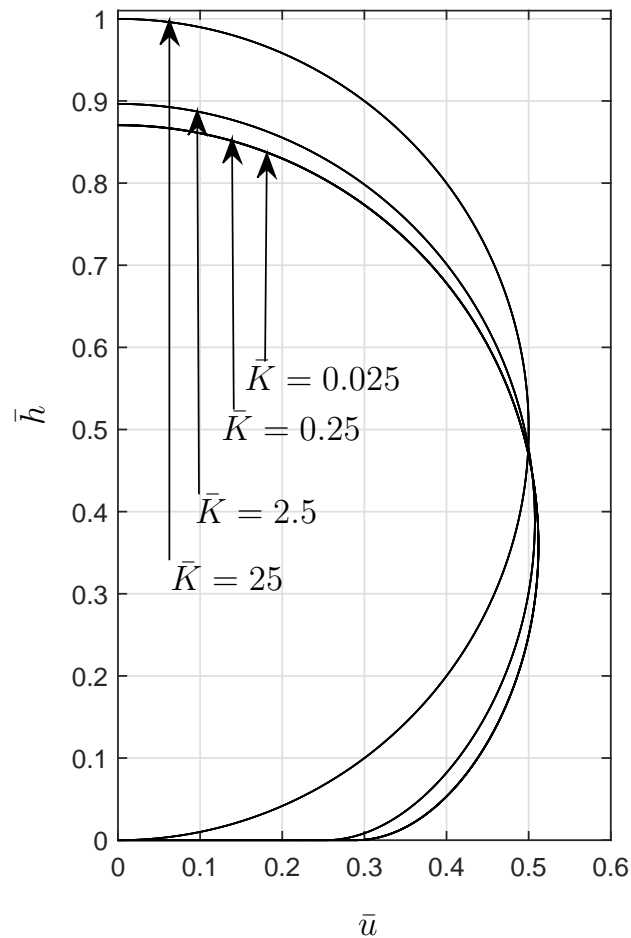


Figure 3.11: Deformed configurations of the cell for different values of Debye length inverse $\bar{K} = \{0.025, 0.25, 2.5, 25\}$ and $\{\bar{r}_0 = 3, \bar{\gamma} = 10^{-4}, \gamma_3 = 10^{-5}, \bar{\zeta} = 0.5, \bar{h}_0 = 0.35, \bar{\rho}_l = 1.0\}$ [26].

Larger cell deformation induced by longer Debye length, rises the pressure of the

enclosed fluid, which grants a stiffness to the cell membrane and slows the rate of cell deformation. Additionally, receptor diffusion toward the substrate is enhanced by the strengthened receptor-ligand bindings, however since total number of receptors is fixed the receptor diffusion saturates, which does not yield further cell deformation. Due to important role of cell adhesion force F_{ad} in determination of required detachment effort for specific adhesion condition, the influence of electrolytic characteristic of environment is discussed. Fig.3.12 depicts that the cell adhesion force increases in electrolytic environment with longer Debye length. This increase in adhesion force is strongly consistent with growth in binding force (as explained above) and increase in contact area.

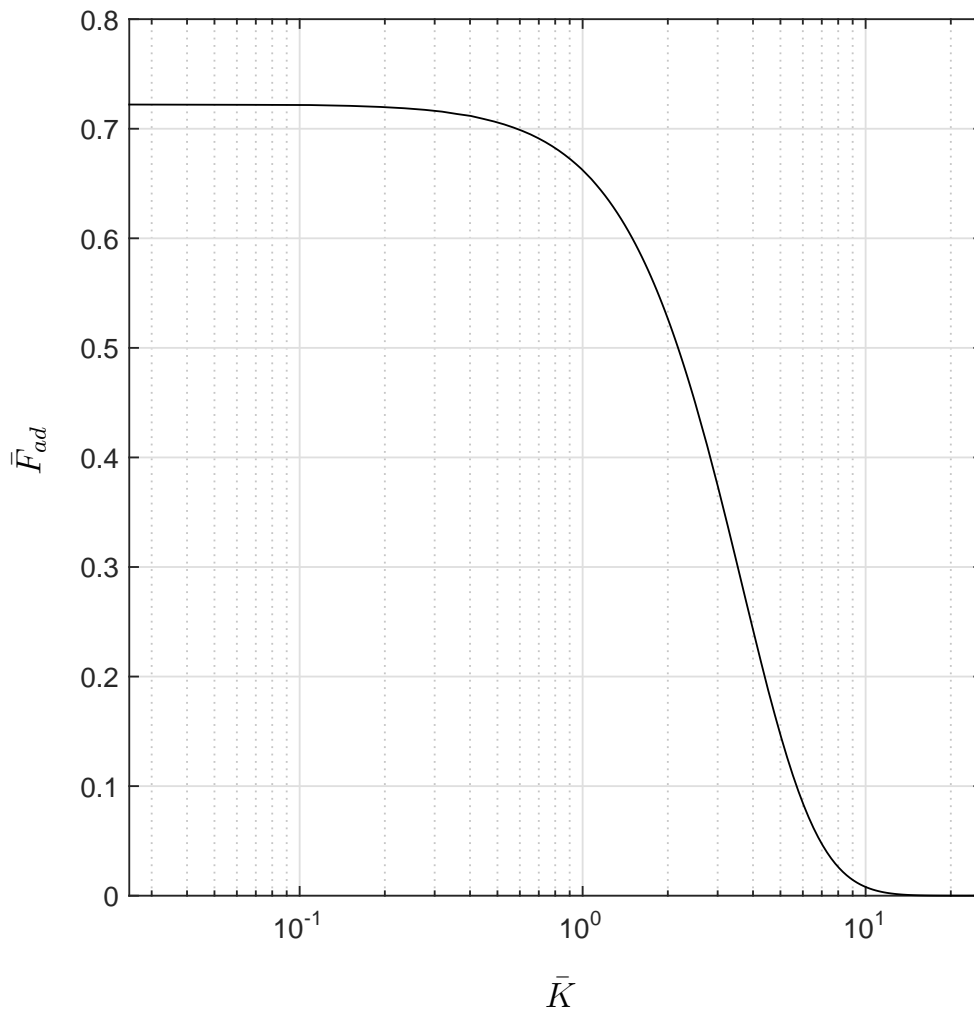


Figure 3.12: The nondimensionalized adhesion force of the cell \bar{F}_{ad} versus the inverse of the Debye length \bar{K} and $\{\bar{r}_0 = 3, \bar{\gamma} = 10^{-4}, \gamma_3 = 10^{-5}, \bar{\zeta} = 0.5, \bar{h}_0 = 0.35, \bar{\rho}_l = 1.0\}$ [26].

As the Debye length increases the associate adhesion force increases, however as discussed before for large enough Debye length the receptor diffusion saturates and no significant increase in adhesion force is observed with further increase in Debye length.

Next attention is directed to the roles of the characteristic of the receptor-ligand interaction in proportion to the material characteristic of the membrane. Recall that the binding-membrane parameter $\bar{\gamma}$ (2.169) is defined as the dimensionless ratio of the binding parameter γ_2 to the membrane parameter γ_1 . Figs.3.13 and 3.14 present re-

sults for the original-state cell, ligand density $\bar{\rho}_l = 1.0$ and different values of binding-membrane parameter, $10^{-7} \leq \bar{\gamma} \leq 10^{-4}$, which clarifies the effects of binding and membrane stiffness coefficients on the cell behavior. In order to entail the roles of the binding and membrane characteristics in variation of the dimensionless parameter $\bar{\gamma}$, the binding force intensity and the membrane stiffness vary as $10^{-55} \leq C \leq 10^{-52} \text{ Nm}^5$ and $0.1 \leq K_m \leq 0.4 \text{ N/m}$, respectively [8, 23, 25, 28, 38, 51, 56]. Since the dimensionless parameter of diffusion, γ_3 , defined in $(2.169)_2$ depends on the intensity of the receptor-ligand interactions, it takes the relevant values $10^{-8} \leq \gamma_3 \leq 10^{-5}$. The cell deformations depicted in Fig.3.13 demonstrate the influence of the intensity of the receptor-ligand binding, C , on the cell deformation. This physically means that increase in the number of existing charges on a receptor magnifies the generated electrostatic field, which consequently intensifies the polarization imposed on the nonpolar molecules of a ligand. Therefore increase in intensity of receptor-ligand binding C by means of increase in existing charges on a receptor not only reinforces the external electrostatic field but also induces a stronger dipole in a nonpolar ligand, which together strengthen the interaction between a receptor and a ligand. The overall result of these phenomena leads to the enhancement in the cell adhesion and deformation. Additionally an increase in adhesion and deformation is also expected if polarizability of nonpolar molecules of ligands, α , grows. However between number of existing charges and polarizability characteristic the former one shows intenser effect on receptor-ligand interactions and consequent membrane deformation. That is because, charges are involved in both generating the electrostatic field and inducing polarization in ligand molecules, while polarizability characteristic is only committed to polarization of ligands (this dual effect of charges emerges as the power of 2 for charges in relation of coefficient C). The cell deformations depicted in Fig.3.13 decrease, as anticipated, by increase in the membrane stiffness, K_m . In accordance to the rationale discussed above, cell membrane represents 12.9% reduction in cell height for the same ranges of variations of binding and material rigidities used above. The obtained results indicate that the resultant adhesion force increases for larger binding intensity and smaller membrane stiffness.

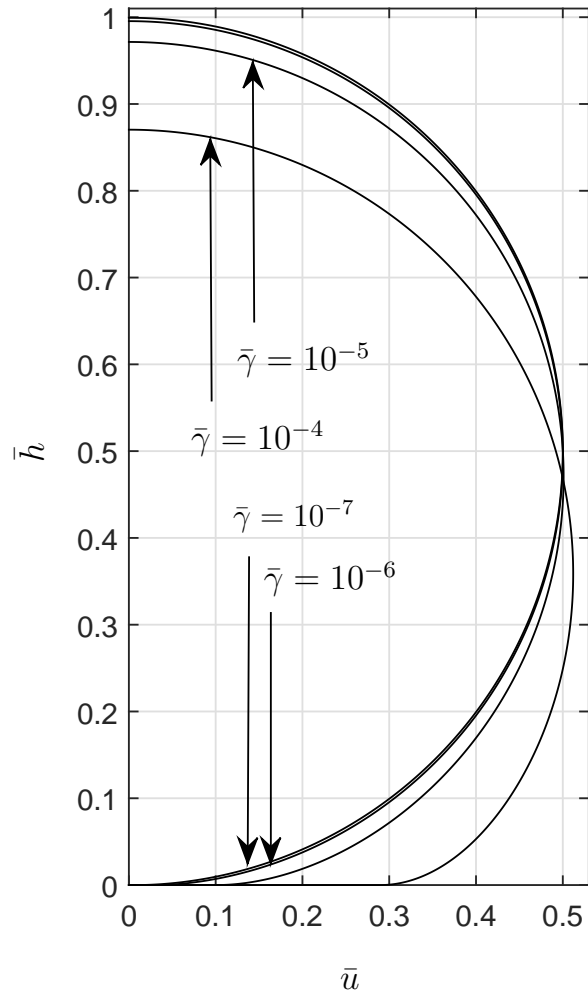


Figure 3.13: Deformed configurations of the cell for different dimensionless binding-membrane parameters $\bar{\gamma} = \{10^{-7}, 10^{-6}, 10^{-5}, 10^{-4}\}$ and $\{\bar{r}_0 = 3, \gamma_3 = \{10^{-8}, 10^{-7}, 10^{-6}, 10^{-5}\}, \bar{K} = 0.025, \bar{\zeta} = 0.5, \bar{h}_0 = 0.35, \bar{\rho}_l = 1.0\}$ [26].

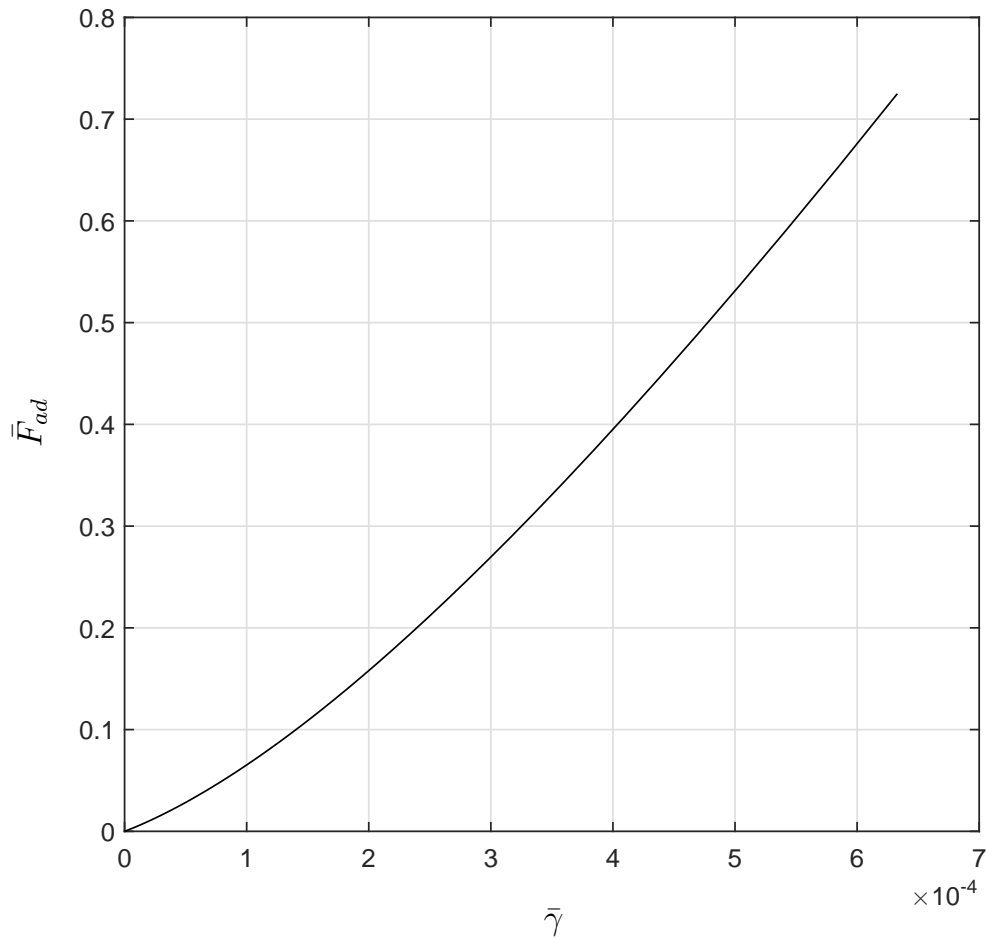


Figure 3.14: The nondimensionalized adhesion force of the cell \bar{F}_{ad} versus dimensionless binding-membrane parameter $\bar{\gamma}$ and $\{\bar{r}_0 = 3, \gamma_3 = \{10^{-8}, 10^{-7}, 10^{-6}, 10^{-5}\}, \bar{K} = 0.025, \bar{\zeta} = 0.5, \bar{h}_0 = 0.35, \bar{\rho}_l = 1.0\}$ [26].

The influence of the dimensionless diffusion parameter γ_3 on the deformation and adhesion of the cell is discussed here. The obtained results show a weak effect of this parameter on the deformation behavior of the cell in which the areal dilation J increases in contact region for larger γ_3 (see Fig.3.15). The increase in areal dilation at contact region is accompanied by the decrease in it at upper segment of the membrane. In fact higher value of the diffusion parameter γ_3 increases the mobility of the receptors on the membrane in a way that the larger number of receptors is attracted toward the substrate and accumulate in the lower segment of the membrane, such that it strengthens the binding force and consequently the adhesion force \bar{F}_{ad} between cell and substrate, as shown in Fig.3.16.

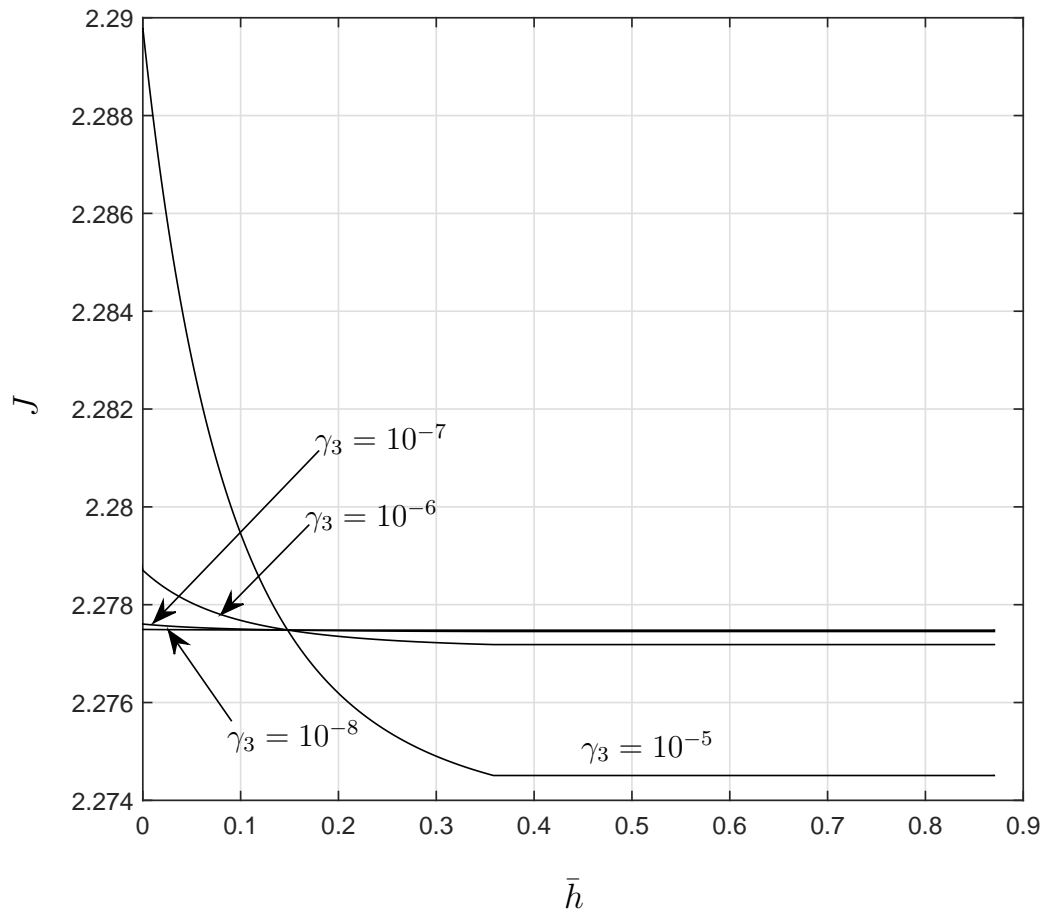


Figure 3.15: The distributions of the areal dilation J versus dimensionless vertical distance \bar{h} for various dimensionless diffusion parameter $\gamma_3 = \{10^{-8}, 10^{-7}, 10^{-6}, 10^{-5}\}$ and $\{\bar{r}_0 = 3, \bar{\gamma} = 10^{-4}, \bar{K} = 0.025, \bar{\zeta} = 0.5, \bar{h}_0 = 0.35\}$.

The increase in receptor-ligand interaction in the form of binding force and consequent adhesion force exerts a larger traction to the lower segment of the cell and increases the areal dilation J of the membrane. It is notable that the deformation of the cell and increase in contact region has a direct impact on the cell adhesion force \bar{F}_{ad} , that means the adhesion force not only grows due to the accumulation of the receptors in lower segment of the membrane and consequent larger binding force but also because of induced increase in contact region. Fig.3.17 illustrates the same behavior of spontaneous areal dilation J_{sp} as of J in upper and lower segments of the cell.

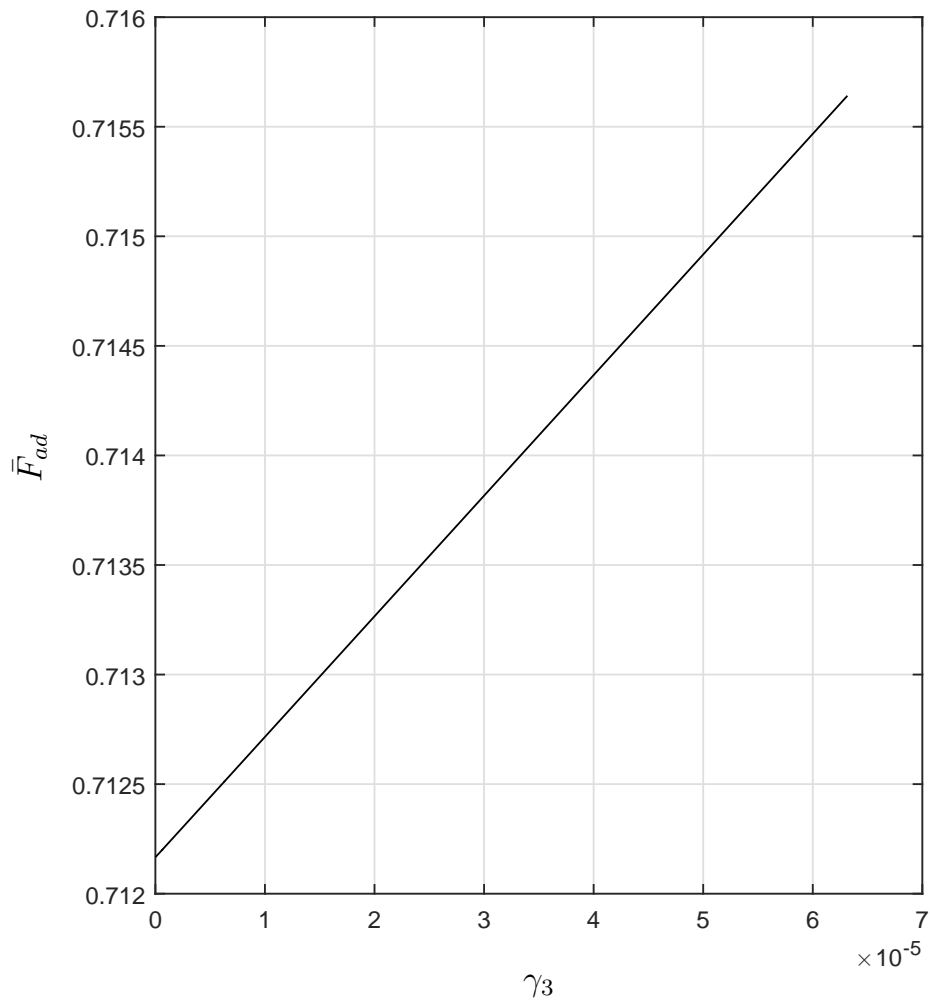


Figure 3.16: The nondimensionalized adhesion force of the cell \bar{F}_{ad} versus dimensionless diffusion parameter γ_3 and $\{\bar{r}_0 = 3, \bar{\gamma} = 10^{-4}, \bar{K} = 0.025, \bar{\zeta} = 0.5, \bar{h}_0 = 0.35, \bar{\rho}_l = 1.0\}$.

It is reasonable that accumulation of the receptors on the lower segment of the cell increases the dilation of the membrane due to the presence of the receptors and vice versa. Also the variation in receptor $\bar{\rho}_r$ distribution by diffusion parameter γ_3 , displayed in Fig.3.18, implies that although the local areal dilation J increases in lower segment of the cell for larger diffusion parameter γ_3 , the accumulation of larger number of receptors on that segment overcomes the dilation in local area such that the consequent local receptor density increases in that region. The effect of decrease in number of receptors in upper segment of cell for larger diffusion parameter γ_3 is

stronger than the decrease in areal dilation and induces lower receptor density in upper segment. It is worth mentioning that some additional figures of the results are provided in appendix to support the presented models in this work.

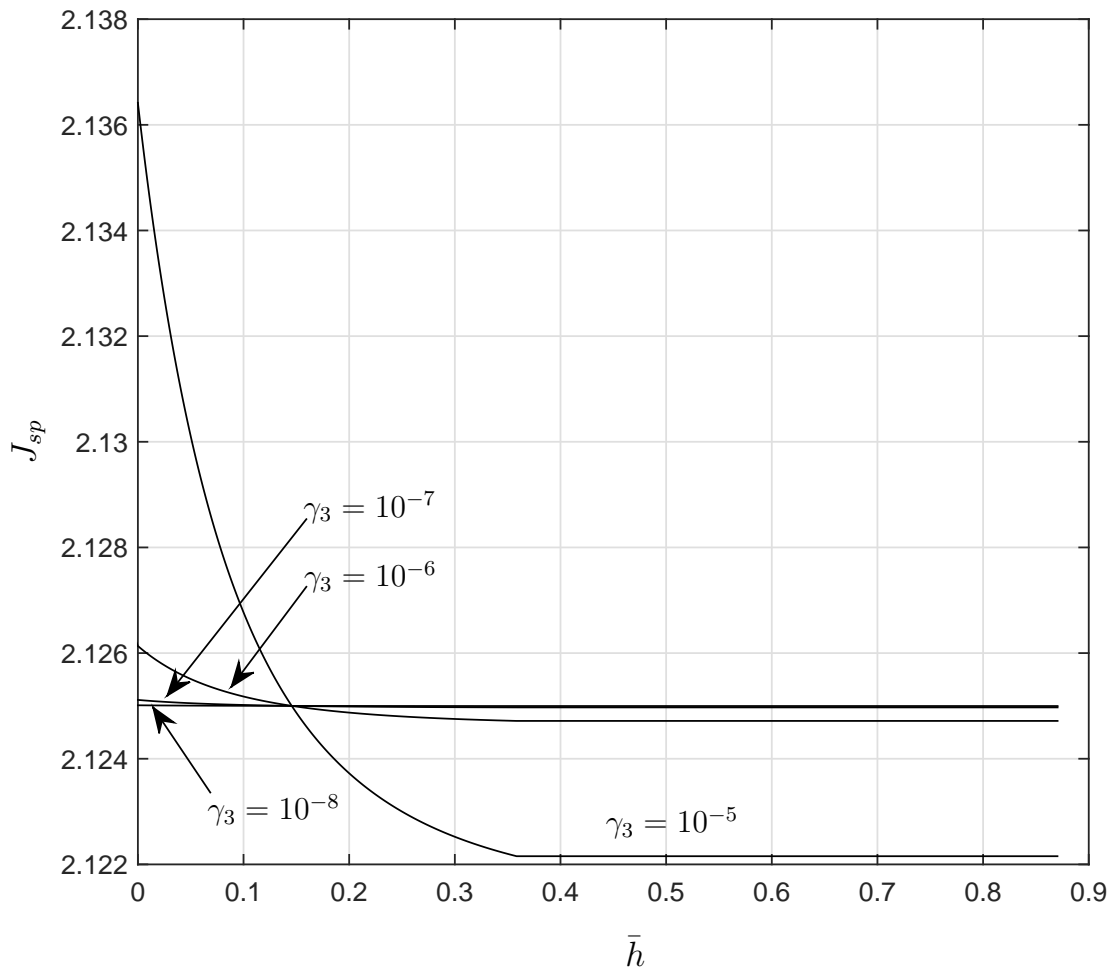


Figure 3.17: The distributions of the spontaneous areal dilation J_{sp} versus dimensionless vertical distance \bar{h} for various dimensionless diffusion parameter $\gamma_3 = \{10^{-8}, 10^{-7}, 10^{-6}, 10^{-5}\}$ and $\{\bar{r}_0 = 3, \bar{\gamma} = 10^{-4}, \bar{K} = 0.025, \bar{\zeta} = 0.5, \bar{h}_0 = 0.35\}$.

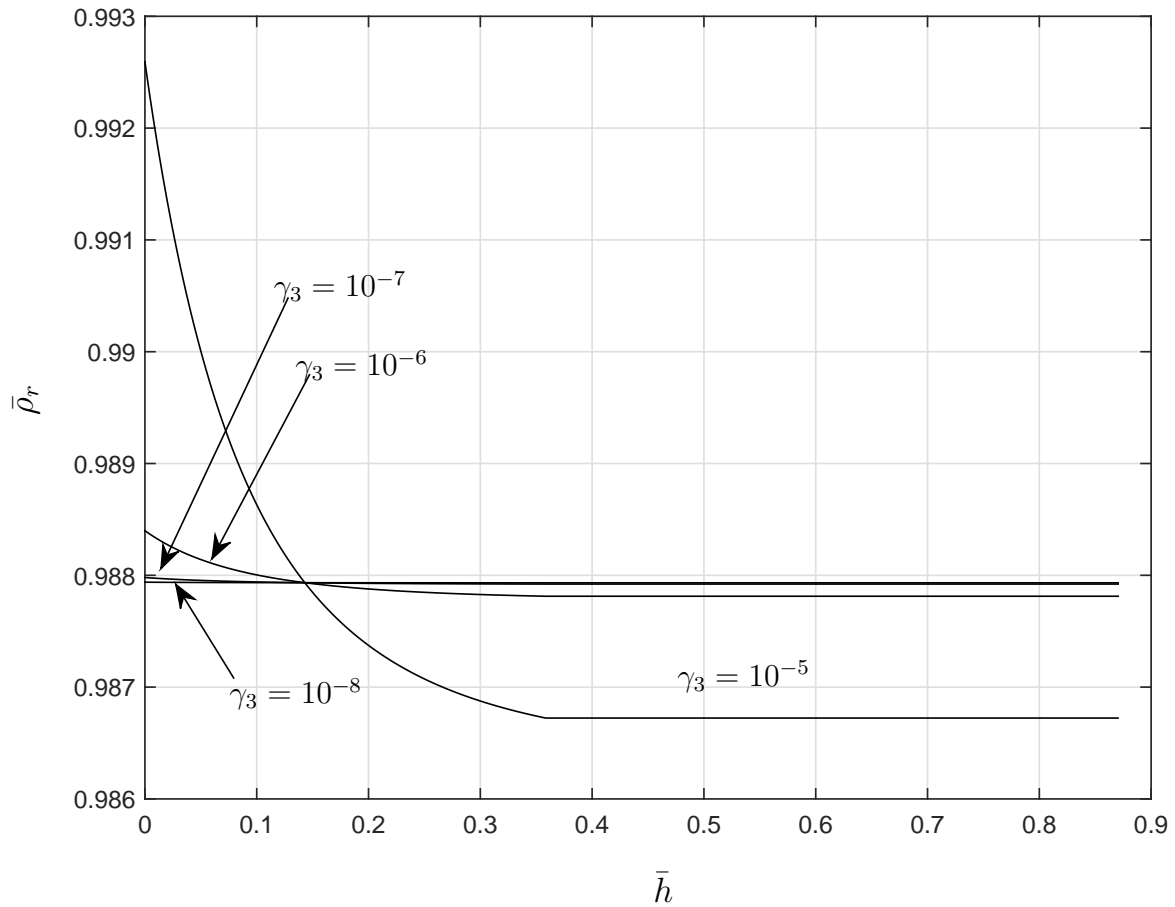


Figure 3.18: The distributions of the nondimensionalized receptor density $\bar{\rho}_r$ versus dimensionless vertical distance \bar{h} for various dimensionless diffusion parameter $\gamma_3 = \{10^{-8}, 10^{-7}, 10^{-6}, 10^{-5}\}$ and $\{\bar{r}_0 = 3, \bar{\gamma} = 10^{-4}, \bar{K} = 0.025, \bar{\zeta} = 0.5, \bar{h}_0 = 0.35\}$.

Chapter 4

Conclusions

In this chapter we were concerned with the formulation of a comprehensive model, which approximated the adhesion and deformation of a biological cell (biocell) to a rigid substrate. The adhesion was mediated by means of two types of proteins, integrin (receptor) on the membrane, and fibronectin (ligand), on the substrate. The behavior of the cell in adhesion and deformation is strongly dependent on the material characteristic of the cell membrane. According to the observed experimental results in literature, the phospholipid molecules as dominant components of the cell membrane are closely held together by non-covalent interaction, such that they can freely move laterally and the cell membrane behavior in dilation and distortion is mostly close to the behavior of an isotropic fluid. It was discussed that, the surface of cell membrane includes sufficient number of molecules, such that the fluctuation and effects of one individual molecule are negligible. Additionally, in the current analysis any considered characteristic length was sufficiently larger than the molecular distances and gaps, such that the material behavior was never addressed from molecular point of view. Therefore, an isotropic continuum fluid-like model was proposed for the cell membrane and a strain energy function was proposed to approximate the mechanical behavior of the cell membrane. This strain energy accounted for the resistance of the fluid-like membrane to the in-plane dilation, however neglected any distortion in the membrane. As a novelty and since the influence of the receptor presence on the adhesion and deformation of the cell has not been sufficiently studied, in the present work the effect of the presence of the receptors on the areal dilation of the membrane was addressed through the introduction of spontaneous areal dilation. The conception of spontaneous areal dilation also affected the material behavior of the membrane through the proposed strain energy function. In the current work,

the membrane theory was used for modeling, since the membrane of the cell was considered to be comprised of phospholipid molecules and other components of the membrane plus the cytoskeleton underneath the membrane were ignored. Therefore, the behavior of the cell membrane was better modeled by using membrane theory. That means, the bending stiffness of the membrane was ignored and the normal forces to the membrane are tolerated as in-plane stresses. Additionally a nonlinear binding force relation was proposed based on charge-induced dipole interaction between receptors and ligands, which was enriched by a consideration of shielding phenomenon which is in agreement with intrinsic behavior of bonds. According to the mobility of the receptors on the membrane and the electrostatic characteristics of the receptors and ligands, the migration of the receptors on the membrane was considered to be under the influence of receptor-receptor and receptor-ligand interactions. Therefore, a diffusion model was developed, which governed the distribution of the receptors on the membrane.

The current study was allocated to investigate the adhesion and deformation of a cell by applying the developed model. Additionally, the influences of variety of membrane, binding and electrolytic constitutive coefficients on the cell adhesion and deformation behaviors were investigated. The results obtained show that the ligands density on the substrate has strong effect on the adhesion and deformation the cell. This result is admissible due to the essential role of the ligands in cell adhesion. The novelty in this work is the introduction of the intrinsic membrane area dilation due to the presence of receptors. Based on the results obtained in the current work, the area dilation due to the presence of receptors possesses a significant effect on the cell adhesion and deformation, which emphasizes the important of the consideration of this effect in cell adhesion modeling. The Debye length as the electrolytic characteristic of extracellular environment also shows intense effect on the adhesion and deformation of the cell. Additional significant parameter is the ratio of the receptor-ligand binding coefficient to the membrane stiffness, $\bar{\gamma}$, which was shown to have a considerable influence on cell behavior. However, the influence of the dimensionless diffusion parameter γ_3 on the adhesion and deformation of the cell is small, although the migration of the receptors on the cell membrane is biological fact.

Chapter 5

Future Work

In the current work, the membrane theory was used for modeling, since the membrane of the cell was considered to be comprised of phospholipid molecules and other components of the membrane plus the cytoskeleton underneath the membrane were ignored. Therefore, the behavior of the cell membrane was better modeled by using membrane theory. That means, the bending stiffness of the membrane was ignored and the normal forces to the membrane are tolerated as in-plane stresses. For the future work, the influences of the membrane thickness and bending stiffness of the membrane on the deformation and consequently adhesion of the cell, can be considered by using the shell theory for modeling the behavior of the cell membrane. That model can better account the several different protein components in the cell membrane and the cytoskeleton, which exists underneath the membrane and analyze the behavior of the cell membrane. Additionally, due to the existence of the protein components in the cell membrane, beside the fluid-like behavior of the phospholipid molecules, a fluid-solid constitutive model can be proposed, which can approximate the behavior of the membrane by considering the dilation and distortion happen in the cell membrane. As discussed in the present work the diffusion of the receptors on the membrane due to the interactions between receptors was modeled by Fick's law. As an prospective work, a nonlinear constitutive relation can be proposed based on the electrostatic interaction of the charges exist on the receptor proteins to improve the diffusion of the receptors on the membrane.

Appendix A

Additional Results

In this chapter, additional figures are provided to further analyze the cell adhesion and deformation.

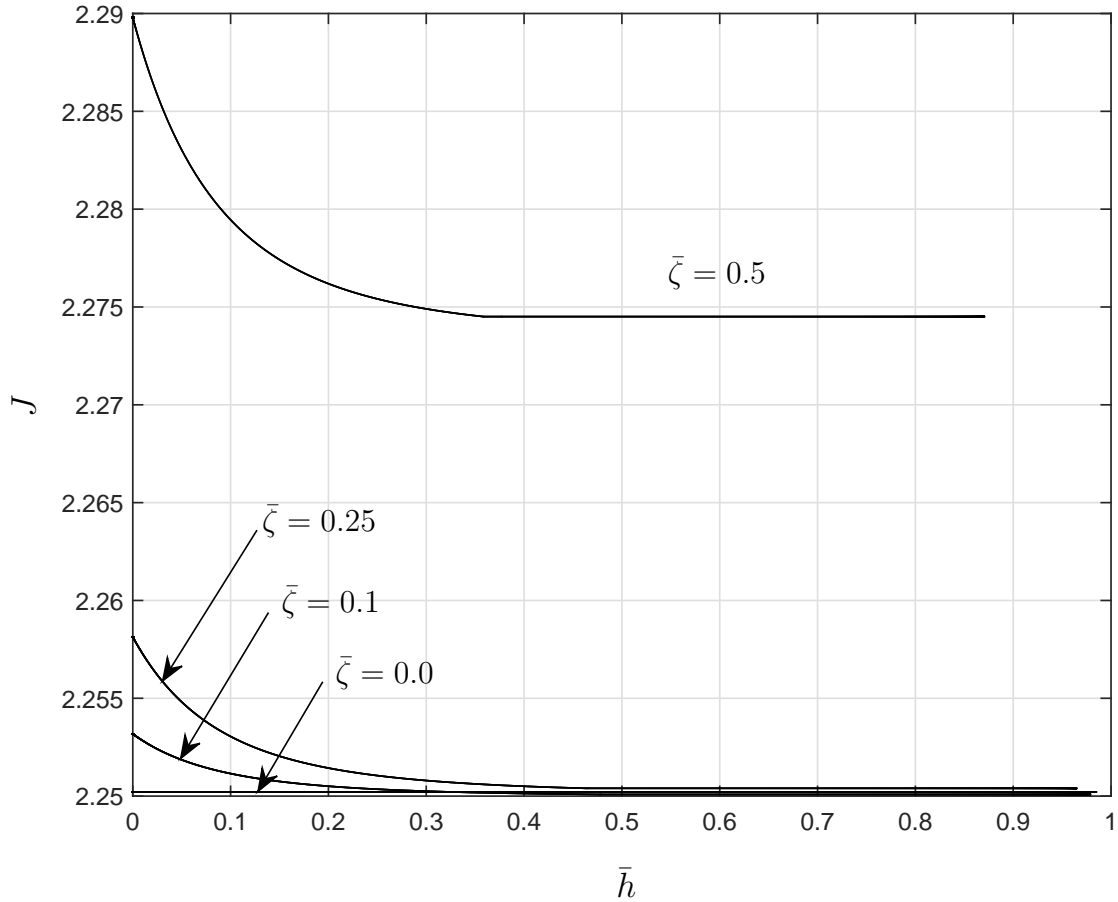


Figure A.1: Variation of the membrane area dilation, J , for various values of the dimensionless coefficient of spontaneous area dilation $\bar{\zeta} = \{0.0, 0.1, 0.25, 0.5\}$ and $\{\bar{r}_0 = 3, \bar{\gamma} = 10^{-4}, \gamma_3 = 10^{-5}, \bar{K} = 0.025, \bar{h}_0 = 0.35, \bar{\rho}_l = 1.0\}$.

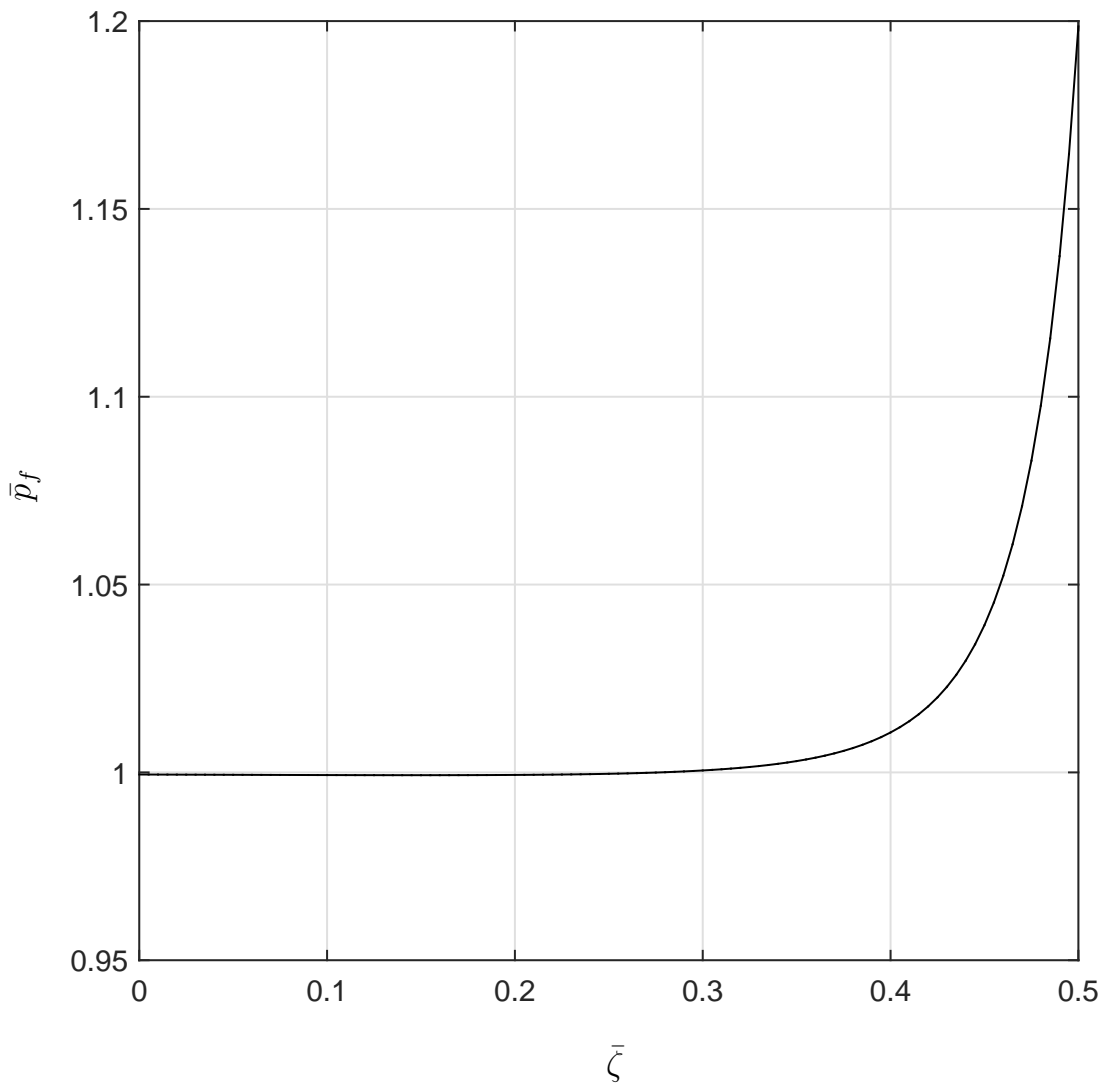


Figure A.2: The nondimensionalized pressure of the enclosed fluid, \bar{p}_f versus nondimensionalized coefficient of spontaneous area dilation $\bar{\zeta}$ and $\{\bar{r}_0 = 3, \bar{\gamma} = 10^{-4}, \gamma_3 = 10^{-5}, \bar{K} = 0.025, \bar{h}_0 = 0.35, \bar{\rho}_l = 1.0\}$.

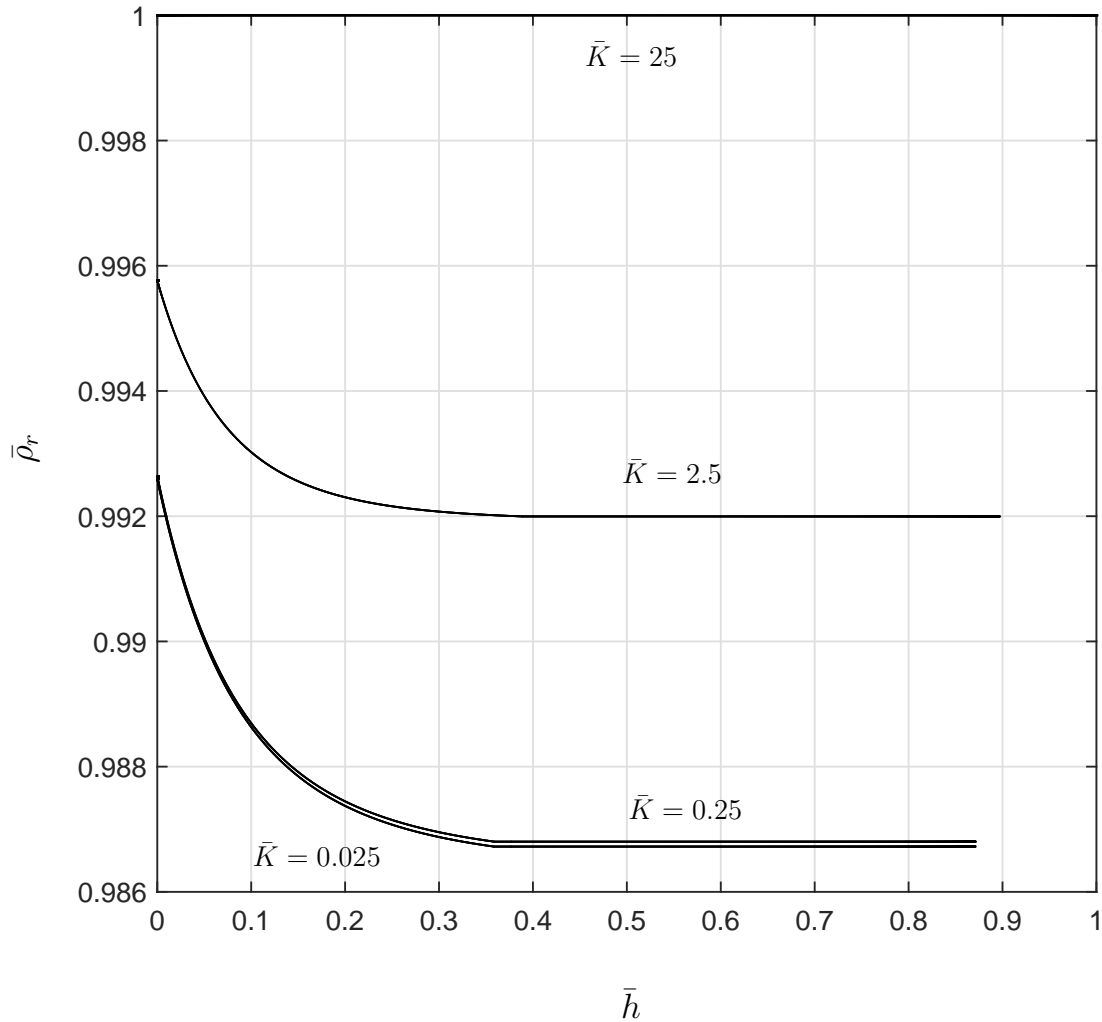


Figure A.3: The distribution of the dimensionless receptor density $\bar{\rho}_r$ versus dimensionless \bar{h} for various values of Debye length inverse $\bar{K} = \{0.025, 0.25, 2.5, 25\}$ and $\{\bar{r}_0 = 3, \bar{\gamma} = 10^{-4}, \gamma_3 = 10^{-5}, \bar{\zeta} = 0.5, \bar{h}_0 = 0.35, \bar{\rho}_l = 1.0\}$.

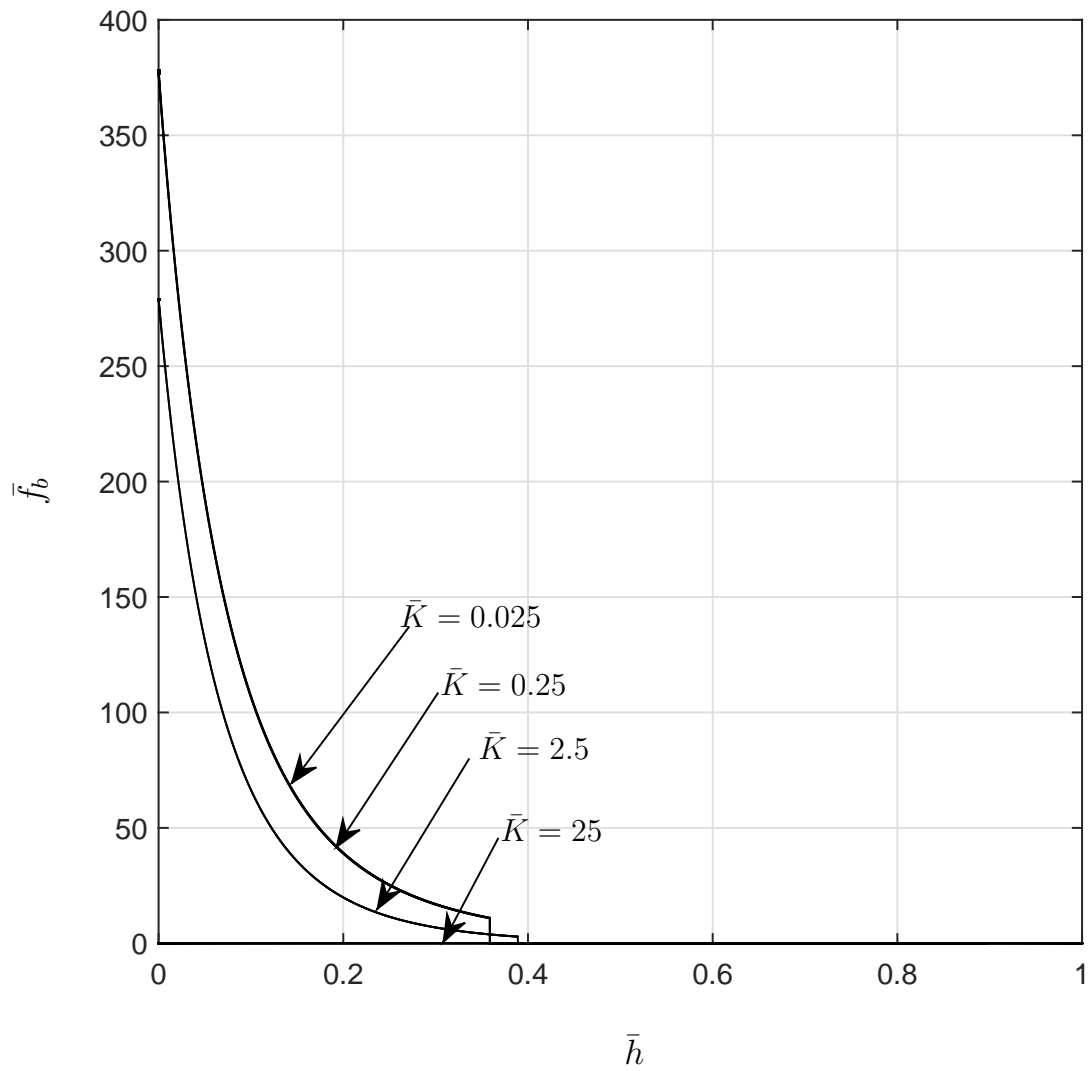


Figure A.4: Variation of the dimensionless binding force \bar{f}_b on the membrane versus dimensionless vertical distance \bar{h} for various values of Debye length inverse $\bar{K} = \{0.025, 0.25, 2.5, 25\}$ and $\{\bar{r}_0 = 3, \bar{\gamma} = 10^{-4}, \gamma_3 = 10^{-5}, \bar{\zeta} = 0.5, \bar{h}_0 = 0.35, \bar{\rho}_l = 1.0\}$.

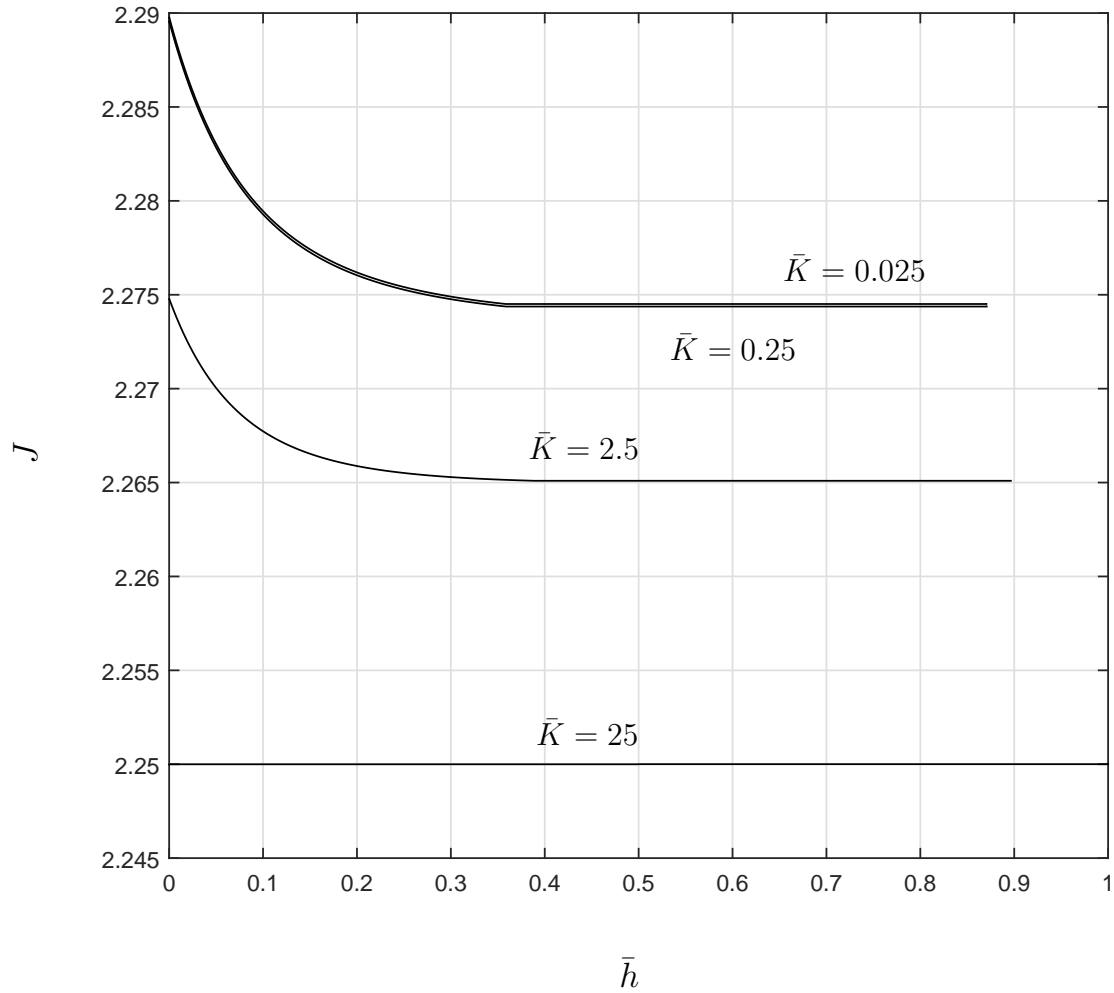


Figure A.5: Variation of the membrane area dilation J on the membrane versus dimensionless vertical distance \bar{h} for various values of Debye length inverse $\bar{K} = \{0.025, 0.25, 2.5, 25\}$ and $\{\bar{r}_0 = 3, \bar{\gamma} = 10^{-4}, \gamma_3 = 10^{-5}, \bar{\zeta} = 0.5, \bar{h}_0 = 0.35, \bar{\rho}_l = 1.0\}$.

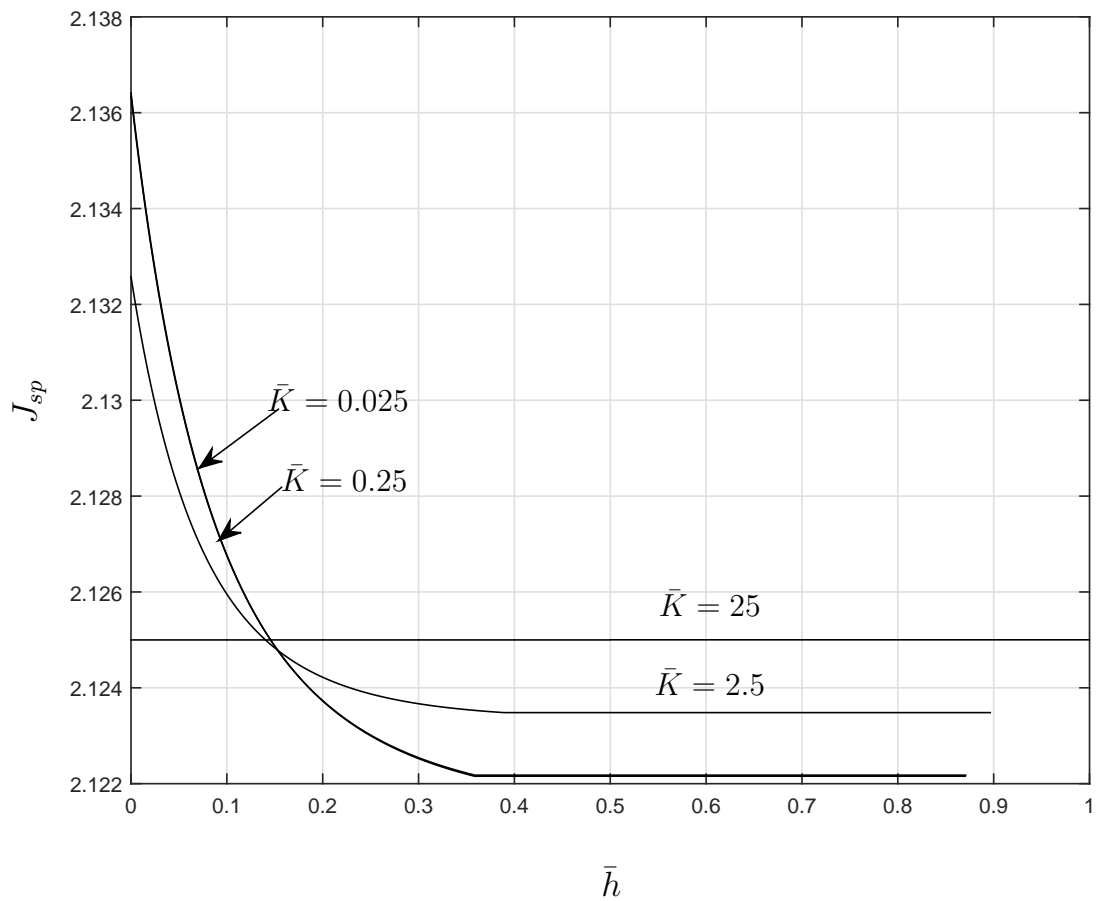


Figure A.6: Variation of the spontaneous area dilation J_{sp} on the membrane versus dimensionless vertical distance \bar{h} for various values of Debye length inverse $\bar{K} = \{0.025, 0.25, 2.5, 25\}$ and $\{\bar{r}_0 = 3, \bar{\gamma} = 10^{-4}, \gamma_3 = 10^{-5}, \bar{\zeta} = 0.5, \bar{h}_0 = 0.35, \bar{\rho}_l = 1.0\}$.

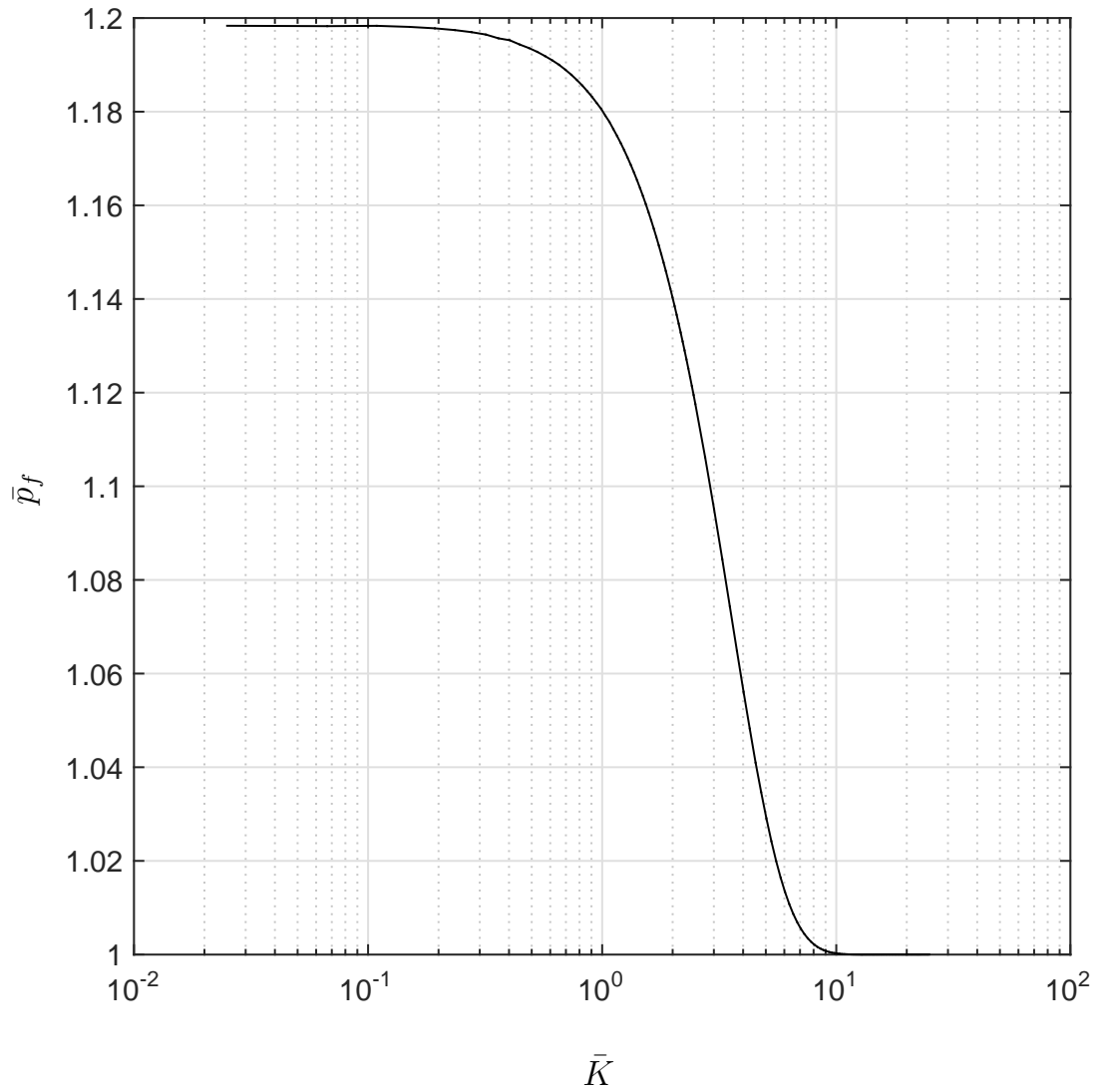


Figure A.7: The dimensionless pressure of the enclosed fluid, \bar{p}_f , versus Debye length inverse $\bar{K} = \{0.025, 0.25, 2.5, 25\}$ and $\{\bar{r}_0 = 3, \bar{\gamma} = 10^{-4}, \gamma_3 = 10^{-5}, \bar{\zeta} = 0.5, \bar{h}_0 = 0.35, \bar{\rho}_l = 1.0\}$.

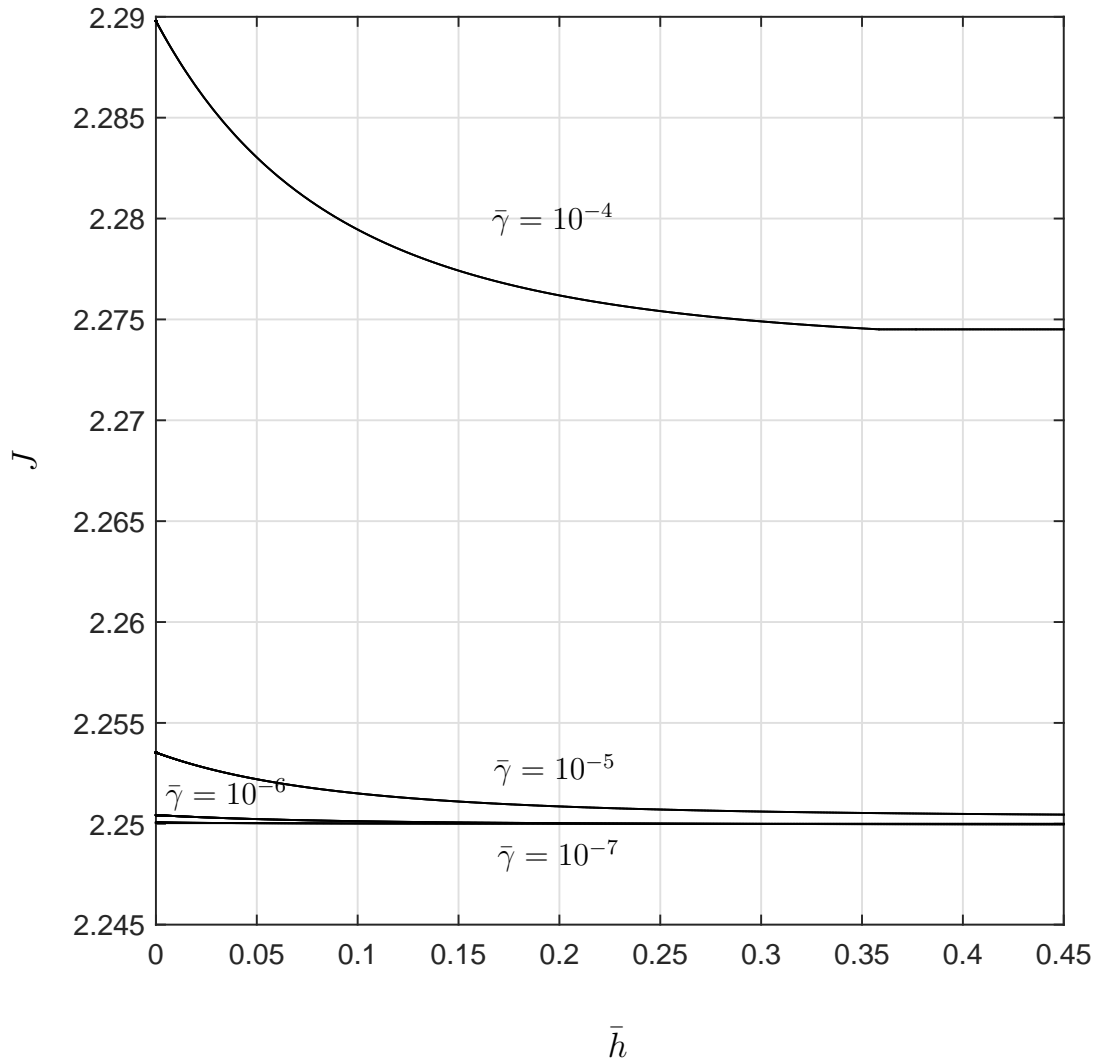


Figure A.8: Variation of the membrane area dilation J versus the dimensionless vertical distance \bar{h} for various dimensionless binding-membrane parameters $\bar{\gamma} = \{10^{-7}, 10^{-6}, 10^{-5}, 10^{-4}\}$ and $\{\bar{r}_0 = 3, \gamma_3 = \{10^{-8}, 10^{-7}, 10^{-6}, 10^{-5}\}, \bar{K} = 0.025, \bar{\zeta} = 0.5, \bar{h}_0 = 0.35, \bar{\rho}_l = 1.0\}$.

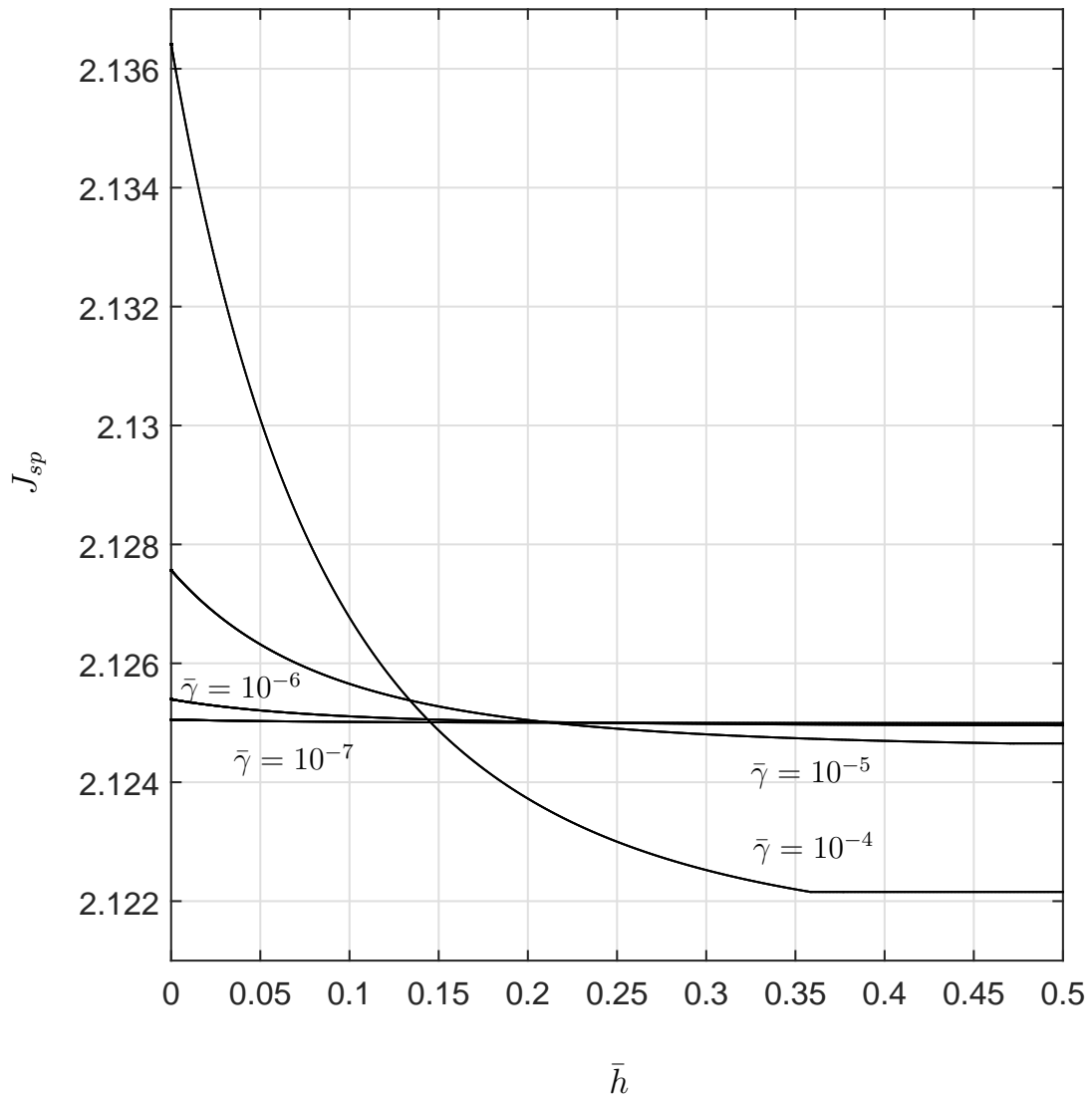


Figure A.9: Variation of the spontaneous area dilation J_{sp} versus the dimensionless vertical distance \bar{h} for various dimensionless binding-membrane parameters $\bar{\gamma} = \{10^{-7}, 10^{-6}, 10^{-5}, 10^{-4}\}$ and $\{\bar{r}_0 = 3, \gamma_3 = \{10^{-8}, 10^{-7}, 10^{-6}, 10^{-5}\}, \bar{K} = 0.025, \bar{\zeta} = 0.5, \bar{h}_0 = 0.35, \bar{\rho}_l = 1.0\}$.

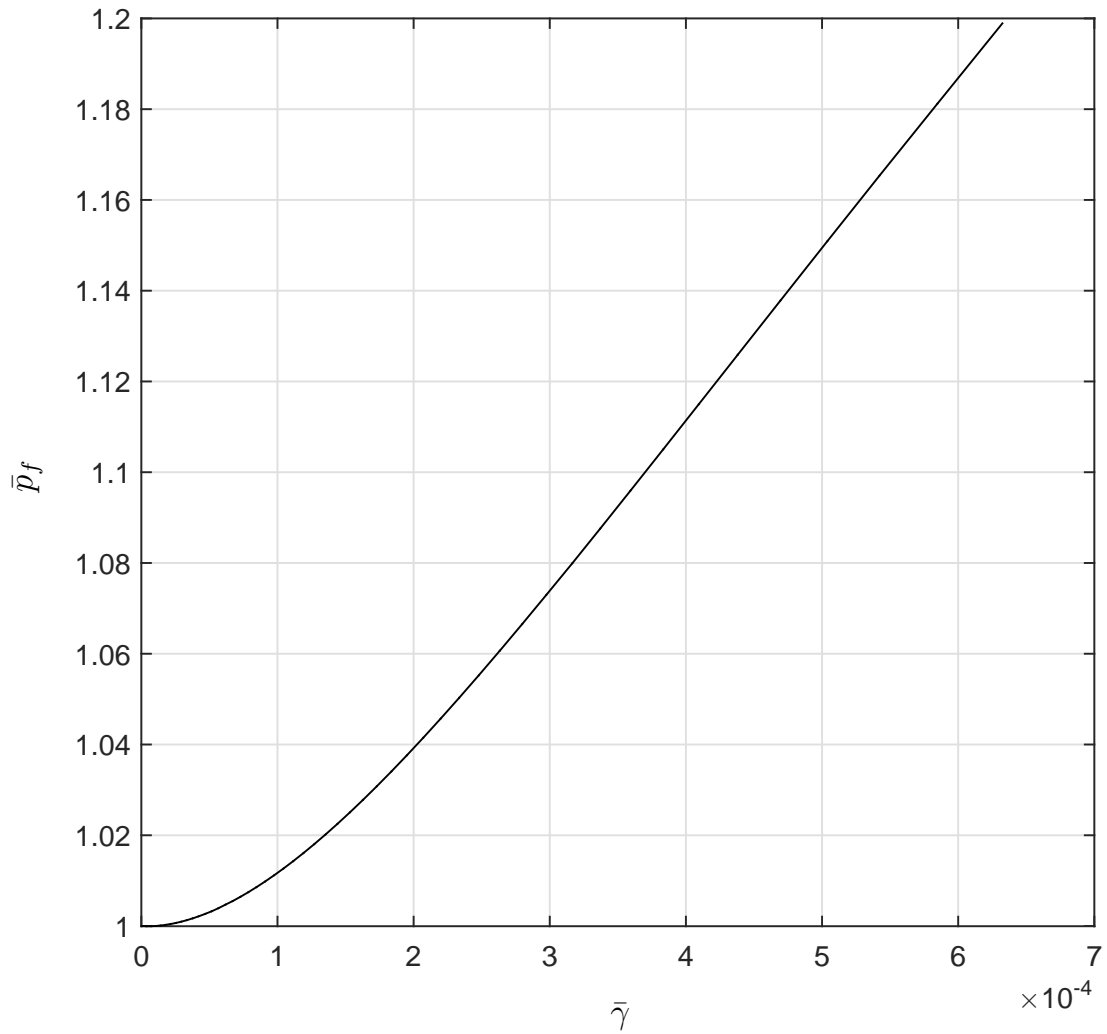


Figure A.10: The dimensionless pressure of the enclosed fluid, \bar{p}_f , versus dimensionless binding-membrane parameters $\bar{\gamma} = \{10^{-7}, 10^{-6}, 10^{-5}, 10^{-4}\}$ and $\{\bar{r}_0 = 3, \gamma_3 = \{10^{-8}, 10^{-7}, 10^{-6}, 10^{-5}\}, \bar{K} = 0.025, \bar{\zeta} = 0.5, \bar{h}_0 = 0.35, \bar{\rho}_l = 1.0\}$.

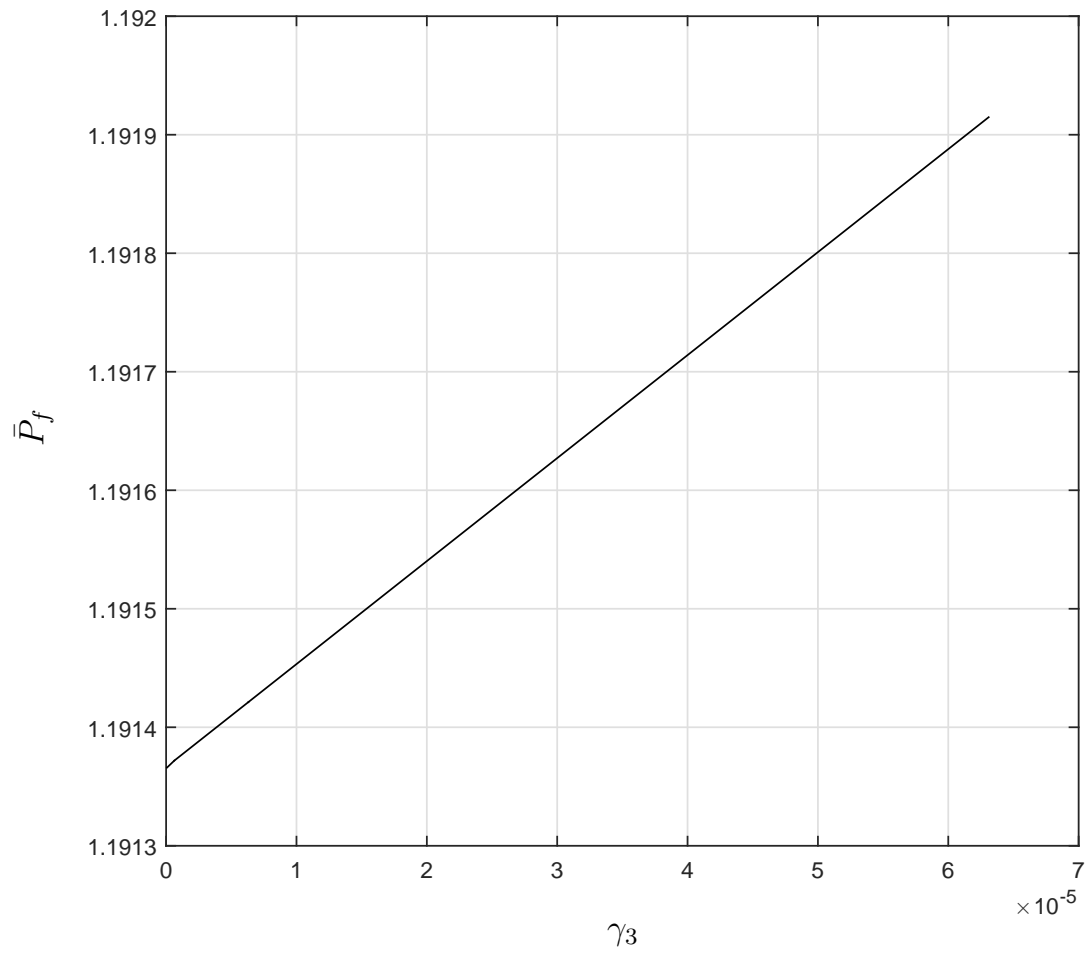


Figure A.11: The nondimensionalized pressure of the enclosed fluid \bar{p}_f versus dimensionless diffusion parameter γ_3 and $\{\bar{r}_0 = 3, \bar{\gamma} = 10^{-4}, \bar{K} = 0.025, \bar{\zeta} = 0.5, \bar{h}_0 = 0.35, \bar{\rho}_l = 1.0\}$.

Bibliography

- [1] B. Alberts, D. Bray, K. Hopkin, A. Johnson, J. Lewis, M. Raff, K. Roberts, and P. Walter. *Essential cell biology*. Garland Science, second edition, 2004.
- [2] B. Alberts, A. Johnson, J. Lewis, M. Raff, K. Roberts, and P. Walter. *Molecular biology of the cell*. Garland Science, New York, 4th edition, 2002.
- [3] S.S. Antman. *Nonlinear problems of elasticity*. Springer-Verlag, New York, 1995.
- [4] G. Bao and S. Suresh. Cell and molecular mechanics of biological materials. *Nature Materials*, 2(11):715–725, 2003.
- [5] M.V. Bayas, K. Schulten, and D. Leckban. Forced detachment of the cd2-cd58 complex. *Biophysical Journal*, 84(4):2223–2233, 2003.
- [6] G.I. Bell. Models for the specific adhesion of cells to cells. *Science*, 200(4342):618–627, 1978.
- [7] G.I. Bell, M. Dembo, and P. Bongrand. Cell adhesion competition between nonspecific repulsion and specific bonding. *Biophysical Journal*, 45(6):1051–1064, 1984.
- [8] D.H. Boal. *Mechanics of the cell*. Cambridge University, Cambridge, UK, 2002.
- [9] P. Chadwick. *Continuum Mechanics Concise Theory and Problems*. Dover, Mineola, New York, second edition, 1999.
- [10] Q.H. Cheng, P. Liu, H.J. Gao, and Y.W. Zhang. A computational modeling for micropipette-manipulated cell detachment from a substrate mediated by receptor–ligand binding. *Journal of the Mechanics and Physics of Solids*, 57:205–220, 2009.

- [11] S. Chien, S. Usami, K.M. Jan, and R. Skalak. Macrorheological and microrheological correlation of blood flow in the macrocirculation and microcirculation, in rheology of biological systems. *Rheology of Biological Systems*, pages 12–48, 1973.
- [12] P.G. Ciarlet. *An introduction to differential geometry with applications to elasticity*. Springer, Dordrecht, Netherlands, 2005.
- [13] E. Evans and Y.C. Fung. Improved measurements of the erythrocyte geometry. *Microvascular Research*, 4(4):335–347, 1972.
- [14] E. Evans and W. Rawics. Entropy-driven tension and bending elasticity in condensed-fluid membranes. *Physical Review Letters*, 64(17):2094–2097, 1990.
- [15] E.A. Evans. New membrane concept applied to the analysis of fluid shear and micropipette-deformed red blood cells. *Biophysical Journal*, 13(9):941–954, 1973.
- [16] E.A. Evans. Minimum energy analysis of membrane deformation applied to pipet aspiration and surface adhesion of red blood cells. *Biophysical Journal*, 30(2):265–284, 1980.
- [17] E.A. Evans. Bending elastic modulus of red blood cell membrane derived from buckling instability in micropipet aspiration tests. *Biophysical Journal*, 43(1):27–30, 1983.
- [18] E.A. Evans. Detailed mechanics of membrane-membrane adhesion and separation. i. continuum of molecular cross-bridges. *Biophysical Journal*, 48(1):175–183, 1985.
- [19] E.A. Evans and P.L. LaCelle. Intrinsic material properties of the erythrocyte membrane indicated by mechanical analysis of deformation. *Blood*, 45(1):29–43, 1975.
- [20] E.A. Evans and D. Needham. Physical properties of surfactant bilayer membranes: Thermal transitions, elasticity, rigidity, cohesion, and colloidal interactions. *The Journal of Physical Chemistry*, 91(16):4219–4228, 1987.
- [21] E.A. Evans and V.A. Parsegian. Energetics of membrane deformation and adhesion in cell and vesicle aggregation. *Annals New York Academy of Sciences*, 416:13–33, 1983.

- [22] E.A. Evans and W. Rawics. Elasticity of fuzzy biomembranes. *Physical Review Letters*, 79(12):2379–2382, 1997.
- [23] E.A. Evans and R. Skalak. *Mechanics and thermodynamics of biomembranes*. CRC Press, Florida, 1980.
- [24] E.A. Evans and R. Waugh. Osmotic correction to elastic area compressibility measurements on red cell membrane. *Biophysical Journal*, 20(3):307–313, 1977.
- [25] E.A. Evans, R. Waugh, and L. Melnik. Elastic area compressibility modulus of red cell membrane. *Biophysical Journal*, 16(6):585–595, 1976.
- [26] A. F.Golestaneh and B. Nadler. Modeling of cell adhesion and deformation mediated by receptor-ligand interactions. *Biomechanics and Modeling in Mechanobiology*, June 2015.
- [27] Y.C. Fung. Theoretical considerations of the elasticity of red cells and small blood vessels. *Federation proceedings*, 25(6):1761–1772, 1966.
- [28] Y.C. Fung. *Biomechanics, mechanical properties of living tissues*. Springer-Verlag, New York, 2nd edition, 1993.
- [29] N.D. Gallant and A.J. Garcia. Model of integrin-mediated cell adhesion strengthening. *Journal of Biomechanics*, 40(6):1301–1309, 2007.
- [30] H. Gao, W. Shi, and L.B. Freund. Mechanics of receptor-mediated endocytosis. *Proceedings of the National Academy of Sciences of the United States of America*, 102(27):9469–9474, July 2005.
- [31] A.E. Green and W. Zerna. *Theoretical elasticity*. Dover, New York, 2nd edition, 1992.
- [32] M.E. Gurtin. *An introduction to continuum mechanics*. Academic Press, New York, 1981.
- [33] M.E. Gurtin, E. Fried, and L. Anand. *The mechanics and thermodynamics of continua*. Cambridge University, New York, 2010.
- [34] W. Hanley, O. McCarty, S. Jadhav, Y. Tseng, D. Wirtz, and K. Konstantopoulos. Single molecule characterization of p-selectin/ligand binding. *The Journal of Biological Chemistry*, 278(12):10556–10561, 2003.

- [35] H. Hirata, K. Ohki, and H. Miyata. Mobility of integrin 51 measured on the isolated ventral membranes of human skin fibroblasts. *Biochimica et Biophysica Acta*, 1723(1-3):100–105, 2005.
- [36] R.M. Hochmuth and N. Mohandas. Uniaxial loading of the red cell membrane. *Journal of Biomechanics*, 5(5):501–504, 1972.
- [37] R.M. Hochmuth, N. Mohandas, and J.P.L. Blackshear. Measurement of the elastic modulus for red cell membrane using a fluid mechanical technique. *Biophysical Journal*, 13(8):747–762, 1973.
- [38] J. Israelachvili. *Intermolecular and surface forces*. Academic Press, London, UK, 2nd edition, 1991.
- [39] R. Lipowsky. The conformation of membranes. *Nature*, 349:475–481, 1991.
- [40] P. Liu, Y.W. Zhang, Q.H. Cheng, and C. Lu. Simulations of the spreading of a vesicle on a substrate surface mediated by receptor-ligand binding. *Journal of the Mechanics and Physics of Solids*, 55(6):1166–1181, 2007.
- [41] J.E. Marsden and T.J.R. Hughes. *Mathematical foundations of elasticity*. Prentice-Hall, New Jersey, 1983.
- [42] L. Martin. The fluid mosaic model of the cell membrane - the mosaic. connexions module.
- [43] E.J. Martinez, Y. Lanir, and S. Einav. Effects of contact-induced membrane stiffening on platelet adhesion. *Biomechanics and Modeling in Mechanobiology*, 2(3):157–167, 2004.
- [44] B. Nadler. On the contact of a spherical membrane enclosing a fluid with rigid parallel planes. *International Journal of Non-Linear Mechanics*, 45(3):294–300, 2010.
- [45] B. Nadler and T. Tang. Decohesion of a rigid punch from non-linear membrane undergoing finite axisymmetric deformation. *International Journal of Non-Linear Mechanics*, 43(8):716–721, 2008.
- [46] C.H. Norris. The tension at the surface and other physical properties of the nucleated erythrocyte. *Journal of Comparative Physiology*, 14(1):117–133, 1939.

- [47] R.W. Ogden. *Nonlinear elastic deformations*. Dover, Mineola, New York, 1997.
- [48] R.P. Rand. Mechanical properties of the red blood cell membrane ii. viscoelastic breakdown of the membrane. *Biophysical Journal*, 4(4):303–316, 1964.
- [49] U.S. Schwarz, T. Erdmann, and I.B. Bischofs. Focal adhesions as mechanosensors: The two-spring model. *Biosystems*, 83(2-3):225–234, 2006.
- [50] V.B. Shenoy and L.B. Freund. Growth and shape stability of a biological membrane adhesion complex in the diffusion-mediated regime. *Proceedings of the National Academy of Sciences of the United States of America*, 102(9):3213–3218, March 2005.
- [51] S.D. Shoemaker and T.K. Vanderlick. Intramembrane electrostatic interactions destabilize lipid vesicles. *Biophysical Journal*, 83:2007–2014, 2002.
- [52] S.J. Singer and G.L. Nicolson. The fluid mosaic model of the structure of cell membranes. *Science*, 175(4023):720–731, 1972.
- [53] R. Skalak. Modeling the mechanical behavior of red blood cells. *Biorheology*, 10:229–238, 1973.
- [54] T. Sohail, T. Tang, and B. Nadler. Adhesive contact of the fluid filled membrane driven by electrostatic forces. *International Journal of Solids and Structures*, 50(16-17):2678–2690, 2013.
- [55] K.M. Yamada. Fibronectin peptides in cell migration and wound repair. *The Journal of Clinical Investigation*, 105(11):1507–1509, 2000.
- [56] P.R. Zarda, S. Chien, and R. Skalak. Elastic deformations of red blood cells. *Journal of Biomechanics*, 10(4):211–221, 1977.